OPTIMIZATION OF SHALLOW ARCHES AGAINST SNAP-THROUGH BUCKLING

A THESIS

Presented To

The Faculty of the Division of Graduate Studies and Research

By

Hartley McMullin Caldwell, III

In Partial Fulfillment

of the Requirements for the Degree

Doctor of Philosophy in the School of Engineering Science and Mechanics

Georgia Institute of Technology

March, 1977

OPTIMIZATION OF SHALLOW ARCHES

AGAINST SNAP-THROUGH BUCKLING

Approved:

George J. Simitses, Chairman

C. V. Smith

S. Atluri

Date Approved by Chairman MAR 14 1977

This Dissertation is Dedicated

To

Thornwell, A Home and School for Children

Clinton, South Carolina

ACKNOWLEDGMENTS

Special appreciation is extended to Professor George J. Simitses, the author's thesis advisor, for his patience and encouragement during the course of this investigation. The many enlightening discussions and remarkable insights shared with the author will always be a constant source of motivation. Thanks are also extended to Professors C. V. Smith, S. Atluri, C. E. S. Ueng and R. L. Carlson who served on the thesis committee and provided invaluable comments and advice.

A special note of thanks to Ms. Brenda Smiley and Ms. Barbara Geiger for an excellent job in typing the final manuscript and to Ms. Sharon Flores for her assistance in putting the early drafts into a readable form.

And finally, sincere appreciation is extended to my family for whose encouragement and devotion I will be forever indebted.

TABLE OF CONTENTS

LIST OF TABLES

LIST OF ILLUSTRATIONS

Figure Page

Figure Page

SUMMARY

The field of structural optimization, that is, obtaining the best performance for a structure within a specified class which satisfies certain given constraints, has occupied investigators for many years. Only in the last two decades, however, have large strides been made in this area, primarily due to the advent of large capacity digital computers coupled with novel numerical approximation techniques. In an effort to learn more about optimum structural systems, studies have been made in search of optimum structural elements (i. e., beams, plates, shells, arches.)

Consider a shallow arch of specified volume and length, under arbitrary boundary restraint and loaded symmetrically in the plane. The problem is to find, among all shallow arches of equal volume, boundary restraints, initial shape and load distribution, the one with the highest buckling load. This problem, unlike the high arch, is complicated by the fact that instability can occur through either a limit point (symmetric snapping) or unstable bifurcation (anti-symmetric mode). Because of this dual mode instability, which depends upon the arch rise, the technical approach is to separately consider each form of instability as the failure constraint; produce the optimum design; and then compare the various designs for the same value of arch

rise to determine the one with the maximum buckling load.

The problem is formulated on the basis of displacement and discretized via the finite element method. Equilibrium equations are then obtained from the principle of the stationary value of total potential. The buckling criteria is obtained from Trefftz' interpretation of the energy criterion for stability. In the case of unstable bifurcation, critical conditions are found by requiring a nontrival buckled mode. In the case of limit point (symmetric mode) instability critical conditions are those at which the second variation of the total potential becomes positive semi-definite. With the equations now obtained, sufficient for the analysis of any given design, the construction of the optimality criterion necessary for the optimal design for each type of instability is made. By equating to zero the second variation of the total potential, a functional is obtained which defines the axial thrust within the arch at the critical point. Constraining this functional to meet the constant volume constraint as well as specifying the mode shape by its relation to the primary path equilibrium mode, upon extremization one obtains the optimality criterion for each type of buckling failure. Interpreting the optimality criterion in terms of energy density, an iterative scheme is devised which uniformly converges to an optimal design for a given set of system parameters. Using this approach, numerous designs are generated which satisfy the respective

optimality criterion for a specified load distribution, initial configuration and boundary restraint.

The designs obtained differ significantly under varying degrees of rotational restraint at the boundaries for a given failure mode. There are also fundamental differences in the optimal designs for the two different failure modes.

To determine the strongest design for a low or high value of arch rise, an analysis is made to determine the critical response of the optimal designs. For low values of rise, the strongest design is obtained with respect to the limit point optimality criterion; for high values of arch rise, the strongest design is obtained with respect to the unstable bifurcation optimality criterion. For moderate values of arch rise, the optimization process presented, which is based on an assumed failure mode, does not yield the strongest design since the failure mode in this region changes during the optimization. It is seen, however, that for moderate values of arch rise the uniform arch may have a higher buckling load than either of the designs which separately meet the optimality criteria. This phenomena is strongly dependent upon the degree of boundary restraint and is almost non-existent for the simply supported arch.

The demonstrated methodology allows one to systematically analyze a shallow arch of arbitrary shape and to determine for extreme values of arch rise the shape of the strongest shallow arch.

NOTATIONS

$A(x)$	Dimensional cross-sectional area, z, x-coordinates
$A(\xi)$	Dimensional cross-sectional area, z, ξ-coordinates
$\bar{A}(\xi)$	$A(\xi)/A_u$ non-dimensional area
A_u	Cross-sectional area of uniform column
$A_{opt}(\xi)$	The function $A(\xi)$ satisfying the optimality criteria
E	Young's Modulus
e	Rise parameter = $\eta_o(\pi/2)$
F^*	Dimensional concentrated load
F	Non-dimensional concentrated load
H	Critical energy
$I(x)$	Dimensional moment of inertia
I_u	Moment of inertia of uniform column of length L
$I(\xi)$	Non-dimensional arch moment of inertia
$\bar{I}(\xi)$	$I(\xi)/I_u$
$\overset{A}{I}_{opt}$	Design obtained by optimizing for anti-symmetric buckling modes
$(e)\overset{S}{I}_{opt}$	Design obtained by optimizing for symmetric buckling modes for a specific value of rise parameter, e.
J	constant = $\dfrac{1}{2\left[\int_o^\pi \dfrac{d\xi}{A(\xi)} + \hat{\alpha}\right]}$
L	Length in the x, z-coordinate system
$M^*(x)$	Dimensional moment
$M(\xi)$	Non-dimensional moment

$\bar{m}$, m	Integer
n	Integer, 1, 2, 3
$\bar{p}_{cr}$	The value of $\bar{p}$ in the buckled state for an $A(\xi)$
$\bar{p}_{opt}$	The value of $\bar{p}_{cr}$ for $A(\xi) = A_{opt}(\xi)$
P	Dimensional axial thrust = $\int_A \sigma dA$
p	Non-dimensional axial thrust = $\frac{P}{P_E}$
$\bar{p}$	$= -p$
P_E	Critical axial load for simply supported column = $\frac{\pi^2 E I_u}{L^2}$
$Q^*(x)$	Dimensional lateral load
$q(\xi)$	Non-dimensional lateral load
q_{cr}	Critical value of amplitude of applied lateral load
U^*_T	Dimensional total potential
U_T	Non-dimensional total potential
$u(x)$	Horizontal displacement of a point in x, z coordinates
$v(\xi)$	Horizontal displacement of a point in ξ, z coordinates
$\bar{v}$	Prescribed volume
V	Non-dimensional second variation $\delta^2 U_T$
$w_o(x)$	Dimensional initial configuration
$w(x)$	Dimensional deformed configuration
$y(\xi)$	$= \eta(\xi) - \eta_o(\xi)$ · non-dimensional displacement
α	positive proportionality constant

$\hat{\alpha}$	Constant = $\frac{1}{\varepsilon_E} \frac{2}{\alpha_o}$
α_o^*	Modulus of elastic support in horizontal direction
α_o	Non-dimensional α_o^*
β_o^*	Modulus of rotational elastic restraints at $\xi=0$
β_o	Non-dimensional β_o^*
β^*	Dimensional modulus of elastic foundation
$\gamma(\xi)$	Kinematically admissible variations in $\eta(\xi)$; buckled modes
δ	Denotes Dirac delta function for concentrated load; variation
ε_E	Strain of column subjected to P_E
$\varepsilon, \varepsilon_1, \varepsilon_2, \varepsilon_3$	Small quantities
ε_x^o	Reference surface strain
$\bar{\eta}_o(\xi)$	$=\eta_o(\xi)/e$
$\eta(\xi)$	Non-dimensional deformed configuration
$\eta_o(\xi)$	Non-dimensional initial configuration
θ	Admissible function in the variation of V
κ_x	Change in curvature
λ	Lagrange multiplier
$\bar{\rho}$	Constant $\bar{I}(\xi) = \bar{\rho}\bar{A}(\xi)^n$, n integer 1,2,3
ρ	Radius of gyration; $= \frac{I_u}{A_u}$
σ	Linear mass density; stress
$(\underline{\ })$	Vector quantity
$(\underline{\underline{\ }})$	Matrix quantity
$(\ )'$	Spatial derivative
β	Non-dimensional β^*

$( )^T$	Transpose of matrix or vector quantity
$( )^{-1}$	Inverse of matrix
$(\hat{})$	Equilibrium and buckling equation solutions at critical loading conditions

CHAPTER I

INTRODUCTION

Complicated structural systems such as buildings, bridges, water, air, and space vehicles are composed of basic structural elements. On the basis of their geometry and mission, these basic elements are called bars, columns, straight and curved beams, high and shallow arches, flat and curved thin plates and others. The constant demand for light weight, low cost, efficient structural systems has led many investigators to the field of structural optimization. The effort along these lines can be grouped into a) structural system optimization and b) basic structural element optimization. Successes and failures have been reported in both groups through the past few years. In the second group one might differentiate between elements whose design is governed by buckling (columns, rings, arches, and compression panels) and elements which are designed on the basis of strength and deflection limitations (beams, bars, transversely loaded plates, etc.,).

The interest in the low arch is of great importance because this particular structural geometry has been used as a basic structural element in large structural systems as well as a fundamental structural configuration by itself.

1.1 Statement of the Problem

The investigation reported herein is carried out within the framework of the following problem statement:

Given a symmetric shallow arch (see Fig. 1) of specified mass, length, rise and various boundary conditions (mixed or not - with or without elastic supports) resting on an elastic foundation and loaded by a symmetric transverse load, find the optimum distribution of stiffness such that its load carrying capacity against buckling is a maximum. The design objective is thus to maximize the buckling load.

The shallow arch presents an interesting and challenging problem primarily because it is the simplest structural configuration that exhibits the known mechanisms of buckling: namely, snapping symmetrically (limit point instability), snapping anti-symmetrically (unstable bifurcation), and classical stable bifurcation. Thus, any attempt to produce an "optimum" design must be done with the possible types of instabilities as the primary failure criteria. The design space is composed of all those shallow arches of specified volume and with the same set of system parameters (i.e., those parameters that collectively describe the initial shape, loading and boundary conditions). It will be shown in subsequent chapters that the analysis-synthesis process leading to a local optimum design can be broken into two separate investigations depending upon whether the arch is constrained to buckle symmetrically (limit point) or

anti-symmetrically (unstable bifurcation) with respect to the primary (unbuckled) equilibrium path. Furthermore, the arch rise parameter, the height of the arch at its mid-point, plays a dominant role in differentiating between the type of failure modes experienced by the arch for a given destabilizing lateral load.

Since the design objective is to maximize the critical load for each type of failure mode, this necessitates the introduction of certain optimality criteria which are met via an iterative scheme. The optimality criterion is different for each type of failure mode, but both depend upon meeting a criterion of uniform energy density for the optimum geometry.

Although the unstable bifurcation analysis is amenable to an eigenvalue solution, the limit point analysis, due to the coupled non-linearity of the governing equation enjoys no such simplification. Moreover, the synthesis process, with limit point instability as failure mechanism depends explicitly upon the rise parameter whereas the corresponding process with unstable bifurcation as failure mechanism does not.

Finally, optimum designs are obtained in each case within the restriction that the cross-sectional inertia and area are related by $I(\xi) = \bar{\rho} A(\xi)^n$, where $\bar{\rho}$ is a specified shape factor and the exponent n is given the values 1, 2, or 3, meaning respectively that the thickness of the arch cross-section varies and the height is constant; the thickness

and height vary proportionally; or the height varies and the thickness is constant.

1.2 Historical Review

The search for optimum designs transcends the spectrum of structural shapes including beams and columns, (1-6, 19, 21, 22), stiffened and unstiffened plates and shells (7), and finally complex indeterminate trusses and advanced aerospace structural systems composed of numerous basic elements. (8-10, 15, 17, 25) Moreover, these optimum designs are sought for many different failure criteria including strength, deflection, stability and dynamic response.

The earliest published effort in man's attempt to find the best or optimum design within a given framework of constraints is generally attributed to T. Clausen (11) who in 1851 correctly solved the problem for the optimal shape of a simply supported column of minimum weight with a prescribed buckling load as the failure criterion. The column problem was later independently solved by Keller (1) in 1960.

The optimum column for various classes of system parameters has received wide and varied attention in the past decade and a half, and appears to have served as impetus for a broad range of structual optimization investigations as well as for cohesive theoretical studies, a comprehensive review of which was made by Sheu and Prager in 1968 (12). Tadjbakhsh and Keller (3) extended the work of Ref.(1) to

columns with different supports and gave the first proof of the optimal character of the design. A reformulation of the optimality criterion from energy concepts, rather than the incremental equilibrium equations, was presented by Taylor (4), and Prager and Taylor (13). The last reference, together with Taylor and Liu (5), also introduced minimum cross-sectional area constraints into the formulation. The effect of self-weight on the optimal design of the column has been investigated by Keller and Niordson (2), and Huang and Sheu (14). Growing efforts during the late 1950's to utilize the computational speed and capacity of digital computers resulted in the development of numerous algorithms for the automated structural design of complex systems.

The developments in structural optimization based on numerical search techniques mushroomed quickly because it suddenly opened up a new promising area for research work with computer applications attracting the interest of many capable researchers to a territory formerly almost the exclusive domain of the structural engineer. In the wake of the demonstrated successes, and anticipating further improvements in numerical search techniques, computer capability and structural analysis methods, an effort was initiated to investigate the feasibility of applying mathematical programming techniques to the optimization of large structural systems using finite element methods as the analysis module. It was hoped not only to replace fully

stressed design methods, applicable to strength design only, but to couple the general purpose optimization capability of direct numerical search techniques with the general purpose analysis capability of the finite element methods to handle structural optimization problems with a wide range of behavioral and side constraints. (15) These efforts met with limited success when applied to large structural systems due to the exorbitant amount of computer time and capacity required coupled with the result of degradation in accuracy (16).

To avoid the pitfalls of direct search techniques utilized for the optimum design of large structural systems, indirect methods built around optimality criteria were developed by Venkayya and others (17, 18). These approaches frequently result in a specification of the energy distribution when the optimum design is reached. Similar observations are made by Taylor (4) and Prager and Taylor (13) for the column problem mentioned previously.

While much effort is currently being expended in industry to automate the design of complex structure, equally important efforts have been made in the study of the optimal character of basic structural elements themselves. Simitses, Kamat and Smith (6) have studied the optimal column through a finite element formulation utilizing redesign methods based upon the satisfaction of the optimality criterion. The optimal design of simply supported beams with given structural volume having the highest fundamental frequency was obtained by Niordson (19). Numerous investigations have subsequently

considered the optimization of basic elements and structural systems subject to dynamic constraints (20-26).

In addition to the column problem, more complicated structural elements have been the target of optimization methods. Simitses and Ungbhakorn (7) presented a two-stage methodology for obtaining a minimum weight design of stiffened cylinders subjected to axial compression. For the fuselage type circular cylindrical shells considered, the primary design constraint was taken to be general instability. Reference (7) contains a bibliography of important contributions regarding optimum design of stiffened plates and shells. A critical review of these efforts is contained in reference (9).

The study of the instability of the shallow arch with prescribed geometry has occupied investigators for many years. Timoshenko and Gere (27) provide several examples of arch buckling under various loads and boundary conditions. Reference to early initial work is given. Marguerre (28) discusses the snap buckling of the slightly curved beam subjected to destabilizing lateral loads and formulates the buckling criterion by enforcing the stationality of the second variation of the total potential. Kaplan and Fung (29) reported analytical and experimental results for the classical buckling of shallow arches using a Fourier representation for displacements under various loads and boundary conditions. Schreyer and Masur (30) studied analytically both symmetric and anti-symmetric

instability of a clamped circular arch under uniform pressure as well as a concentrated load. Walker (31) used a finite element formulation to study the bifurcation and post buckling behavior of a clamped and simply supported circular arch under dead loading. Thomas (32) presented a finite element formulation using a cubic displacement function for the instability of beams, frames, and arches. He considered three different cases of load behavior: loads remain normal to deformed element; loads remain parallel to their original direction; and the loads remain directed toward a fixed point. Only classical buckling was considered and no attempt was made to include the limit point instability associated with the shallow arch.

In addition to instability for static load cases mentioned above, extensive results have been published [Ref. Simitses (33), Hsu, Kuo, Lee (34), Hoff and Bruce (35)] regarding the buckling, both snapping and bifurcation, of shallow arches under a wide variety of dynamic loads.

Owing to the large volume of interest over the years in the character of instability of shallow arches, it is a natural consequence that investigators would extend their efforts to the determination of those designs which have the greatest capability of withstanding destabilizing loads. Utilizing the theoretical base provided by Keller (1) and Tadjbakhsh and Keller (3) for the column, in addition to the energy interpretation given by Taylor (4), Wu (36) successbully attacked the problem of generating the strongest simply

supported high circular arch subjected to uniform pressure. Subsequently, Wu's perturbation approach was extended by Budiansky, Frauenthal and Hutchinson (37) to a general class of high circular arches for which a Rayleigh quotient can be given and buckling occurs via an anti-symmetric mode. Rapp (38) investigated the instability of shallow arches for symmetric buckling modes within a specified class of nonuniform area distributions. He demonstrated that the distribution of area significantly affects the critical conditions. Recently, Christensen (39) studied the optimization of a shallow, clamped, uniformly loaded, circular arch for symmetric buckling using a perturbation technique. The design space was restricted to small changes from the uniform arch and small values of arch rise so that snapping was assured to be the failure mode.

Several investigators over the past decade have sought to unify the numerous approaches to structual optimization problems by placing them on a firmer theoretical foundation. Optimality criterion approaches have thus come under close scrutiny.

Following Taylor (4), Salinas (40) provided a comprehensive presentation of the variational basis for problems in optimal structural design, and demonstrated the duality of potential energy and minimum volume formulations. He considered one and two dimensional conservative elastic systems from both minimum weight and maximum load carrying capability points of view, and demonstrated that the optimum structure for both

minimum weight (volume) and maximum load are the same for unconstrained and (linear) buckling problems. Prager and Taylor (13) present a uniform method for treating the optimization of sandwich type structures for maximum stiffness, fundamental frequency, buckling load, and safety. Venkayya, Khot and Reddy (18) discuss the energy distribution in optimal structural designs. Gellatly and Berke (16) discuss the applicability of optimality criteria approaches to stress and displacement limited designs. Prager, Marcal et. al. (41) treat the minimum weight design of various structural forms subjected to static, dynamic and thermal loads. Berke (42) points out that iterative resizing techniques based upon optimality criteria may be subject to some convergence problems. The introduction of scaling factors has been successfully used to smooth the convergence process. Prager (43) has presented necessary and sufficent conditions for global optimality for certain truss layouts subjected to displacement as well as energy constraints.

It is seen that most previous methods attempting to optimize structural elements with buckling as the failure mechanism are necessarily dependent up the formulation of a Rayleigh quotient for the critical load parameter. To date, no attempt has been made to extend this idea of an "energy quotient" to the non-linear snap-through problem. The search for the strongest arch for specified end restraints must be made with both limit point instability as well as unstable

bifurcation in mind since the character of the failure changes dramatically for certain ranges of system parameters. Thus, a unified approach is presented herein that considers instability through snapping as well as bifurcation and converges to a local optimum design via the iterative redistribution of inertia based upon optimality criteria which demand uniform energy density.

Even with the extensive work being conducted in the field of automated structural design on both the applied and theoretical levels (see Refs. 44 and 45 for recent reviews), numerous general questions remain unsolved. It is hoped that the specific problem treated herein will provide further insight into the applicability of the optimality criterion approach to the optimization of basic structural components and thus be beneficial to the understanding of the related problems for structural systems.

CHAPTER II

MATHEMATICAL FORMULATION

In dealing with the optimization of structural elements which are governed by buckling, initially the attempt was toward linear eigenvalue problems such as the column (4, 5) and the high circular arch, (36) the reason being that for such elements a Rayleigh quotient exists and the derivation of the needed optimality condition is straightforward. Unfortunately, this energy approach cannot be applied directly to shallow arches (a highly nonlinear system) without some modification and reinterpretation because of the dual mechanism through which instability might occur.

It is well known that the shallow arch (or slightly curved beam) subjected to quasi-static lateral loading exhibits two quite distinct mechanisms of instability upon reaching certain load levels; namely, snapping symmetrically (limit point instability) or snapping anti-symmetrically (unstable bifurcation). (48) Furthermore, these load levels can be related directly to the arch geometry for given sets of system parameters, namely those parameters that collectively define the load distribution, the initial shape and boundary conditions. A basic ingredient to the solution for the optimum shape for a given set of system parameters is the buckling analysis for intermediate designs. Therefore, one must first derive equations

which relate the buckling load to the structural geometry, by considering the inertia (or area) as position dependent, and then formulate the optimization problem. To this end the technical approach shall be divided into two parts. Part I deals with the relation of the critical load to the structural geometry and the response of the system. It is instructive to derive these relationships at first analytically by means of the principle of the stationary value of the total potential and utilize Trefftz' interpretation of the energy criterion for instability to relate the critical load to the primary path response and the buckling modes. Afterward, the continuous system will be discretized via the finite element displacement formulation yielding a system of algebraic governing equations through which a solution becomes tractable. Part II will focus on the derivation of the optimality criteria associated with limit point instability and unstable bifurcation separately.

2.1 Buckling Analysis

Consider the symmetric shallow arch shown on Fig. 1. The arch is resting on an elastic foundation and is elastically supported at both ends. Its cross-sectional area and, consequently, its flexural stiffness is in general nonuniform, but symmetric with respect to $x = L/2$. The transverse loading consists of a concentrated load F^* applied through the plane of structural symmetry and a symmetrically

distributed load $Q^*(x)$.

The equilibrium equations for the deformed configuration are obtained within the limitations imposed by the following:

(1) homogeneous and isotropic material obeying a linear constitutive law;

(2) the arch is shallow, $[\frac{dw_o}{dx}]^2 << 1$

(3) the arch is thin, $h << L$;

(4) normals to cross-sections remain normal during deformation;

(5) the load is applied quasi-statically; thus no dynamic response of the structure is accounted for;

(6) the loads and reactions occur in and remain in the plane of deformation.

With reference to Fig. 1, and employing the above assumptions, the following kinematic relations apply (46): when z is measured from a centroidal plane of the arch cross-section,

$$\varepsilon_x = \varepsilon_x^o + z\kappa_x \tag{1}$$

where

$$\varepsilon_x^o = u_{,x} + \tfrac{1}{2}(w_{,x}^2 - w_{o,x}^2) \tag{2}$$

$$\kappa_x = -w_{,xx} + w_{o,xx} \tag{3}$$

Note that the comma denotes differentiation with

respect to the spatial coordinate that follows.

Assuming that the behavior of the material is linearly elastic, one may derive the following expression for the axial load P and the bending moment M*.

$$P = \int_A E\varepsilon_x dA = EA(x)\varepsilon_x^o \tag{4}$$

$$M^* = \int_A zE\varepsilon_x dA = EI(x)\kappa_x \tag{5}$$

The total potential consists of the strain energy (sum of stretching, U_m^*, and bending, U_B^*, energies), the energy stored into the elastic foundation and springs, U_E^*, and the potential of the external forces, U_p^*. Using the shallow arch kinematic relations and linear constitutive relations these energy contributions become

$$U_m^* = \tfrac{1}{2} \int_o^L EA(x)\ \varepsilon_x dx \tag{6}$$

$$U_B^* = \tfrac{1}{2} \int_o^L EI(w_{,xx} - w_{o,xx})^2 dx \tag{7}$$

$$U_E^* = \tfrac{1}{2} \int_o^L \beta^*(w-w_o)^2 dx + \tfrac{1}{2}\alpha_o^*[u(o)^2 + u(L)^2] \tag{8}$$

$$+ \tfrac{1}{2}\beta_o^* \left[[w_{,x}(o)-w_{o,x}(o)]^2 + [w_{,x}(L)-w_{o,x}(L)]^2 \right]$$

$$U_p^* = -\int_o^L [Q^*(x)+F^*\delta(x-\bar{x})]\ (w-w_o)\ dx \tag{9}$$

where $\delta(x-\bar{x})$ is the Dirac-δ function.

It is convenient to nondimensionalize all the parameters according to the following:

$$\xi = \pi\, x/L \;;\; \delta^*(x-L/2) = \rho\delta(\xi - \bar{\xi}) \tag{10}$$

$$\eta(\xi) = w(x)/\rho;\; v(\xi) = u(x)/\rho \;;\; q(\xi) = Q^*/P_E\varepsilon_E$$

$$p = P/P_E \;;\; \beta = (\beta^*/P_E)\,(\tfrac{L}{\pi})^2 \;;\; F = F^*/P_E\varepsilon_E$$

$$M = M^*/\rho P_E \;;\; \alpha_o = (\alpha_o^*/P_E)\,(\tfrac{L}{\pi}) \;;\; \beta_o = \beta_o^*/P_E L$$

$$\rho^2 = I_u/A_u \;;\; P_E = \pi^2 E I_u/L^2 \;;\; \varepsilon_E = (\pi\rho/L)^2$$

$$\bar{A} = A/A_u \;;\; \bar{I} = I/I_u$$

Note that I_u and A_u are the second moment of the area and the area of an equal volume column of length L and radius of gyration, ρ.

On the basis of the nondimensionalized parameters, we have

$$P = \frac{E\varepsilon_E}{2}\, A\left[\frac{2v'}{\varepsilon_E^{1/2}} + (\eta')^2 - (\eta_o')^2\right] \tag{11}$$

$$M^* = -\frac{E\varepsilon_E}{2}\, I\,(\eta'' - \eta_o'') \tag{12}$$

$$U_m^* = P_E\varepsilon_E\,\frac{L}{8\pi}\int_o^{\pi} \bar{A}\left[\frac{2v'}{\varepsilon_E^{1/2}} + (\eta')^2 - (\eta_o')^2\right]^2 d\xi \tag{13}$$

$$U_B^* = P_E \varepsilon_E \frac{L}{2\pi} \int_o^\pi \bar{I}[\eta'' - \eta_o'']^2 \, d\xi \tag{14}$$

$$U_E^* = P_E \varepsilon_E \frac{L}{2\pi} \left[\int_o^\pi \beta(\eta-\eta_o)^2 \, d\xi + \alpha_o \{ v^2(o)+v^2(\pi) \} \right. \tag{15}$$

$$\left. \beta_o \{\eta'(o) - \eta_o'(o)\}^2 + \beta_o \{\eta'(\pi)-\eta_o'(\pi)\}^2 \right]$$

$$U_p^* = P_E \varepsilon_E \frac{L}{\pi} \int_o^\pi [q(\xi) + F\delta(\xi-\bar{\xi})] \, (\eta-\eta_o) \, d\xi \tag{16}$$

where the prime denotes differentiation with respect to ξ. By introducing the nondimensionalized total potential

$$U_T = \frac{4\pi}{P_E \varepsilon_E L} \, U_T^*$$

we have

$$U_T = -2 \int_o^\pi \frac{p^2}{\bar{A}} \, d\xi + 2 \int_o^\pi \bar{I} \, (\eta''-\eta_o'')^2 d\xi \tag{17}$$

$$+ 2\beta \int_o^\pi (\eta-\eta_o)^2 \, d\xi - 4 \int_o^\pi [q(\xi)+F\delta(\xi-\bar{\xi})] \, (\eta-\eta_o) d\xi$$

$$+ 2 \, \alpha_o \{v^2(o) + v^2(\pi)\} + \beta_o \{ \eta_o'(o)-\eta_o'(o)\}^2$$

$$+\beta_o \{\eta'(\pi)-\eta_o'(\pi)\}^2$$

where $$p = \frac{P}{P_E} = \frac{\bar{A}}{2} \left[\frac{2v'}{\varepsilon_E I^2} + (\eta')^2 - (\eta_o')^2 \right] \tag{18}$$

If we let the equilibrium positions be denoted $\hat{v}$ and $\hat{\eta}$ and if we let v and η in Eq. (17) be

$$v = \hat{v} + \varepsilon_1 \zeta \tag{19}$$

$$\eta = \hat{\eta} + \varepsilon_1 \gamma$$

where ε_1 is a small constant, and $\zeta(\xi)$ and $\gamma(\xi)$ are kinematically admissible functions, then

$$\Delta U_T = U_T[\xi, \hat{v}+\varepsilon_1\zeta, \hat{\eta}+\varepsilon_2\gamma] - U_T[\xi, \hat{v}, \eta] \tag{20}$$

$$= \delta^1 U_T + \delta^2 U_T + \text{higher order variations}$$

where $\delta^1 U_T$, $\delta^2 U_T$ etc., are terms in the expansion of Eq. (17) according to powers of ε_1 and denote first, second etc., variations in the total potential.

Use of the principle of the stationary value of the the total potential ($\delta^1 U_T = 0$) and integration by parts leads to the equilibrium equations and associated boundary conditions, which are:

Equilibrium Equations

$$p' = 0 \tag{21}$$

$$[\bar{I}\ (\eta''-\eta_o'')]'' - p\eta'' + \beta(\eta-\eta_o) - q(\xi) - F\delta(\xi-\bar{\xi}) = 0$$

Boundary Conditions

$$p = v(0)\alpha_o \varepsilon_E^{\frac{1}{2}} \; ; \quad \bar{I}(0)[\eta''(0)-\eta_o''(0)] = +\beta_o[\eta'(0)-\eta_o'(0)] \tag{22}$$

$$p = v(\pi)\alpha_o \varepsilon_E^{\frac{1}{2}} \; ; \quad \bar{I}(\pi)[\eta''(\pi)-\eta_o''(\pi)] = -\beta_o[\eta'(\pi)-\eta'(\pi)]$$

The first of Eq. (21) implies that p, the axial thrust, is independent of ξ (constant w.r.t ξ). Furthermore, because of the geometries considered (see Fig. 1)

$$\eta(0) = \eta(\pi) = \gamma(0) = \gamma(\pi) = 0$$

Next, if we return to the expression for p, we have

$$\frac{p}{\bar{A}(\xi)} = \tfrac{1}{2}\left[\frac{2v'}{\varepsilon_E^{\frac{1}{2}}} + (\eta')^2 - (\eta_o')^2\right] \tag{23}$$

Integration from 0 to π, since p is constant, yields

$$p\int_o^\pi \frac{d\xi}{\bar{A}(\xi)} = \frac{1}{\varepsilon_E^{\frac{1}{2}}}\int_o^\pi v'd\xi + \tfrac{1}{2}\int_o^\pi [(\eta')^2 - (\eta_o')^2]\, d\xi \tag{24}$$

$$= \frac{1}{\varepsilon_E^{\frac{1}{2}}}[v(\pi)-v(0)] + \tfrac{1}{2}\int_o^\pi [(\eta')^2 - (\eta_o')^2]d\xi$$

Expressing the boundary conditions on $v(\xi)$ in terms of p from Eq. (22) yields

$$p = 1/2 \quad \frac{\int_o^{\pi} [(\eta')^2 - (\eta')^2]d\xi}{\left[\int_o^{\pi} \frac{d\xi}{\bar{A}(\xi)} + \frac{2}{\varepsilon_E \alpha_o}\right]} \tag{25}$$

From the same in-plane boundary conditions we obtain that

$$\alpha_o v^2(\pi) = \frac{p^2}{\alpha_o \varepsilon_E} \; ; \quad \alpha_o v^2(0) = \frac{p^2}{\alpha_o \varepsilon_E} \tag{26}$$

This allows us to express the total potential (at equilibrium positions) solely in terms of η, its space-dependent derivatives and the structural geometry.

$$U_T = J \left[\int_o^{\pi} [(\eta')^2 - (\eta_o')^2]d\xi\right]^2 + 2\int_o^{\pi} \bar{I}(\eta'' - \eta_o'')^2 d\xi \tag{27}$$

$$+ 2\beta \int_o^{\pi} (\eta - \eta_o)^2 \, d\xi - 4\int_o^{\pi} [q(\xi) + F\delta(\xi - \bar{\xi})](\eta - \eta_o)]d\xi$$

$$+ 2\beta_o \left[\{\eta'(0) - \eta_o'(0)\}^2 + \{\eta'(\pi) - \eta_o'(\pi)\}^2\right]$$

where $J = \frac{1}{2} \Big/ \left[\int_o^{\pi} \frac{d\xi}{\bar{A}} + \frac{2}{\varepsilon_E \alpha_o}\right]$ (28)

Again, as before, if we let $\hat{\eta}$ denote equilibrium positions and let $\eta = \hat{\eta} + \varepsilon_2 \gamma$, substitute this into Eq. (27)

and obtain the first, second, etc., variations according to the powers of ε_2 we have

$$\Delta U_T = \delta^1 U_T + \delta^2 U_T + \text{etc.}$$

where
$$\frac{\delta^2 U_T}{2\varepsilon_2^2} \equiv V[\xi,\hat{\eta}] = p\int_0^{\pi}(\gamma')^2 d\xi + 2J\left[\int_0^{\pi}\hat{\eta}'\gamma' d\xi\right]^2 \qquad (29)$$
$$+ \beta\int_0^{\pi}\gamma^2 d\xi + \int_0^{\pi}\bar{I}\,(\gamma'')^2 d\xi$$
$$+ \beta_0[\gamma'(0)^2 + \gamma'(\pi)^2]$$

Note that the vanishing of the first variation leads to the same equilibrium equation [second of Eqs. (21)] and corresponding boundary conditions, as before.

According to the energy criterion for stability, when the buckling load is reached the second variation becomes positive semi-definite. In other words, for at least one non-trivial displacement $\gamma(\xi)$, $\delta^2 U_T$ has a minimum value of zero. Trefftz observed that the conditions that $\delta^2 U_T$ have a non-trivial minimum are that the equation $\delta[\delta^2 U_T]=0$ be satisfied for at least one non-trivial $\gamma(\xi)$. This is applicable to both manners by which the primary path can become unstable (existence of limit point as well as of bifurcation point). Thus, at the critical point the first variation, with respect to γ, of the second variation of the

total potential, Eq. (29), must vanish.

Letting $\hat{\gamma}$ denote the nontrivial buckled mode and expressing $\gamma = \hat{\gamma} + \varepsilon_3\theta$ in Eq. (29), we obtain,

$$\Delta V = V[\xi, \hat{\eta}, \hat{\gamma}+\varepsilon_3\theta] - V[\xi, \hat{\eta}, \hat{\gamma}] \tag{30}$$

$$= \delta^1 V + \delta^2 V + \text{higher order variations}$$

$$\text{where} \quad \delta^1 V = 2\varepsilon_3 \left[p \int_o^\pi \hat{\gamma}'\theta' d\xi + 2J \int_o^\pi \hat{\eta}'\hat{\gamma}' d\xi \int_o^\pi \hat{\eta}'\theta' d\xi \right. \tag{31}$$

$$+ \beta \int_o^\pi \hat{\gamma}\theta d\xi + \int_o^\pi \bar{I}\hat{\gamma}''\theta'' d\xi$$

$$\left. + \beta_o (\hat{\gamma}'\theta')_o + \beta_o (\hat{\gamma}'\theta')_\pi \right]$$

Integration by parts and use of the admissibility conditions on $\hat{\gamma}$ and θ lead to the following differential equation (necessary condition on $\hat{\gamma}$ at q_{cr}) and boundary conditions. (omitting $\hat{}$ on γ)

$$[\bar{I}(\xi)\gamma''(\xi)]'' - p\gamma'' + 2J\eta'' \int_o^\pi \eta''\gamma d\xi + \beta\gamma = 0 \tag{32}$$

$$\beta_o \gamma' = \bar{I}\gamma'' \quad \text{at } \xi = 0 \tag{33}$$

$$\beta_o \gamma' = -\bar{I}\gamma'' \quad \text{at } \xi = \pi$$

Also, because of the admissibility condition on γ

$$\gamma(0) = \gamma(\pi) = 0$$

Through this approach $\gamma(\xi)$ actually denotes the buckling modes at a critical point of the primary equilibrium path, while $\eta(\xi)$ need only represent the primary equilibirum path (symmetric response of the arch).

In summary, the field equations for the general symmetric arch are:

Equilibrium Equation

$$[I(\eta''-\eta_o'')]'' - p\eta'' + \beta(\eta-\eta_o) = q(\xi) + F\delta(\xi-\bar{\xi}) \qquad (21)$$

Boundary Conditions in η

$$\eta(0) = \eta(\pi) = 0 \qquad (22)$$

$$\bar{I}(0)[\eta''(0)-\eta_o''(0)] = \beta_o[\eta'(0)-\eta_o'(0)]$$

$$\bar{I}(\pi)[\eta''(\pi)-\eta_o''(\pi)] = -\beta_o[\eta'(\pi)-\eta_o'(\pi)]$$

Buckling Equation

$$[\bar{I}(\xi)\gamma''(\xi)]'' - p\gamma'' + 2J\eta''\int_o^\pi \eta''\gamma d\xi + \beta\gamma = 0 \qquad (32)$$

Boundary Conditions in γ

$$\gamma(0) = \gamma(\pi) = 0 \tag{33}$$

$$\bar{I}(0)\gamma''(0) = \beta_o \gamma'(0)$$

$$\bar{I}(\pi)\gamma''(\pi) = -\beta_o \gamma'(\pi)$$

where p and J are given by Eqs. (25) and (28), respectively. The simultaneous solution of the field equations yields the primary equilibrium path at the critical load η, the critical load parameters $[Q_{cr}, p_{cr}]$ for any load distribution, and the shape of the buckled mode γ. As reported in Ref.(10) and outlined in Appendix A, numerous examples are presented for which the critical conditions for a uniform arch are determined utilizing for the bifurcation problem the direct solution of Eq. (32). For the snapping problem, two methods are demonstrated: (1) combining Eqs. (21) and (32) at the midpoint $\xi = \pi/2$ or (2) utilizing as the buckling criterion the vanishing of the second variation of the total potential. The finite element formulation to follow and the solution methodology presented in the next chapter will rely for the limit point analysis upon method two above, primarily because of numerical simplicity. (Refer to Appendix B for details of the finite element discretization).

It is convenient to express the total potential, Eq. (27) in terms of displacement $y(\xi)$ by letting $y(\xi)=\eta(\xi)-\eta_o(\xi)$. Thus obtaining

$$U_T[y] = J\left[\int_o^\pi (y'^2 + 2y'\eta_o')d\xi\right] + 2\beta\int_o^\pi y^2 d\xi \quad (34)$$
$$+ 2\int_o^\pi \bar{I}(y'')^2 d\xi - 4\int_o^\pi [q(\xi) + F\delta(\xi-\bar{\xi})]y d\xi$$
$$+ 2\beta_o\{y'(0)^2 + y'(\pi)^2\}$$

By discretizing the continuous system into m elements and assuming a displacement function for an arbitrary element in the form of a cubic, one may express the displacement in the i^{th} element in terms of the generalized coordinates a_i as,

$$y^i(\xi) = a_0 + a_1\xi + a_2\xi^2 + a_3\xi^3 = \underline{L}^T\underline{a} \quad (35)$$

Letting the vector of generalized nodal degrees of freedom be $\underline{u}$ and interpolating the element displacement function in terms of its nodal values of displacement and rotation, one obtains

$$y^i(\xi) = \underline{L}^T{}_i\underline{\underline{B}}_i{}^{-1}\underline{u}_i \quad (36)$$

where matrix $\underline{\underline{B}}_i$ is a 4 x 4 relating the $\underline{a}_i$ to the $\underline{u}_i$.

Using Eq. (36) in Eq. (34), performing the appropriate

element integrations and summing over the m elements, one obtains the following matrix representation for the total potential U_T:

$$U_T[\underline{u}] = J[\underline{u}^T \underline{\underline{K}}_2 \underline{u} + 2\underline{V}_6^T \underline{u}]^2 + 2\beta \underline{u}^T \underline{\underline{K}}_3 \underline{u} \tag{37}$$

$$+ 2\underline{u}^T \underline{\underline{K}}_1 \underline{u} - 4Q\underline{V}_5^T \underline{u} + 2\beta_o \underline{u}^T \underline{\underline{R}} \underline{u}$$

In obtaining Eq. (37) from Eq. (34) the load $q(\xi)$ was expressed as $QN(\xi)$, where $N(\xi)$ is some specified symmetric load distribution. The initial configuration $\eta_o(\xi)$ was expressed as $e\bar{\eta}_o(\xi)$ where $\bar{\eta}_o(\xi)$ is some specified symmetric initial shape function.

Likewise, we may express the definition of p, Eq. (25), as

$$\bar{p} = -J[\underline{u}^T \underline{\underline{K}}_2 \underline{u} + 2\underline{V}_6^T \underline{u}]. \tag{38}$$

Now Eqs. (37) and (38) are the fundamental relations from which the field equations will be derived. Expanding $U_T(\underline{u})$ about some arbitrary vector $\varepsilon \underline{v}$ obtain

$$\Delta U_T[\underline{u},\underline{v}] = \delta^1 U_T[\underline{u},\underline{v}] + \delta^2 U_T[\underline{u},\underline{v}] + \text{higher order terms}$$

Setting $\delta^1 U_T(\underline{u},\underline{v}) = 0$ for arbitrary non-trivial $\underline{v}$ we obtain

$$[\underline{\underline{K}}_1 - \bar{p}\underline{\underline{K}}_2 + \beta \underline{\underline{K}}_3 + \beta_o \underline{\underline{R}}]\underline{u} = \bar{p}\underline{V}_6 + Q\underline{V}_5 \tag{39}$$

The equilibrium configuration given by Eqs. (38) and (39) reaches a critical state in accordance with Trefftz' interpretation of the energy criterion for stability whenever the second variation is stationary for non-trivial $\underline{v}$.

Let
$$V(\underline{v}) = \delta^2 U_T(\underline{v}) \tag{40}$$

setting $\delta^1 V(\underline{\theta},\underline{v}) = 0$ for arbitrary non-trivial $\underline{\theta}$, the buckling equations representing the discrete analog to Eq. (32) are

$$[\underline{\underline{K}}_1 - \bar{p}\underline{\underline{K}}_2 + \beta\underline{\underline{K}}_3 + \beta_o\underline{\underline{R}} + \underline{\underline{K}}_{NL}(\underline{u})]\underline{v} = 0 \tag{41}$$

$$\underline{\underline{K}}_{NL}(\underline{u}) \equiv 2J[\underline{\underline{K}}_2\underline{u}\underline{u}^T\underline{\underline{K}}_2 + \underline{\underline{K}}_2\underline{u}\underline{V}_6^T + \underline{V}_6^T\underline{u}\underline{\underline{K}}_2 + \underline{V}_6\underline{V}_6^T]$$

An alternative, but theoretically equivalent, [see Ref. (49)] statement of the instability criterion is to require the second variation to vanish at both the limit point as well as bifurcation point. This yields the following expression:

$$\underline{v}^T[\underline{\underline{K}}_1 - \bar{p}\underline{\underline{K}}_2 + \beta\underline{\underline{K}}_3 + \beta_o\underline{\underline{R}} + 2J\{\underline{\underline{K}}_2\underline{u}\underline{u}^T\underline{\underline{K}}_2 + 2\underline{\underline{K}}_2\underline{u}\underline{V}_6^T + \underline{V}_6\underline{V}_6^T\}]\underline{v} = 0 \tag{42}$$

The simultaneous solution of Eqs. (38) and (39) and either (41) or (42) yields those load conditions at which the arch becomes unstable. In other words, for some externally applied load Q, there is an internal reaction $\bar{p}$ and a

displacement $\underline{u}$ such that the coefficient matrix of Eq. (41) is singular or Eq. (42) vanishes for non-trivial buckling mode shape $\underline{v}$. The solution methodology for each type of instability will be developed in detail in the next chapter.

The solution to the buckling problem for any set of system parameters can be greatly simplified by specifying apriori the mode shape $\underline{v}$ (or γ) as being either symmetric (in the case of limit point), or anti-symmetric (unstable bifurcation) with respect to the pre-buckled equilibrium displacement field $\underline{u}$ (or y). This is accomplished in the following manner. During the quasi-static loading process, the pre-buckled deformation is symmetric about the mid-line $\xi = \pi/2$. At the point of incipient bifurcation, Hoff and Bruce (35) have shown that the buckled mode $\gamma(\xi)$ is anti-symmetric with respect to $\xi = \pi/2$, hence, the orthogonality of $\gamma(\xi)$ and $\eta(\xi)$ causes the integral in the buckling equation (32) (or similarly $\underline{\underline{K}}_{NL}\underline{v}$) to vanish when $\bar{p} = \bar{p}_{cr}$, and $Q = Q_{cr}$. Imposing this condition apriori reduces the determination of the critical internal thrust $\bar{p}$ to an eigenvalue analysis utilizing either the discrete or continuous formulations given by Eqs. (41) or (32) respectively.

In the case of limit point instability, the symmetric buckled mode $\underline{v}$ and the symmetric primary path $\underline{u}$ are assumed to be related by $\underline{v} = c\underline{u}$ for some constant c at the critical point. The buckling criterion for this case is then obtained from (42) as

$$\underline{u}^T[K_1 - \bar{p}K_2 + \beta K_3 + \beta_o R + \underline{\underline{K}}_{NL}(\underline{u})]\underline{u} = 0$$

Utilizing this modified version of the buckling condition in the simultaneous solution with Eqs. (38) and (39) provides a simple, direct and efficient means for finding the limit point critical conditions for any inertia distribution and set of system parameters.

At this point we have obtained in discretized form the necessary equations which describe the arch in its buckled state (either limit point or unstable bifurcation) for arbitrary condition of geometry, loading and boundary restraint.

Upon development of the optimality criteria in the next section, a complete set of equations will have been derived, the solution of which yields the optimum design and associated critical conditions.

2.2 Development of Optimality Criteria

The solutions obtained for the foregoing system of governing equations by either formulation require specification of the inertia (or area) distribution as well as a set of system parameters. Extensive experience (App. A) indicates the validity of the following assertion: namely, that the axial force $\bar{p}$ increases monotonically with increasing applied lateral load values, Q, on the primary equilibrium path.

Thus, one can examine the second variation of U_T, (Eq. (29), in terms of displacement) and at the critical point, $\delta^2 U_T(\hat{\gamma}) = 0$, obtain the following representation for the

critical value of $\bar{p}$:

$$\bar{p}_{cr} = \frac{2J\left[\int_o^\pi (y'+\eta_o')\gamma' d\xi\right]^2 + \int_o^\pi \bar{I}(\gamma'')^2 d\xi + \beta \int_o^\pi \gamma^2 d\xi + R(\beta_o)}{\int_o^\pi (\gamma')^2 d\xi} \qquad (43)$$

where, $$R(\beta_o) \equiv \beta_o \left[\gamma'(0)^2 + \gamma'(\pi)\right]^2$$

$$y(\xi) \equiv \eta(\xi) - \eta_o(\xi)$$

and $y(\xi)$ and $\gamma(\xi)$ are respectively the primary equilibrium path transverse displacement and buckling mode [solutions of Eqs. (21) and (32) at the critical loading condition $\{Q_{cr}, P_{cr}\}$]. Recalling the functional relationship between J, and $A(\xi)$, Eq. (28), and considering those cross sections for which the inertia-area relation is of the form $I = \bar{\rho}A^n$, $\bar{\rho}$ = constant and n = 1, 2, or 3, one seeks for a given loading, initial shape and boundary conditions, that geometry given by $\{I(\xi), J(I)\}$ such that $\bar{p}_{cr}$ and thus Q_{cr} is a maximum (for arches of the same volume). A necessary condition for $\bar{p}_{cr}[I]$ to be a maximum with respect to arbitrary variations in $I(\xi)$ subject to the constant volume integral constraint is for the augmented functional to become stationary. This functional is given by:

$$\bar{p}^*_{cr} = \bar{p}_{cr} - \lambda\left[\int_o^\pi A(\xi)d\xi - \bar{v}\right] \qquad (44)$$

where $\bar{v}$ is a specified volume, $\bar{p}_{cr}$ is given by Eq. (43), and λ is a Lagrange multiplier. Equating the first variation of $\bar{p}^*_{cr}$ with respect to changes in inertia, $\delta_I \bar{p}^*_{cr}$, to zero one obtains the following optimality condition:

$$\frac{1}{A(\xi)}\left[2J\int_0^{\pi}(\hat{y}'' + \eta_o'')\hat{\gamma}d\xi\right]^2 + nI(\xi)\left[\hat{\gamma}(\xi)''\right]^2 = \gamma\int_0^{\pi}(\hat{\gamma}')^2 d\xi A(\xi) \quad (45)$$

This integro-differential equation relates the optimum shape $I_{opt}(\xi)$ to the primary path response $\hat{y}(\xi)$, the initial symmetric shape $\eta_o(\xi)$, and the buckled mode $\hat{\gamma}(\xi)$. Furthermore, it is easily shown that $\bar{p}^*_{cr}$ and thus $\bar{p}_{cr}$ are stationary with respect to the buckled mode $\hat{\gamma}(\xi)$, since in accordance with Trefftz' criterion, $\hat{\gamma}(\xi)$ is a non-trivial solution of Eq. (32), obtained through the extremization of the second variation of the total potential, U_T.

One can specialize the optimality criterion Eq. (45), for those buckled mode shapes $\hat{\gamma}(\xi)$ which are either symmetric, corresponding to limit point instability, or anti-symmetric, corresponding to unstable bifurcation. In the former case, the form of Eq. (45) does not change while in the latter the criterion becomes

$$A^{n-1}(\xi)(\hat{\gamma}'')^2 = \text{constant} \quad (46)$$

The vanishing of the integral in Eq. (45), in effect, has negated the dependence of the optimum shape upon the prebuckled

shape $y(\xi)$ and the initial shape $\eta_o(\xi)$. This representation has been developed and utilized by Prager and Taylor (13) and many others (see Refs. 5, 6, and 18).

In summary, the governing equations which upon solution yield the optimum geometry and the associated critical condition for arbitrary loading, initial shape and boundary conditions are the following:

Unstable Bifurcation: (anti-symmetric mode buckling)

A. Equilibrium condition (primary path)

$$[\underline{\underline{K}}_1 - \bar{p}\underline{\underline{K}}_2 + \beta\underline{\underline{K}}_3 + \beta_o\underline{\underline{R}}]\underline{u} = \bar{p}\underline{V}_6 + Q\underline{V}_5 \tag{39}$$

$$\bar{p} = -J[\underline{u}^T\underline{\underline{K}}_2\underline{u} + 2\underline{V}_6^T\underline{u}] \tag{38}$$

B. Buckling condition:

$$[\underline{\underline{K}}_1 - \bar{p}\underline{\underline{K}}_2 + \beta\underline{\underline{K}}_3 + \beta_o\underline{\underline{R}}]\underline{v} = \underline{0} \tag{41}$$

C. Optimality criterion: (continuous form)

$$[A(\xi)]^{n-1}\,[\gamma''(\xi)]^2 = \text{constant} \tag{46}$$

Limit Point Instability: (symmetric mode snapping)

D. Equilibrium conditions: (primary path)

$$[\underline{\underline{K}}_1 - \bar{p}\underline{\underline{K}}_2 + \beta K_3 + \beta_o \underline{\underline{R}}]\underline{u} = \bar{p}\underline{V}_6 + Q\underline{V}_5 \tag{39}$$

$$\bar{p} = -J[\underline{u}^T \underline{\underline{K}}_2 \underline{u} + 2\underline{V}_6^T \underline{u}] \tag{38}$$

E. Buckling Condition:

$$\underline{u}^T[\underline{\underline{K}}_1 - \bar{p}\underline{\underline{K}}_2 + \beta\underline{\underline{K}}_3 + \beta_o \underline{\underline{R}} + \underline{\underline{K}}_{nL}]\underline{u} = 0 \tag{42}$$

$$\underline{\underline{K}}_{nL} = 2J[\underline{\underline{K}}_2 \underline{u}\underline{u}^T \underline{\underline{K}}_2 + 2\underline{\underline{K}}_2 \underline{u}\underline{V}_6^T + \underline{V}_6 \underline{V}_6^T]$$

assuming $\underline{u}$ and $\underline{v}$ are related by $\underline{u} = c\underline{v}$

F. Optimality Criterion: (continuous form)

$$\frac{1}{A(\xi)}\left[2J\int_o^\pi (\hat{y}'' + \eta_o'')\hat{\gamma}\,d\xi\right]^2 + n\bar{I}(\xi)\left[\hat{\gamma}''(\xi)\right]^2 \tag{45}$$

$$= [\lambda \int_o^\pi (\gamma')^2 d\xi]A(\xi)$$

During the solution process the coefficient matrix in Eq. (41) is assembled on the basis that $\underline{v}$ is anti-symmetric, while the coefficient matrix of Eq. (39), although appearing the same, is assembled on the basis that $\underline{u}$ is symmetric. Thus, at $\bar{p} = \bar{p}_{cr}$ Eq. (41) is singular while Eq. (39) is not.

CHAPTER III

SOLUTION PROCEDURE

In the previous chapter, all the necessary equations were derived governing the solution for the optimum shape using both an anlytic as well as a discretized approach via the finite element formulation. The analytic formulation was presented to clarify the finite element analog, whereas the finite element system of equations will actually be developed further and used in a computer program (see Appendix D) to yield optimum designs.

The optimization process is quite naturally divided into discrete stages for a given set of system parameters, namely

(a) For a given initial design, a buckling analysis is performed yielding the critical conditions and the buckling mode.

(b) The critical conditions are then used in conjunction with the optimality criterion to generate a better design.

Such an analysis-synthesis process is used by practically all investigators who employ an optimality criterion approach. The synthesis process, step (b) above, depends upon the formulation of a workable process for incorporating the requirements of the previously derived optimality

criterion, Eq. (45). In the next section, the discretized versions of Eq. (45) will be obtained for both symmetric (limit point) and anti-symmetric (unstable bifurcation) mode instability.

3.1 Energy Interpretation of the Optimality Criterion

In order to systematically produce an optimum design for a given set of system parameters, an iterative technique is employed whereby the general optimality criterion, Eq. (45) is subjected to an energy interpretation. On the basis of this interpretation, iterative relations are formulated which are used to produce stronger designs. By integrating Eq. (45) over the entire length and over the length of the i^{th} element respectively, one obtains,

$$\frac{U^I}{\bar{v}} + n\,\frac{U^B}{\bar{v}} = \text{constant} = c^2 \tag{47}$$

and

$$\frac{JU^I}{J_i\bar{v}_i} + n\,\frac{U_i^B}{\bar{v}_i} = \text{constant} = c^2 \tag{48}$$

where

$$U^B = \int_o^\pi I(\gamma'')^2 d\xi = \underline{v}^T \underline{\underline{K}}_1 \underline{v}$$

$$U^I = 2J\left\{\int_o^\pi (y''+\eta_o'')\gamma d\xi\right\}^2 = 2J[\underline{u}^T \underline{\underline{K}}_2 \underline{u} + \underline{V}_6^T \underline{u}]^2$$

and $$J_i = \frac{A_i}{2L_i}$$

The energy term U^I is defined as interaction energy since from the second variation of U_T it can be interpreted as that additional energy term resulting from the interaction of the axial deformation with the curvature changes during the buckling process. Furthermore, note that this term vanishes in the case of bifurcation through an anti-symmetric mode since the buckled mode $\gamma(\xi)$ is orthogonal to the primary path $y(\xi)$ and $\eta_o(\xi)$.

The optimality criterion, as expressed by Eqs. (47) and (48), can be written in terms of the critical energy H, that is the energy state expressed in terms of deformation $\underline{v}$, $\underline{u}$ existing at the point of instability; namely

$$\frac{H}{\bar{v}} = c^2 \tag{49}$$

where $$H = U^I + nU^B$$

and $$\frac{H_i}{\bar{v}_i} = c^2 \tag{50}$$

where $$H_i = \frac{JU^I}{J_i} + nU_i^B$$

The above expressions of optimality can be interpreted as statements that in the optimum configuration, the critical

energy density in each element is a constant, that constant being the average critical energy density for the arch. Such energy interpretations of optimality have been used extensively by Venkayya and others (15, 18) for many structural systems. Also, Simitses, Kamat and Smith (6) used a similar interpretation for column buckling in which case the interaction energy term U^I did not occur, reducing the critical energy to just the bending term U^B.

Development of the Redesign Algorithm:

Suppose for some inertia distribution I^j, during the j^{th} iteration, one obtains the critical loading condition either by a bifurcation analysis [Eqs. (38), (39), (41)] or a limit point analysis [Eqs. (38), (39), (42)], checks the optimality criterion [Eqs. (49), (50)] and it is not satisfied; that is, the energy density is not the same for all elements. It then becomes necessary to redistribute the inertia so that for the next iteration $(j + 1)^{st}$, the energy distribution is more uniform. This requirement is expressed as follows,

$$\left\{\frac{H_i}{\bar{v}_i}\right\}^{j+1} = C^{j+1}\,\frac{H}{\bar{v}} \tag{51}$$

or,
$$\left\{\frac{H_i{}^{j+1}}{H_i{}^{j}}\right\}\left\{\frac{\bar{v}_i{}^{j}}{\bar{v}_i{}^{j+1}}\right\} = b^{j+1}\left\{\frac{H}{\bar{v}}\right\}^{j} \div \left\{\frac{H_i}{\bar{v}_i}\right\}^{j}$$

From the inertia-area relation, $I = \bar{\rho}A^n$, the ratio of

element volumes $\bar{v}_i$ for two successive iterations can be expressed as

$$\frac{\bar{v}_i^{\,j+1}}{\bar{v}_i^{\,j}} = \left\{\frac{I_i^{\,j+1}}{I_i^{\,j}}\right\}^{1/n} \qquad n=1,2,3 \tag{52}$$

If the inertia is reduced under the given load, one would expect an increase in the amount of stored bending energy. Moreover, if the area is reduced under a given load, one would expect a change in the stress (and strain) state to produce an increase in the interaction energy, $U_i^I = \frac{JU^I}{J_i}$, since from Eq. (28) J_i is directly proportional to A_i. Therefore, the critical energy, H_i, in any element may be expressed as inversely proportional to I_i, such that one may write for any iteration j,

$$H_i = \left\{\frac{1}{I_i}\right\}^{\alpha} \tag{53}$$

or

$$\frac{H_i^{\,j+1}}{H_i^{\,j}} = \left\{\frac{I_i^{\,j}}{I_i^{\,j+1}}\right\}^{\alpha} \qquad \alpha=\text{constant} > 0 \qquad i=1,2\ldots m$$

Using (52) and (53) in (51) one obtains the following recurrence relation for the redistribution of the inertia based upon the prevailing critical energy density and geometry:

$$I_i^{j+1} = b^{j+1} \left[\frac{H_i^j / \bar{v}_i^j}{H^j/\bar{v}} \right]^{\frac{n}{n\alpha+1}} \qquad (54)$$

$$i = 1,\ldots m$$

$$n = 1,2, \text{ or } 3$$

The constant b^{j+1} can be found during each iteration by imposing the volume constraint:

$$\sum_{i=1}^{m} \int_{\text{element}} \left\{ \frac{I_i}{\bar{\rho}} \right\}^{\frac{1}{n}} d\xi_i = \bar{v}$$

$$\xi_{i-1} \leq \xi_i \leq \xi_{i+1}$$

The parameter α in Eq. (54) effectively controls the rate at which the inertia is redistributed. Further discussion will be made when results are presented, and in Appendix D.

In summary, for the case of unstable bifurcation for which the buckling mode is orthogonal to the primary path equilibrium response, the critical energy reduces to

$$H = U^B \qquad (55)$$

and the recurrence relation, Eq. (54), is expressed solely in terms of the bending energy as

$$I_i^{j+1} = b^{j+1} \left\{ \frac{\left(U_i^B/\bar{v}_i\right)^j}{(U^B)^j/\bar{v}} \right\}^{\frac{n}{n\alpha+1}} \tag{56}$$

For the case of limit point instability, the critical energy retains the interaction term and is given by Eqs. (49) and (50). The recurrence relation is given by Eq. (54).

3.2 Optimization for Anti-symmetric Modes:

For the case of bifurcation the buckling mode shape, $\gamma(\xi)$, in Eqs. (32) or (29) is orthogonal to the symmetric pre-buckled configuration, $\eta(\xi)$, and hence the integral vanishes yielding the eigen system

$$[\bar{I}(\xi)\gamma''(\xi)]'' + \bar{p}\gamma''(\xi) = 0$$

subject to the following boundary and symmetry conditions:

$$\gamma(0) = \gamma(\pi/2) = 0$$

$$\bar{I}(0)\gamma''(0) - \beta_o\gamma'(0) = \gamma'''(\pi/2) = 0$$

The lowest positive eigenvalue corresponds to $\bar{p}_{cr}$. Analogously, one may seek the lowest positive eigenvalue for a given inertia distribution and elastic constants of the following discrete system,

$$[\underline{\underline{K}}_1 - \bar{p}\underline{\underline{K}}_2 + \beta\underline{\underline{K}}_3 + \beta_o\underline{\underline{R}}]\underline{v} = \underline{0} \tag{57}$$

where anti-symmetry of $\underline{v}$ has been imposed through the appropriate transformation of the coefficient matrix during its assembly. Upon obtaining $\bar{p}_{cr} = \min\{\bar{p}\}$, one may return to the equilibrium equation, Eq. (39) with $\bar{p} = \bar{p}_{cr}$ and express the equilibrium solution explicitly in terms of the magnitude of the critical lateral load Q_{cr}, the given load distribution $N(\xi)$ through $\underline{V}_5$, and the given initial shape function $\bar{\eta}_o(\xi)$ through $\underline{V}_6$ as

$$\underline{u} = [\underline{\underline{K}}^*(\bar{p}_{cr})]\ [\bar{p}_{cr}\underline{V}_6 + Q_{cr}\underline{V}_5] \tag{58}$$

$$\underline{\underline{K}}^*(\bar{p}_{cr}) \equiv [\underline{\underline{K}}_1 - \bar{p}_{cr}\underline{\underline{K}}_2 + \beta\underline{\underline{K}}_3 + \beta_o\underline{\underline{R}}]^{-1}$$

Even though the coefficient matrices of Eqs. (57) and (39) are of the same general form, $\underline{\underline{K}}^*[\bar{p}_{cr}]$ exists since the elements of Eq. (39) include the fact that $\underline{u}$ is symmetric while the elements of Eq. (57) reflect the anti-symmetry of $\underline{v}$. For further details regarding the appropriate transformations the reader is referred to Appendix B.

The equilibrium configuration $\underline{u}$ must also satisfy Eq. (38) at $\bar{p} = \bar{p}_{cr}$. By eliminating $\underline{u}$ between Eqs. (58) and (38), an explicit relationship can be obtained relating the magnitude of the critical load Q to the set of system parameters. This expression, referred to as the $(\bar{p},Q)$ relation, is

$$Q^2 f_1(\bar{p}) + Q f_2(\bar{p},e) + f_3(\bar{p},e) = 0 \tag{59}$$

where $f_1(\bar{p}) = \underline{V}_5^T \underline{\underline{K}}^* \underline{\underline{K}}_2 \underline{\underline{K}}^* \underline{V}_5$

$$f_2(\bar{p},e) = 2e[\underline{V}_6^T(\bar{p}\underline{\underline{K}}^* \underline{\underline{K}}_2 \underline{\underline{K}}^* + \underline{\underline{K}}^*)\underline{V}_5]$$

$$f_3(\bar{p},e) = (\bar{p}e)^2 \underline{V}_6^T \underline{\underline{K}}^* \underline{\underline{K}}_2 \underline{\underline{K}}^* \underline{V}_6 + 2\bar{p}e^2 \underline{V}_6^T \underline{\underline{K}}^* \underline{V}_6 + \frac{\bar{p}}{J}$$

Note that for a given design one can easily plot the load deflection curve by iterating on $\bar{p} > 0$ in Eq. (59), solving for two values of Q and computing the corresponding characteristic deflection from Eq. (58). For the particular value of $\bar{p}$ corresponding to the lowest positive eigenvalue of Eq. (57), which for the case of unstable bifurcation is independent of the initial configuration, Eq. (59), becomes

$$Q_{cr}^2 f_1(\bar{p}_{cr}) + Q_{cr} f_2(\bar{p}_{cr},e) + f_3(\bar{p}_{cr},e) = 0 \tag{60}$$

which yields the required relationship between the critical load Q_{cr} and the rise parameter, e.

In summary, for the case in which instability occurs through an anti-symmetric mode (bifurcation), the solution for the strongest arch among those of equal volume $\bar{v}$, can be produced by a systematic application of the following general procedure for a given set of system parameters:

1. By specifying boundary conditions and the anti-symmetry of the buckled mode $\underline{v}$ and given some arbitrary initial m-dimensional inertia vector, assembly of the relevant matrices in Eq. (57) can be made.

2. Eq. (57) is then solved for the lowest eigenvalue $\bar{p}_{cr}$ and the associated displacement vector $\underline{v}$.

3. The critical energy density distribution H_i/v_i is computed, which for this case is U_i^B/v_i.

4. In the event U_i^B/v_i is <u>not</u> uniform, Eq. (56) is utilized to redistribute the inertia among those elements which have not violated a constraint on the inertia (or area). Steps 2, 3, 4 are repeated until energy convergence is obtained, at which point the inertia distribution is optimum.

5. Once $\{I, \bar{p}_{cr}\}_{opt}$ have been determined through the above iterative process, the corresponding lateral destabilizing load Q_{cr} can be found from Eq. (60) as a function of initial configuration $\eta(\xi)$ and load distribution $N(\xi)$. The scalar coefficients of Eq. (60) are formed on the basis of the <u>symmetric</u> assembly of the relevant matrices since the equilibrium configuration $\underline{u}$ from Eq. (39) is symmetric.

3.3 Optimization for Symmetric Modes

In order to solve the optimization problem subject to the restriction of symmetric mode instability, first a consideration will be given to the buckling analysis methodology. The governing equations summarized below are:

Equilibrium:

$$[\underline{\underline{K}}_1 - \bar{p}\underline{\underline{K}}_2 + \beta\underline{\underline{K}}_3 + \beta_o\underline{\underline{R}}]\underline{u} = \bar{p}\underline{V}_6 + Q\underline{V}_5 \tag{39}$$

$\bar{P}$-Q Relation:

$$\underline{u}^T\underline{\underline{K}}_2\underline{u} + 2\underline{V}_6{}^T\underline{u} + \bar{p}/_J = 0 \tag{38}$$

Buckling Criterion:

$$\underline{v}^T[\underline{\underline{K}}_1 - \bar{p}\underline{\underline{K}}_2 + \beta\underline{\underline{K}}_3 + \beta_o\underline{\underline{R}}]\underline{v} \tag{42}$$

$$+ 2J\underline{v}^T[\underline{\underline{K}}_2\underline{u}\underline{u}^T\underline{\underline{K}}_2 + 2\underline{\underline{K}}_2\underline{V}_6{}^T\underline{u} + \underline{V}_6\underline{V}_6{}^T]\underline{v} = 0$$

The simultaneous satisfaction of the above relations characterize the solution at the limit point for a given geometry. By explicitly solving for $\underline{u}$ from Eq. (39) and eliminating $\underline{u}$ from Eqs. (38) and (42), one obtains the following two algebraic equations relating the internal thrust $\bar{p}$ with the externally applied lateral load Q.

Using Eq. (39) in (38) we obtain as before Eq. (59) which is independent of the buckled mode $\underline{v}$, namely

$$Q^2 f_1(\bar{p}) + Q f_2(\bar{p},e) + f_3(\bar{p},e) = 0 \tag{49}$$

where the scalar coefficients are as previously defined.

Furthermore, by noting that just prior to snapping the displacement $\underline{u}$ is symmetric, at the load level for which snapping occurs through a symmetric mode the buckled mode $\underline{v}$ and the equilibrium solution $\underline{u}$ are approximately related by $\underline{v} = c\,\underline{u}$ for some constant c. Equation (39) can then be used to eliminate $\underline{u}$ from Eq. (42) yielding a fourth order algebraic equation in the critical lateral load Q_{cr}.

$$Q_{cr}^2 \underline{V}_5^T \underline{\underline{K}}^*(\bar{p}) \underline{V}_5 + 2Q_{cr}\bar{p}e\underline{V}_6^T \underline{\underline{K}}^*(\bar{p})\underline{V}_5 \tag{61}$$

$$+ \bar{p}^2 e^2 \underline{V}_6^T \underline{\underline{K}}^*(\bar{p})\underline{V}_6 + F(Q_{cr}^4, \bar{p}, e) = 0$$

where

$$F(Q_{cr}^4, \bar{p}, e) \equiv 2J\{Q_{cr}^2 \underline{V}_5^T \underline{\underline{K}}^* \underline{\underline{K}}_2 \underline{\underline{K}}^* \underline{V}_5$$

$$+ Q_{cr}[2\bar{p}\underline{V}_6^T \underline{\underline{K}}^* \underline{\underline{K}}_2 \underline{\underline{K}}^* \underline{V}_5 + \underline{V}_6^T \underline{\underline{K}}^* \underline{V}_5]e$$

$$+ [\bar{p}^2 \underline{V}_6^T \underline{\underline{K}}^* \underline{\underline{K}}_2 \underline{\underline{K}}^* \underline{V}_6 + \bar{p}\underline{V}_6^T \underline{\underline{K}}^* \underline{V}_6]e^2\}^2$$

The above system can be solved for the solution set $\{Q_{cr}, \bar{p}_{cr}\}$ for any specified geometry used in the assembly of the stiffness matrix $\underline{\underline{K}}_1$, and the scalar J; initial shape $\eta_o(\xi)$ used in the assembly of $\underline{V}_6$; load distribution $N(\xi)$ used in the assembly of $\underline{V}_5$; and the boundary conditions. Unlike the bifurcation problem, for this case all coefficients in

Eqs. (59) and (61) are produced from the symmetric assembly of the relevant matrices. As noted, the buckling analysis involves solving two non-linear algebraic equations simultaneously. The problem can be re-stated by asking oneself the question: given a set of specified system parameters, what is the smallest positive value of the internal thrust parameters $\bar{p}$ such that there is a value of $Q<0$ which satisfies Eqs. (59) and (61)? Q is restricted less than zero due to the sign convention from Fig. 1. The solution proceeds by iteration on $\bar{p}>0$ until the solution set $\{Q_{cr},\bar{p}_{cr}\}$ is found for some value of the inertia and some rise parameter e. With these critical conditions one may return to the equilibrium equations to determine, within a magnitude factor c, the buckled mode shape $\underline{v} = c\ \underline{u}$ at the critical point.

Having established the method of analysis which yields the loading and displacement at the limit point for an arbitrary inertia vector, one may systematically redesign the arch for a given set of system parameters by using the recurrence relation Eq. (54). The critical energy H for this case, depends explicitly upon the specified initial configuration $\bar{\eta}_o(\xi)$ and rise parameter e through the vector $\underline{V}_6$; thus the critical energy is composed of both bending energy as well as interaction energy.

In summary, with instability through a symmetric mode as the failure mechanism (limit point), the solution for the strongest arch among those of equal volume $\bar{v}$, can be produced

by systematic application of the following general procedure for a given set of system parameters:

1. By specifying and imposing boundary conditions and other system parameters, notably the rise parameter e, and assuming some arbitrary m-dimensional inertia vector, the symmetric assembly of all relevant vectors and matrices is made.

2. Equations (49) and (61) are then solved simultaneously for the solution set $\{\bar{p}_{cr}, Q_{cr}\}$ subject to the restriction that $\bar{p} > 0$ and $Q < 0$.

3. With the critical conditions corresponding to a particular value of rise parameter, e, and inertia distribution, the equilibrium equations can be solved for the displacement vector $\underline{u}$.

4. The critical energy density is computed through the use of Eq. (48) and checked for uniformity.

5. In the event $\frac{H_i}{V_i}$ is not uniform for all i,

Eq. (54) is utilized to redistribute the inertia among those elements which have not violated some imposed constraint on the inertia (or area). Steps 2 through 5 are repeated until such time as the energy density is essentially uniform at which point the design is optimum.

An alternative approach for the limit point critical conditions [ie., the simultaneous satisfaction of Eqs. (38), (39), and (41)] which does not depend upon assuming a relationship apriori between the symmetric primary path $\underline{u}$ and

the symmetric buckled mode $\underline{v}$ can be established as follows:

1. Select a value of $\bar{p}$ and compute Q from Eq. (49).

2. Determine the corresponding primary path $\underline{u}$ from Eq. (39).

3. Substitute $\underline{u}$ and $\bar{p}$ into coefficient matrix of Eq. (41).

4. If the coefficient matrix is singular then the buckled mode $\underline{v} \neq 0$ and the corresponding conditions are critical.

Although this approach was not examined extensively, a cursory comparison between this method and the method of choice indicated greater complexity in programming; greater use of computer resources (ie., time, memory); and numerical instability during the determinant computation phase. The method of choice, on the other hand, being based on the approximation that $\underline{v} = c\ \underline{u}$ at the limit point, reduces to solving two algebraic equations simultaneously and can be carried out by iterating on $\bar{p}$ alone.

Whether anti-symmetric or symmetric mode instability is chosen as the failure criterion, it is important to start the interation scheme with a design for which buckling is possible. The bifurcation problem is complicated on the one hand by the need for both symmetric and anti-symmetric reduction of relevant matrices; and simplified on the other, due to standard routines available for solving symmetric eigenvalue problems. Furthermore, since one is ultimately

interested in determining the relationship between critical lateral load Q_{cr} and rise parameter e, the symmetric transformations do not occur until the optimization process yields the optimum design and the associated critical thrust parameter $\bar{p}_{cr}$. On the other hand, for instability through a symmetric mode, the critical thrust parameter $\bar{p}_{cr}$ depends upon the initial shape (the rise parameter e) due to the coupling of Eqs. (42) and (39). Thus, the rise parameter e must be specified and held constant, and an iterative solution for the critical conditions obtained during each analysis phase of the optimization process. The result of this requirement imposed by the non-linearity of the problem is that optimum designs are generated for each value of rise parameter e.

The overall impact of this distinction in the optimization process for symmetric modes will be demonstrated quite clearly upon presentation and discussion of results in the next chapter for particular cases of rise parameter e and boundary conditions.

CHAPTER IV

RESULTS AND DISCUSSION

The optimization process formulated and described in the previous chapters is based upon an a priori specification of the failure mode. That is, for unstable bifurcation the failure mode is anti-symmetric and for limit point instability the failure mode is symmetric.

The general formulation provides for investigation over a wide range of system parameters. Such a program, while certainly within the scope of present day computer capabilities, would yield a vast array of design spectra, but with the possibility of obscuring the more important features of the analysis. One could, for example, vary load distribution $N(\xi)$, initial shape $\eta_o(\xi)$, boundary conditions including elastic foundation modulus, number and spacing of finite elements, inertia-area parameters $\bar{\rho}$ and n, or constraint on inertia or area.

The results and discussion to be presented herein are predicated upon the following:

(a) The loading is taken to be uniform; that is, during the assembly of $\underline{V}_5$, $N(\xi) = 1$.

(b) The initial configuration is half sine; that is during the assembly of $\underline{V}_6$, $\bar{\eta}_o(\xi) = \sin \xi$.

(c) There is no elastic foundation; $\beta \equiv 0$.

(d) Elastic restraint at the boundaries is: $\beta_o = 0$, simply supported case; $\beta_o = 10.0$, restrained case; and $\beta_o \to \infty$, clamped case. The axial restraint is $\alpha_o \to \infty$ and is reflected in the definition of J.

(e) The inertia-area parameters are $\bar{\rho} = 1$, and n = 1, 2, or 3.

(f) The minimum allowable inertia in any element is specified to be zero.

(g) Optimal designs meeting the symmetric optimality criterion are produced for rise parameters of e=6, 8, and 10.

It is important to keep in mind that, for the symmetric optimization process, designs meeting the optimality criterion are obtained only for e = 6, 8, 10. In the $\{Q_{cr}, e\}$ space, the designs are optimum for only the specific value of rise parameter e for which they were obtained. The optimization process does not imply that the resulting design will, in fact, buckle symmetrically at a limit point, only that it is mathematically possible. To determine the actual response at a specified value of e of a particular optimum design, one must subject the design to a complete buckling analysis, including both the possibility of snapping symmetrically (through a limit point), as well as anti-symmetrically (unstable bifurcation). On the other hand, designs satisfying the anti-symmetric optimality criterion are, in fact, optimum for all values of rise, e, for which unstable bifurcation is

mathematically possible. Again, these designs must be subjected to further buckling analysis to determine the range of rise parameters for which they might become unstable via a symmetric (limit point) mode.

One cannot judge that a particular design is, in fact, the strongest design for a given value of rise parameter without first studying the complete response of those designs obtained through symmetric as well as anti-symmetric optimality criterion. Furthermore, it will be shown that there is a range of rise parameters for which the mode of failure changes during the optimization process and the final design, even though satisfying a particular optimality criterion, is not the strongest arch.

4.1 Analysis of Anti-Symmetric Optimal Designs

It is informative to consider first the case of unstable bifurcation, that is, the analysis-synthesis process resulting from the linearization of the buckling equations by imposing the anti-symmetry conditions of Article 3.2. The analysis process for the bifurcation problem depends primarily upon the boundary conditions through the eigenvalue problem, Eq. (57), while the synthesis process, that is, the redesign, depends additionally upon the inertia-area paramters through Eq. (54). Figures (2), (3), and (4) show that the critical response, obtained at $\bar{p} = \bar{p}_{cr}$ and $I = I_{opt}$ in Eq. (59) of the optimum designs varies by factors of 2 or 3 for given values of the rise parameter, e, as the boundary restraint

changes from simply supported to fully clamped. This significant influence of stiffness at the boundaries dominates the optimum inertia distributions depicted in Fig. (5) as well as the response. For a given case of boundary conditions (i.e., β_o), the strongest arch was obtained for n = 3 in the inertia-area relation; that is, one for which the height of the cross-section varies while the base remains constant (see Ref. 48, p. 136, for details). The optimum designs, of course, have in all cases higher bifurcation loads than the uniform arch of equal volume for the same set of system parameters. It is found that the response curve indicating bifurcation for the optimum designs is located above and to the right of the similar response curve for the uniform arch. As can be seen from Figs. (6), (7), and (8) there is a lower bound on the rise parameter e for each design below which bifurcation is not possible. At values of e below the lower bound, the mode of failure is by symmetric snapping (limit point) rather than unstable bifurcation. Thus, the optimum designs not only experience an increase in critical load over the uniform arch for a given value of e for which unstable bifurcation is possible, but the character of the buckling mode could be changed from bifurcation to snapping through a symmetric mode. This phenomenon is much more pronounced for the clamped boundary conditions in Fig. (6) than for the simply supported case in Fig. (8). Returning to Figs. (2), (3), and (4), one may also see that as n is reduced from the value 3, the

lowest value of rise parameter for which bifurcation becomes mathematically possible increases slightly.

For that range of rise parameters beyond the value of e where the optimum response curve indicates a change in buckled mode, Figs. (6), (7), and (8), the optimum design and the uniform arch buckle in the same mode (unstable bifurcation) for the same value of e. At the value of e corresponding to the mode change, the optimum design is a minimum of 10% stronger than the uniform arch for the simply supported case, Fig. (8); and a minimum of 38% stronger than the uniform arch for the clamped case, Fig. (6). For higher values of rise parameter e, the optimum designs are increasingly stronger than the uniform arch.

The complete buckling analysis of these designs, which includes a symmetric (limit point) mode, indicates that their response is similar in character to that of a uniform arch; namely: (1) there is a lower bound on the rise parameter e for which buckling will not occur, (2) there is a range of e for which buckling occurs by snapping through a symmetric mode, and bifurcation is not possible, (3) there is a range of e for which snapping through a symmetric mode occurs, but bifurcation is mathematically possible, and finally, (4) there is a range of e values for which instability occurs through an anti-symmetric mode (bifurcation) while a symmetric mode is mathematically possible, but physically unattainable.

A significant result of the symmetric buckling analysis of these optimum designs is that there is a range of rise

parameters for which these designs exhibit a lower buckling load than the uniform arch. Furthermore, the mode of failure (i. e., limit point or unstable bifurcation) might be different than that of the uniform arch. Again, as shown in Fig. (6), (7), and (8), the magnitude of this phenomenon depends heavily upon the stiffness requirements imposed at the boundaries through the rotational restraint factor β_o, the most severe manifestation occurring for the clamped case, Fig. (6), and the least severe, but still present, for the simply supported case, Fig. (8).

Those designs produced by the anti-symmetric optimization process are represented in Fig. (5a), (b), and (c) for different degrees of boundary restraint, and inertia-area parameters n. The designs are in all cases symmetric with respect to the arch centerline. For a given case of boundary conditions, the optimum inertia distribution is seen to change very little with changes in the inertia-area parameter n, whereas for a given value of n, there is a distinct difference in inertia distributions for changing boundary conditions. This boundary restraint effect is directly traceable to the resultant effect on the nodal deformation pattern $\underline{v}$ which, through the use of Eqs. (48) and (54), redistributes the inertia to meet the optimality criterion. In effect, the material is redistributed to reflect the stiffness requirements imposed by the anti-symmetric deformation pattern $\underline{v}$ existing when the thrust, $\bar{p}$, is critical. In all cases, the strongest design is the one obtained for n = 3, this result having been

demonstrated by Budiansky, Frauenthal, and Hutchinson (Ref. 37) for the simply supported high circular arch under uniform pressure. The distribution of inertia in Fig. (5b) for the simply supported case is similar to that reported by Wu (Ref. 36) for the optimum simply supported high circular arch.

Summarizing for the case in which optimum designs are produced based upon buckling failure through an anti-symmetric mode, one finds that:

(a) The degree of elastic restraint at the boundaries significantly affects the shape of the optimum design, as well as its response to destabilizing loads for all values of inertia-area parameter n.

(b) The complete buckling response of the optimum designs to destabilizing loads is similar in character to the response of a uniform arch.

(c) The improvement in load carrying capability over the uniform arch depends upon the rise parameter, boundary restraint and assumed relation between inertia and area.

(d) The mode of failure for the optimum designs may be different from that of the uniform arch, depending upon the rise parameter.

(e) Obtaining the design meeting the optimality criterion does not depend upon apriori specification of the load distribution or the initial shape of the arch (including rise parameter e).

4.2 Analysis of Symmetric Optimal Designs

Having examined the optimum designs produced by the restriction to anti-symmetric instability under various boundary restraints, and their response to both limit point and bifurcation type buckling, it is worthy to pursue an alternative course; namely, what designs are produced by imposing symmetric snapping as the failure criterion? What is their response? How do they differ from optimum designs obtained under anti-symmetric mode restrictions?

Recalling the solution methodology outlined in the previous chapter, the optimization process is restricted to finding the optimum design for a given value of the rise parameter e. The rise parameter [i.e., through the initial shape, $\eta_o(\xi)$] is present and must be specified apriori due to the dependence of the buckled modes on the pre-buckled deformation which, in turn, is a function of the initial configuration. Mathematically, both the critical thrust $\bar{p}_{cr}$ as well as the corresponding critical lateral load Q_{cr} for a given design, depend explicitly upon the initial configuration $\eta_o(\xi)$. The optimization process begins with the uniform design. For the uniform arch, buckling analysis results are obtained and presented in Appendix A. From these results one can determine that for values of e = 6, 8, and 10, both limit point as well as bifurcation instability are well represented for all boundary conditions. Therefore, the optimization results presented herein concentrate on these

representative values of rise parameter e. Additionally, these data points provide a check during the initial optimization stage by confirming previously obtained analytical results.

The response of the symmetric optimum designs (obtained for e = 6, 8, 10) to destabilizing loads for which instability might occur through either an anti-symmetric or a symmetric mode is investigated for various values of boundary restraint β_o and inertia-area relation n.

Consider first the anti-symmetric (bifurcation) response of the symmetric optimum designs. The character of this response is as indicated in Figs. (9a), (b,) and (c) for various boundary restraints and n = 2. In all of these cases after a certain initial value of rise parameter e, the designs exhibited a lower bifurcation load, Q_{cr}, than the uniform arch. That is, for a given value of e for which bifurcation is the primary failure mode, the symmetric optimum designs are <u>weaker</u> than the uniform arch and significantly weaker than the optimum designs obtained through the anti-symmetric optimization process. The magnitude of this phenomena depends upon the degree of rotational boundary restraint β_o and to a much lesser extent upon the inertia-area parameter n.

In Figs. (9d) and (e), the theoretical limit point loads are given for the optimum designs produced at e = 6, 8, and 10, for both the clamped and simply supported boundaries and n = 2. The uniform arch response (limit point) in each

case falls within the clusters of points for each value of e, but somewhat lower than that obtained for the optimum design. For clarity, the uniform data points were omitted. Note also that the designs have maximum limit point load only for the value of e at which they were produced. For other values of e, their limit point load is somewhat less than that for the optimum.

A very important characteristic of the overall response of the symmetric optimal designs [and to which Christensen (39) alluded] is that these designs do not necessarily buckle through a symmetric (limit point) mode at the value of e for which the design is optimum. Moreover, if at a specific value of e at which the uniform arch buckled symmetrically (or anti-symmetrically), a symmetric optimum design is produced, this arch will generally buckle through a symmetric (or anti-symmetric) mode. This observation is seen to hold true particularly for those values of rise where the failure mode is well defined. For example, consider the response of the e = 10 optimal design depicted in Figs. (9a) and (9d). At e = 10, the design meeting the symmetric optimality criterion buckles symmetrically at a theoretical limit point of $Q_{cr} = -69.40$ (Fig. 9d), but the bifurcation analysis for this design indicates that the arch would actually buckle through an anti-symmetric mode at $Q_{cr} = -61.4$ (Fig. 9a). Furthermore, from Fig. (9a) even the uniform arch which buckles in the same mode is stronger. On the other hand, for those values of rise at or near the point at which the failure mode changes from symmetric to anti-symmetric

the mode of failure for the symmetric optimum arch might be different from its uniform counterpart of the same volume. That is, a design produced from the symmetric mode optimality criterion at a value of e very near where the uniform arch changes mode of failure, but buckles via unstable bifurcation, may itself instead buckle symmetrically via a limit point. Although the possibility of changing failure modes might occur, this phenomenon does not affect the optimization process since each failure mode is considered separately; however, interpretation and usefulness of the designs might be affected if the rise parameter is specified and falls in a critical narrow band. It is sufficient for the purposes herein to note the existence of this phenomenon and be aware of its effect upon the interpretation of the results.

For all cases of boundary restraint, the symmetric optimization process yielded designs with a larger theoretical limit point load than the uniform arch. In addition, further improvements in the limit point load can be obtained by varying the inertia-area parameter n. Fig. (10) is typical and, for the clamped case, shows that n = 3 produced the strongest design, with improvements in limit point load from 9.6% for e = 6 to 8% for e = 10 over corresponding values for the uniform arch. On the other hand, for n = 1 improvements were generally of the order of 2% for the various values of e. Finally, boundary conditions do not significantly affect the degree of improvement in limit point load when symmetric

snapping is the failure criterion for optimization.

Figures (11), (12), and (13) show typical optimum designs obtained by varying rise parameter e, boundary restraint, β_o, and inertia-area relation, n. The designs are symmetric about the arch centerline. Significant differences in optimum inertia distribution are noted in Fig. (13) upon varying the elastic restraint at the boundary from fully clamped ($\beta_o \to \infty$) to simply supported ($\beta_o = 0$). In all cases, the optimization process redistributes the material in such a way that the mid-span of the arch "grows" at the expense of other sections. The greatest degree of growth is seen to occur (Fig. 12) for the clamped case and n = 3. Similar distributions for n = 3 occurred for all degrees of boundary restraint. Fig. (11) shows that, as the rise parameter is increased, more material is redistributed away from those elements in close proximity to the boundary. This, too, is a typical occurrence for all degrees of boundary restraint.

In summary, for the case of optimization with respect to symmetric buckling modes, one finds that:

(a) The buckling analysis for a given design as well as the redesign process (through the interaction energy) depends upon the load distribution and the initial configuration.

(b) The optimum shapes are significantly affected by the degree of elastic restraint at the boundaries; and, to a lesser extent, by the rise parameter and inertia-area

relation.

(c) The degree of improvement in theoretical limit point load over the uniform arch depends upon the value of n in the inertia-area relation and, to a somewhat lesser extent, upon the boundary restraint β_o.

(d) Greater improvements in the limit point load occur for n = 3 than for n = 1 and 2.

(e) Although the possibility exists that the symmetric optimum design will buckle via a different mode than its uniform counterpart, this phenomena appears to be localized around the value of e for which the uniform arch changes failure mode.

In the previous sections, the results for each of the optimization processes have been discussed and the appropriate designs have been presented along with the criteria by which they were obtained. For each design, the critical response for both limit point instability as well as bifurcation was compared to that of the uniform arch and its salient features noted.

In the next section, the foregoing results are merged together in a manner that will allow the reader to appreciate the complexity of determining the "strongest" arch as opposed to generating one that meets certain optimality criterion.

4.3 Determination of the Strongest Design

The "optimum" designs produced through either of the two processes for symmetric or anti-symmetric buckling modes

are by definition those designs which meet the governing equations and the respective optimality criterion. It has been demonstrated that an "optimum" design does in fact exhibit a larger value of the theoretical critical load for the assumed mode shape than does the uniform arch of the same volume. But, in order to properly interpret the results, one must view the buckling phenomenon in the broader context of dual mode instability. That is, a given design (optimum or otherwise) may or may not buckle depending upon the initial rise parameter; moreover, the buckling mode depends also upon the rise parameter.

From the point of view of engineering design, one is interested in knowing the shape of the strongest arch for a given set of system parameters and specific rise. That is, what design buckles at the greatest load, Q_{cr}, and what is its mode of failure (i.e., bifurcation or limit point)? As an illustration of the complexity of this question, consider Fig. (14) which presents the response curves for the uniform design; the anti-symmetric optimal design; and the symmetric optimum design for e = 6. The rise parameter axis is subdivided into regions within which a given design is strongest. In addition, within a given region (i.e., design), the mode of failure could change depending upon the value of e selected. Referring to Fig. (14), Region I is composed of those low rise parameter values for which during the design process buckling takes place at a limit point via a symmetric mode.

As indicated in previous sections, for each of these values of e there is a different design that is optimum for the particular chosen e. Figs. (14), (15), and (16) illustrate the response of the symmetric optimum design for e = 6 only, since this design is nearer the response of the uniform arch than optimal designs obtained for e = 8 or 10. For this case, the symmetric optimum design is obviously stronger than the uniform design or the anti-symmetric optimal design in these regions. Moreover, for e = 6 it is the strongest design and buckles via a symmetric mode (limit point) at $Q_{cr} = -24.7$. Region III is composed of those high rise parameter values for which during the design process buckling takes place at a bifurcation point via an anti-symmetric mode. From Fig. (14) for all e > 15.3 the strongest design is the one which satisfies the anti-symmetric optimality criterion, denoted by I^{A}_{opt}.

Referring to Figs. (14), (15), and (16) a region II develops composed of a narrow band of moderate rise parameter values for which the optimization process as presented does not yield the strongest design. The reason is that each design obtained while satisfying the individual optimality conditions does not, during the analysis process, consider the possibility of buckling in an alternate mode. In other words, the methodology as presented, having assumed apriori the failure mode, does not include the possibility of dual failure modes during redesign. In this region, therefore,

to obtain the strongest design one would have to consider at each analysis step what the actual mode of failure was and then use the corresponding redesign algorithm. All of the response curves indicate that for very low values of rise parameter, anti-symmetric optimum designs are relatively weak. This is because (1) buckling is more likely to occur through symmetric snapping at a limit point for low e and (2) the redesign process for maximum bifurcation load inherently produces a design which is weak with respect to a limit point load [compare the respective designs of Figs. (5a), (5b), and (5c) with those of (11), (12), and (13)]. Conversely, all the response curves indicate that for very high values of rise, symmetric optimum designs are relatively weak. This is due in part to the fact that for high rise parameters bifurcation is more likely to be the failure mode. The symmetric mode redesign process, while maximizing the theoretical limit point, in fact produces a design whose actual mode of failure occurs at a bifurcation point via an anti-symmetric mode and is inherently weak (compare again the relative inertia distributions).

The phenomenon reflected in region II is greatly dependent upon the degree of boundary restraint since the region almost vanishes for the simply supported case ($\beta_o=0$) and is greatest for the clamped case ($\beta_o \to \infty$). For example, in Fig. (16) for the simply supported case, for e slightly less than 6.0, the strongest design is obtained from the

symmetric optimality criterion and the failure mode is at a limit point; for values of e slightly greater than 6.0 the strongest design is obtained from the anti-symmetric criterion and buckling occurs at a bifurcation point.

Referring to Figs. (14), (15), and (16), we can observe that for a uniformly loaded shallow arch, with arbitrary boundary restraint (and governed by the stated set of system parameters):

(a) For rise parameters less than 6.0 the strongest design is obtained from the symmetric optimality criterion and the failure occurs at a limit point through a symmetric mode.

(b) For rise parameters greater than 15.3 the strongest design is obtained from the anti-symmetric optimality criterion and the failure occurs at a bifurcation point through an anti-symmetric mode.

(c) For rise parameters between 6.0 and 15.3 the strongest design must be obtained from a dual consideration of each possible failure mode with optimality possibly being achieved at a point for which simultaneous failure (bifurcation and limit point) can occur.

The results presented herein, having been obtained by separating the failure modes into symmetric and anti-symmetric parts according to their relation with the prebuckled equilibrium configuration, have served as a positive demonstration of the methodology. Furthermore, it has been shown that the

optimum designs obtained differ dramatically in their character as well as their critical response for both anti-symmetric and symmetric optimization. These differences are characteristics of the system variables used to define the initial shape, loading, boundary restraints and inertia-area relation, and have important design as well as theoretical implications.

CHAPTER V

CONCLUSIONS AND RECOMMENDATIONS

5.1 Conclusions

It can be stated conclusively that the optimization of the shallow arch is definitely dependent upon its rise parameter, e. For high values of e the optimum design is obtained by employing the unstable bifurcation optimality criterion, Eqs. (55) and (49) while for sufficiently low values of e, the optimum design is obtained by employing the limit point optimality criterion, Eqs. (49) and (50). As indicated by the results for moderate values of arch rise, the optimization process for an assumed failure mode does not yield the strongest design since the mode of failure changes in this region. It does yield, however, designs with the greatest theoretical limit point on the one hand (from symmetric optimization) or possibly lowest actual limit point (from anti-symmetric optimization) on the other. It is seen that optimum designs have similar buckling response characteristics to those of the uniform arch; that is, there is a lower bound on the rise parameter for which no buckling takes place; a range for which failure occurs by snapping through a symmetric mode; and finally, a range for which buckling takes place by bifurcation through an anti-symmetric mode.

Among the most important conclusions of this investigation

one may list the following:

(a) The optimality criterion for both symmetric and anti-symmetric buckling reduces to uniform energy density.

(b) The finite element formulation allows the buckling analysis methodology to produce critical response for any given set of system parameters and any inertia distribution.

(c) Judicious choice of the proportionality constant α in Eq. (54) allows one to control, to a certain extent, the rate of change of redesign and hence the rate of convergence to the final optimum design (see Appendix D).

(d) The optimum designs obtained by imposing anti-symmetry upon the buckling mode are in all cases stronger than the corresponding uniform arch beyond some value of rise parameter. The mode of failure for the two designs may be different.

(e) The identification of the strongest arch as well as its mode of failure depends upon specification of the rise parameter.

(f) For inertia-area relations of the form $I = \bar{\rho}A^n$, the value of $n = 3$ corresponds to designs which are stronger than those of $n = 2$, or 1 for both symmetric and anti-symmetric optimization.

5.2 Recommendations

The presentation of the results on the study of the optimum shallow arch demonstrates the complexity inherent in its buckling behavior. Several questions remain unanswered

and may provide the main course for further research. Of utmost importance are the following:

(a) An amplification of present methods to include the possibility of either bifurcation or snapping during the iterative redesign process.

(b) A continuation and amplification of the present methods for other static load distributions, initial shapes, and degrees of elastic restraint must be pursued. Initial indications are that the load distribution significantly affects the critical response and one then may expect a dramatic change in optimum designs, possibly of the same order as that seen by a change in boundary conditions.

(c) An investigation of the effect of non-symmetric static loading and non-symmetric boundary restraints on the response of arbitrary designs.

(d) An investigation into the response of the optimum designs obtained herein to time dependent loads.

In summary, the investigation has demonstrated the power and versitility obtained through a novel utilization of finite element methods coupled with energy criteria to characterize the response of a highly nonlinear problem. Moreover, the methodology outlined can, with very little modification, be used to obtain results for more general cases of loading; for other boundary and foundation restraints, and a wide assortment of other system parameters. One might even consider adapting the procedure for the case of time dependent loading.

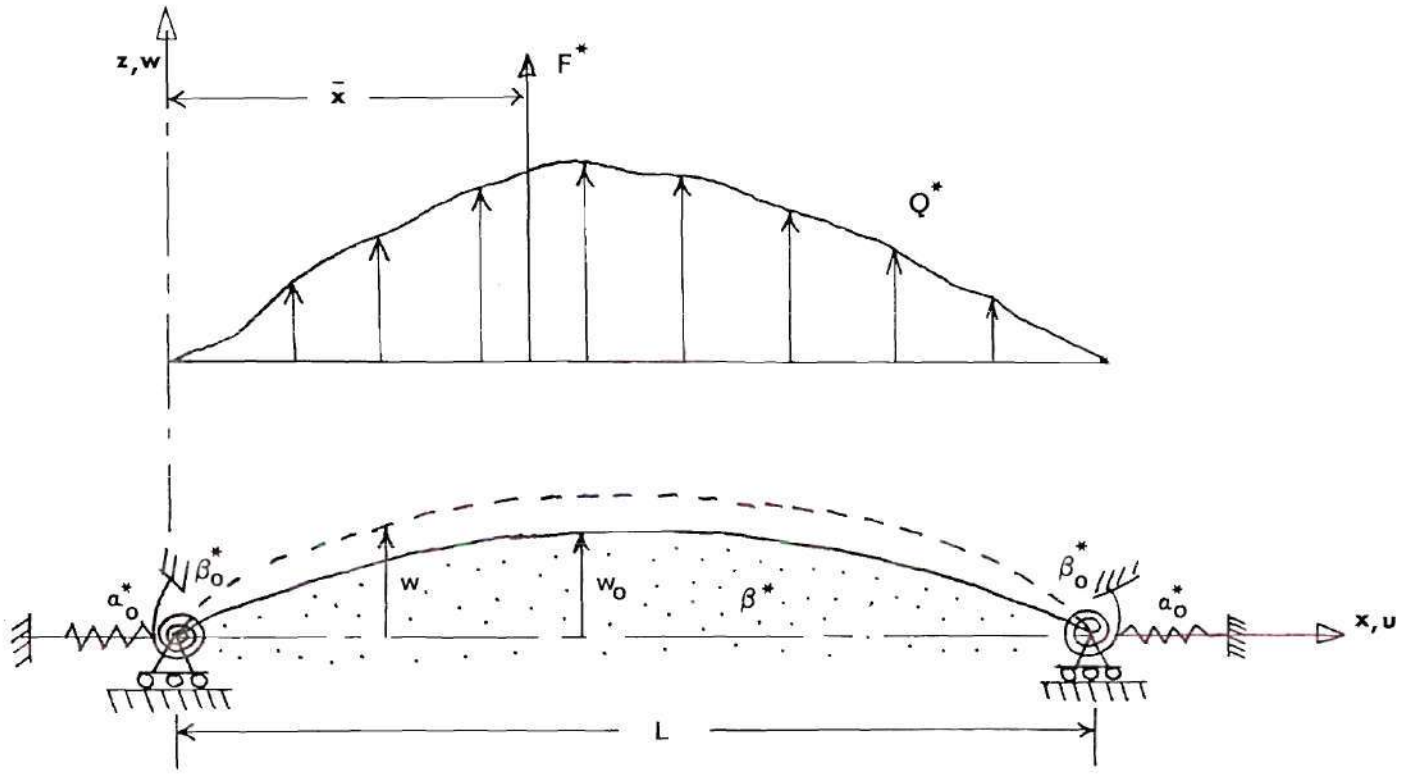

Fig. 1. Shallow Arch Geometry and Sign Convention

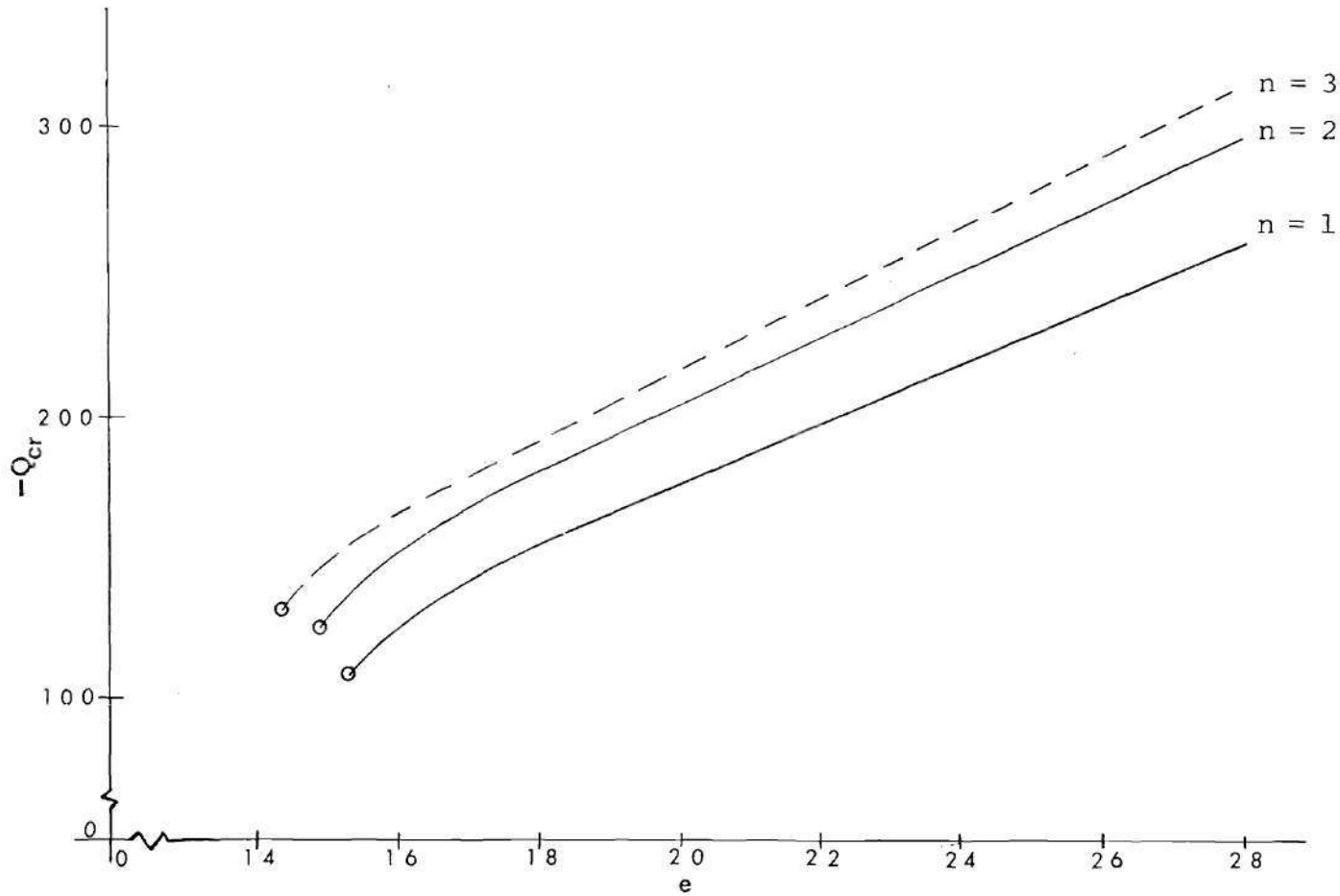

Fig. 2. Anti-Symmetric Response of Optimum Shapes for Various Values of n, $\beta_o = \infty$

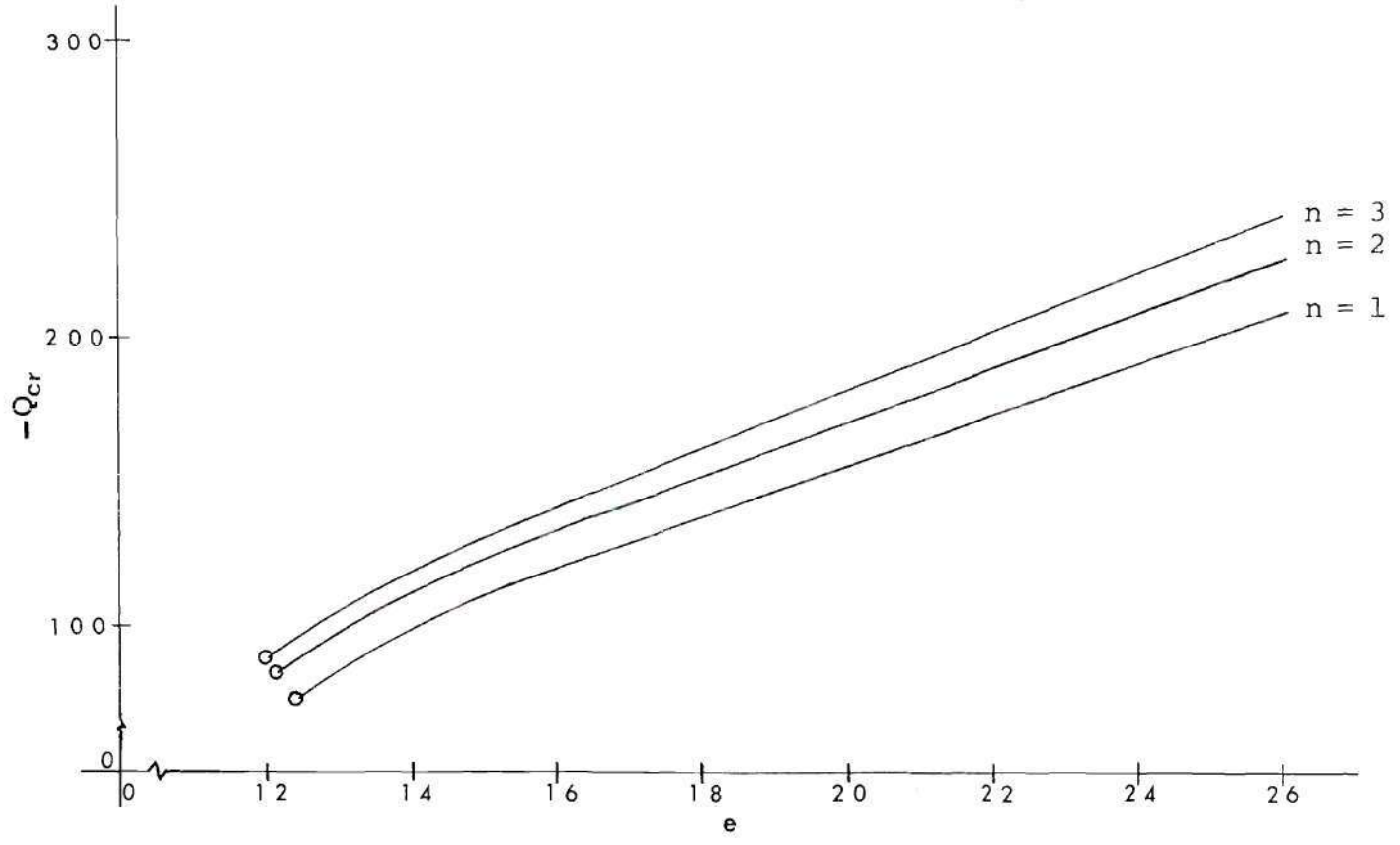

Fig. 3. Anti-Symmetric Response of Optimum Designs for Various Values of n, $\beta_o = 10.0$

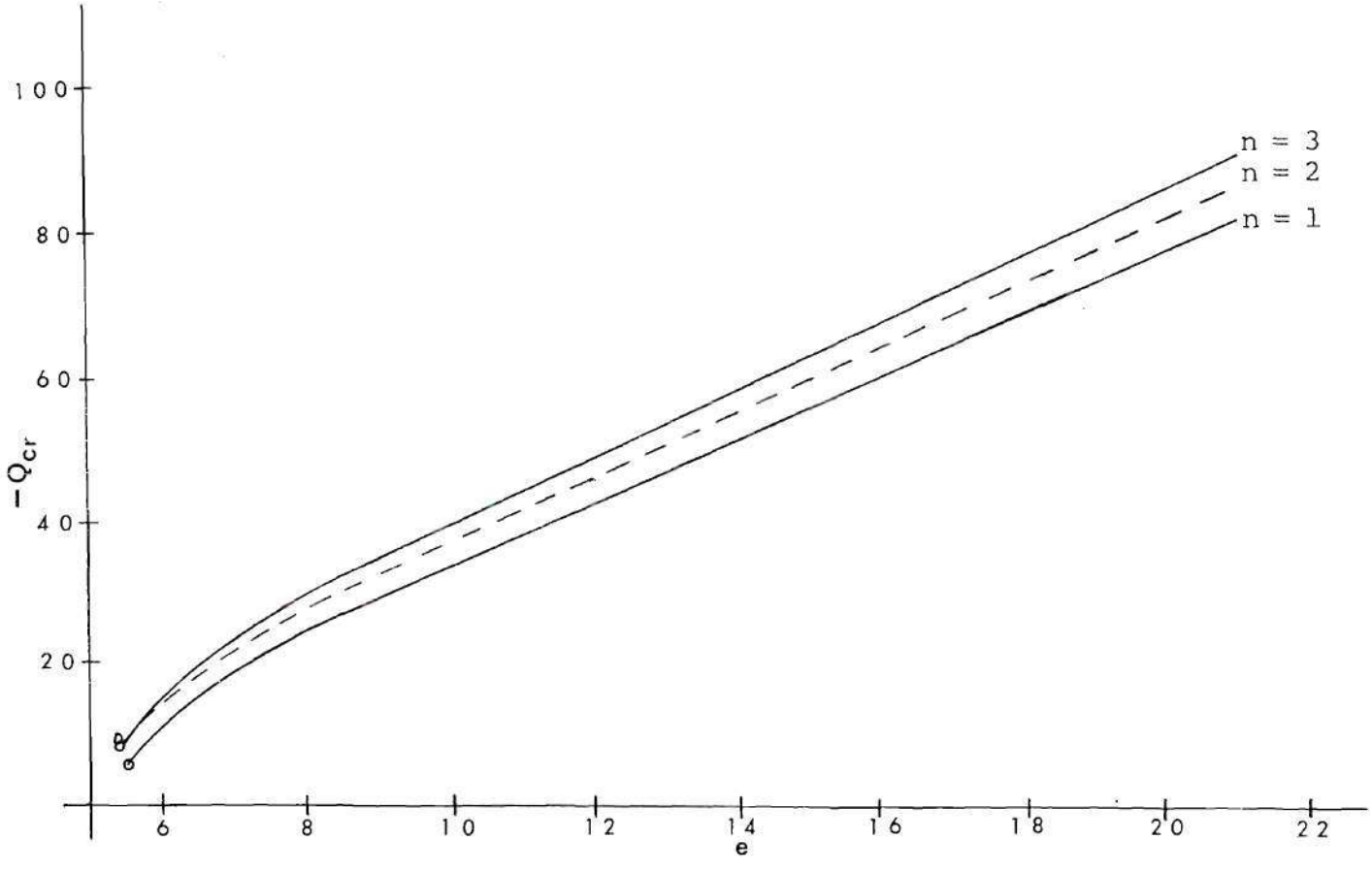

Fig. 4. Anti-Symmetric Response of Optimum Designs for Various Values of n, $\beta_o = 0$.

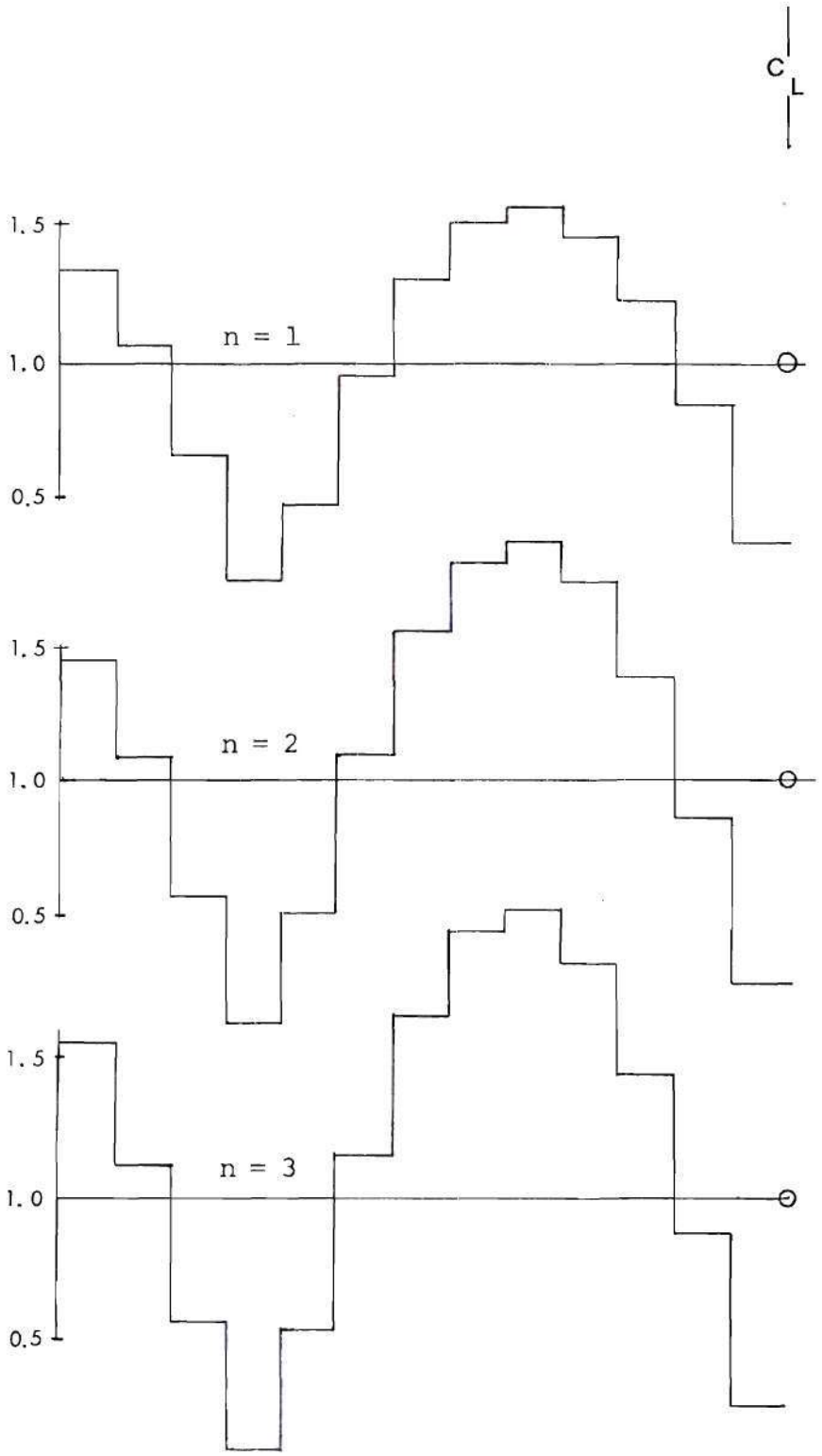

Fig. 5a. Optimum Designs for Various Values of n. Anti-Symmetric Buckling, $\beta_o = \infty$

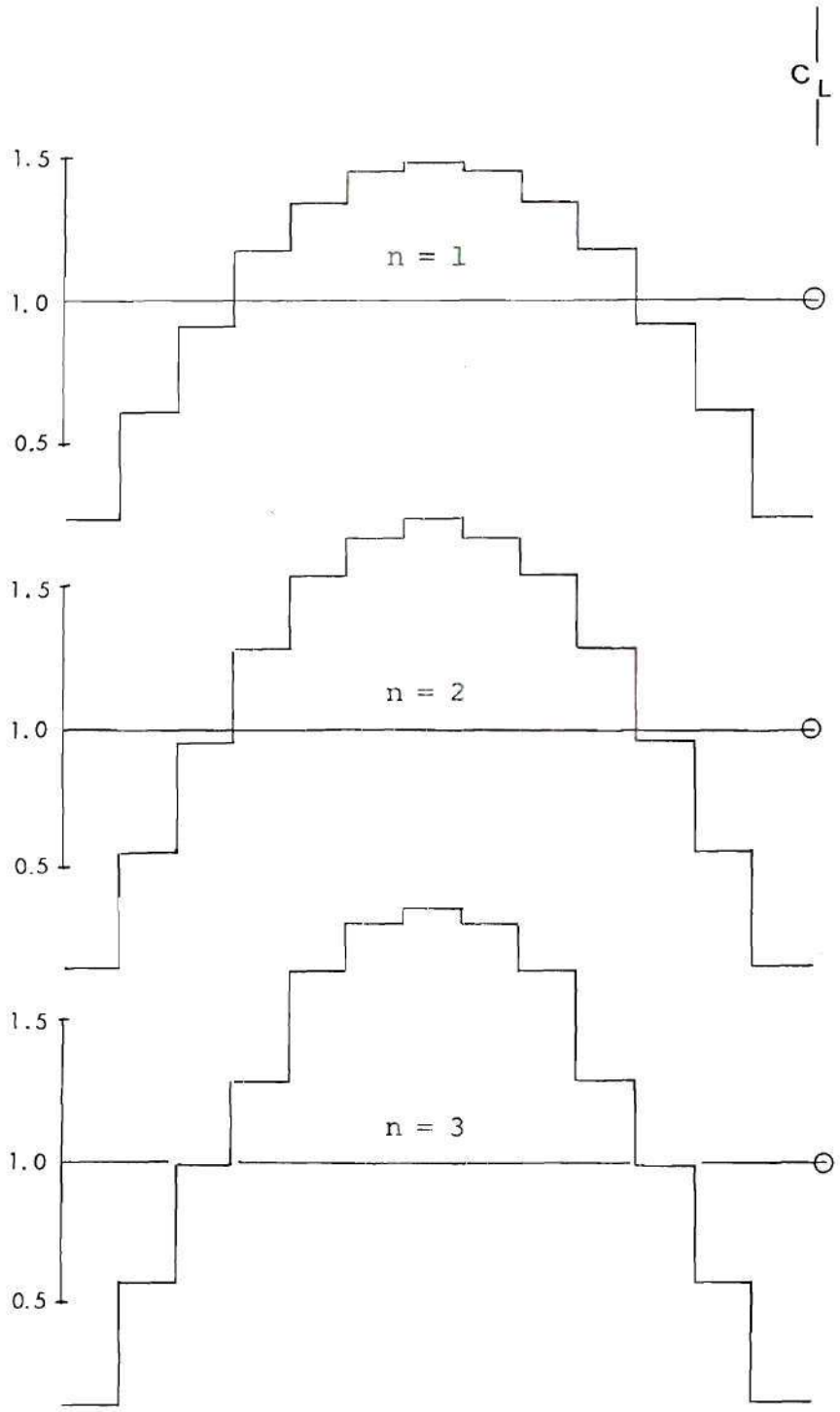

Fig. 5b. Optimum Designs for Various Values of n. Anti-Symmetric Buckling, $\beta_o = 0$.

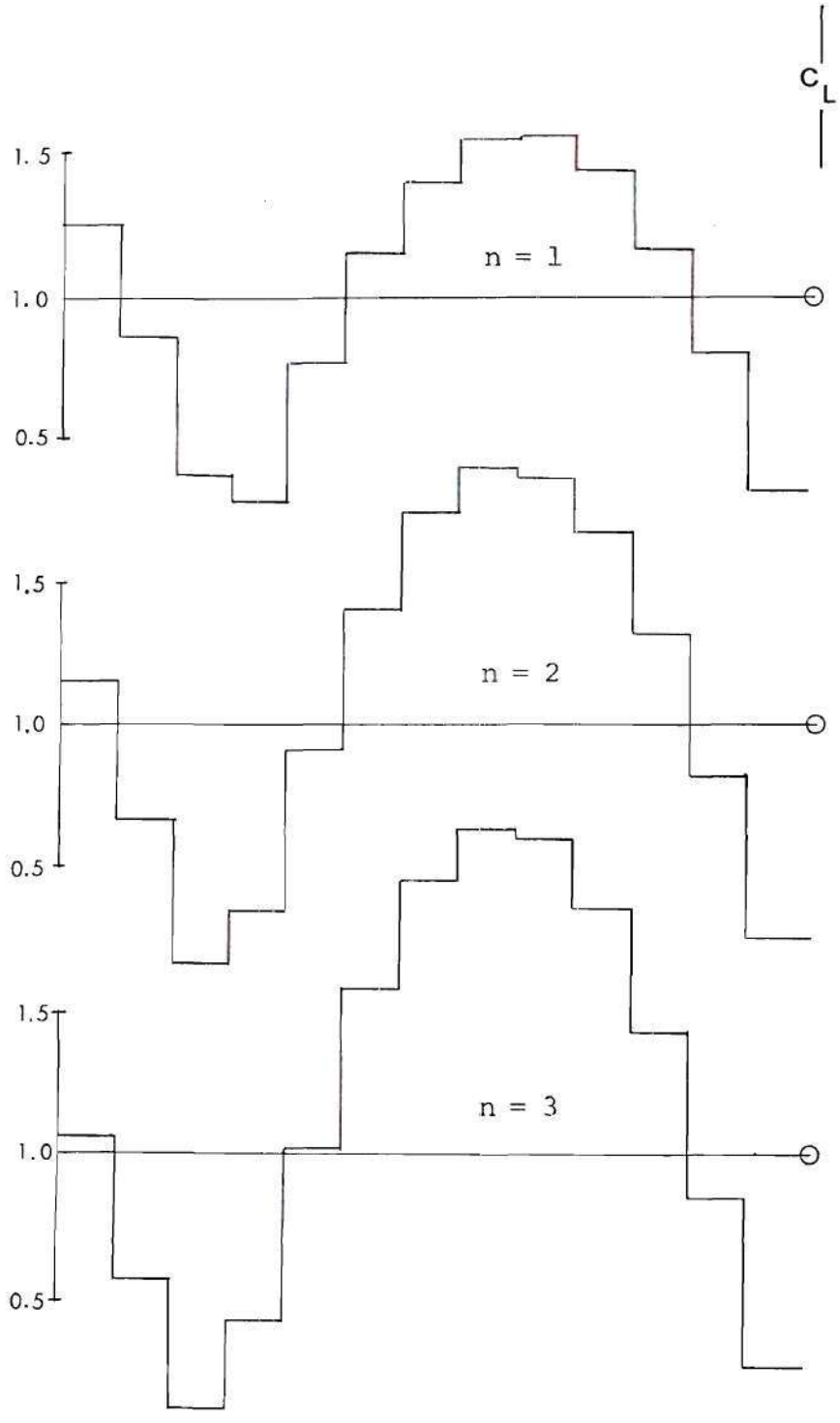

Fig. 5c. Optimum Designs for Various Values of n. Anti-Symmetric Buckling, $\beta_o = 10.0$.

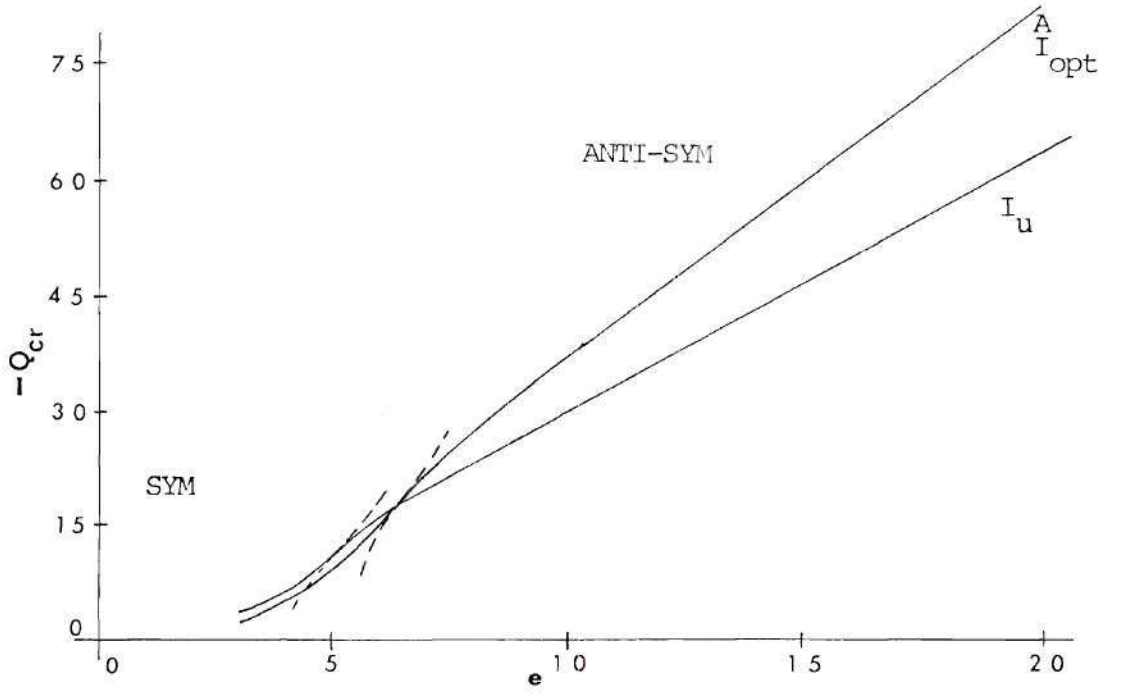

Fig. 7. Critical Load Versus Rise Parameter for I^A_{opt} and I_u, $\beta_o = 10.0$, $n = 2$.

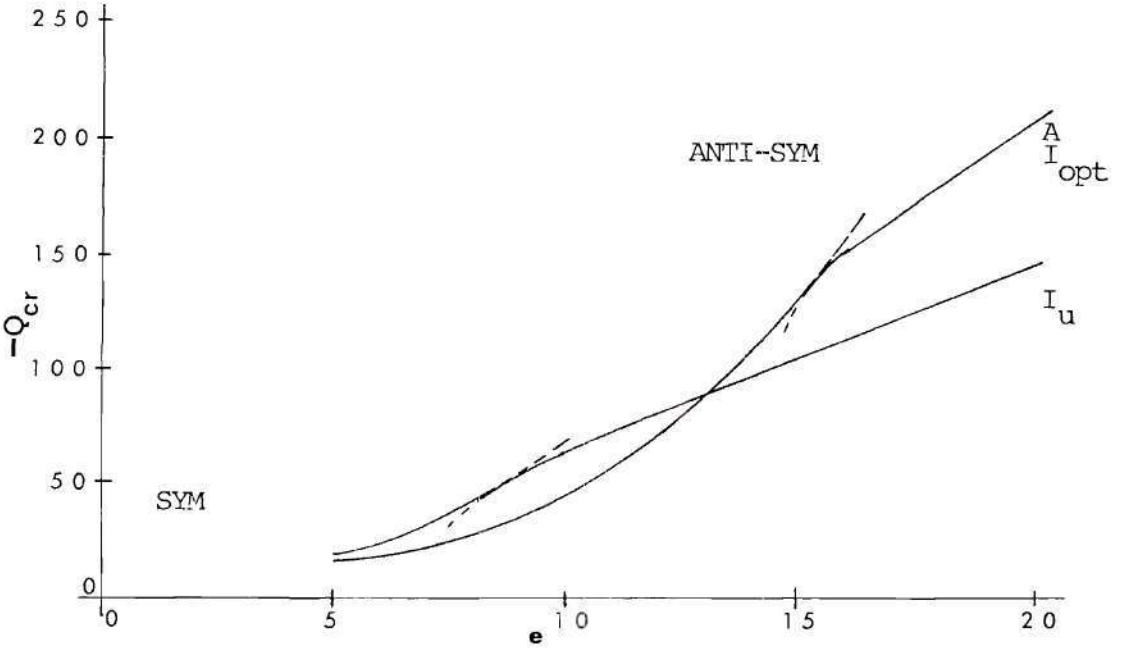

Fig. 6. Critical Load Versus Rise Parameter for I^A_{opt} and I_u, $\beta_o = \infty$, $n = 2$.

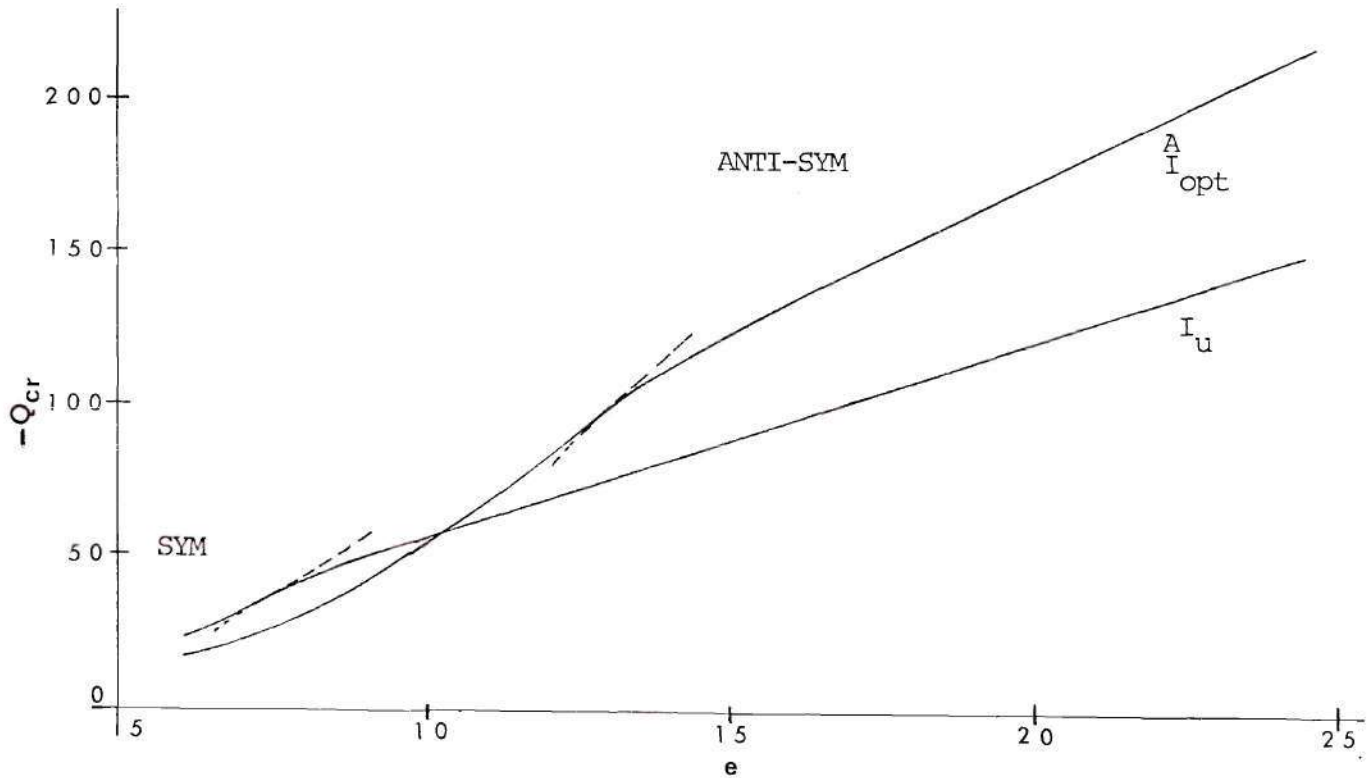

Fig. 8. Critical Load Versus Rise Parameter for I^A_{opt} and I_u, $\beta_o = 0$, $n = 2$.

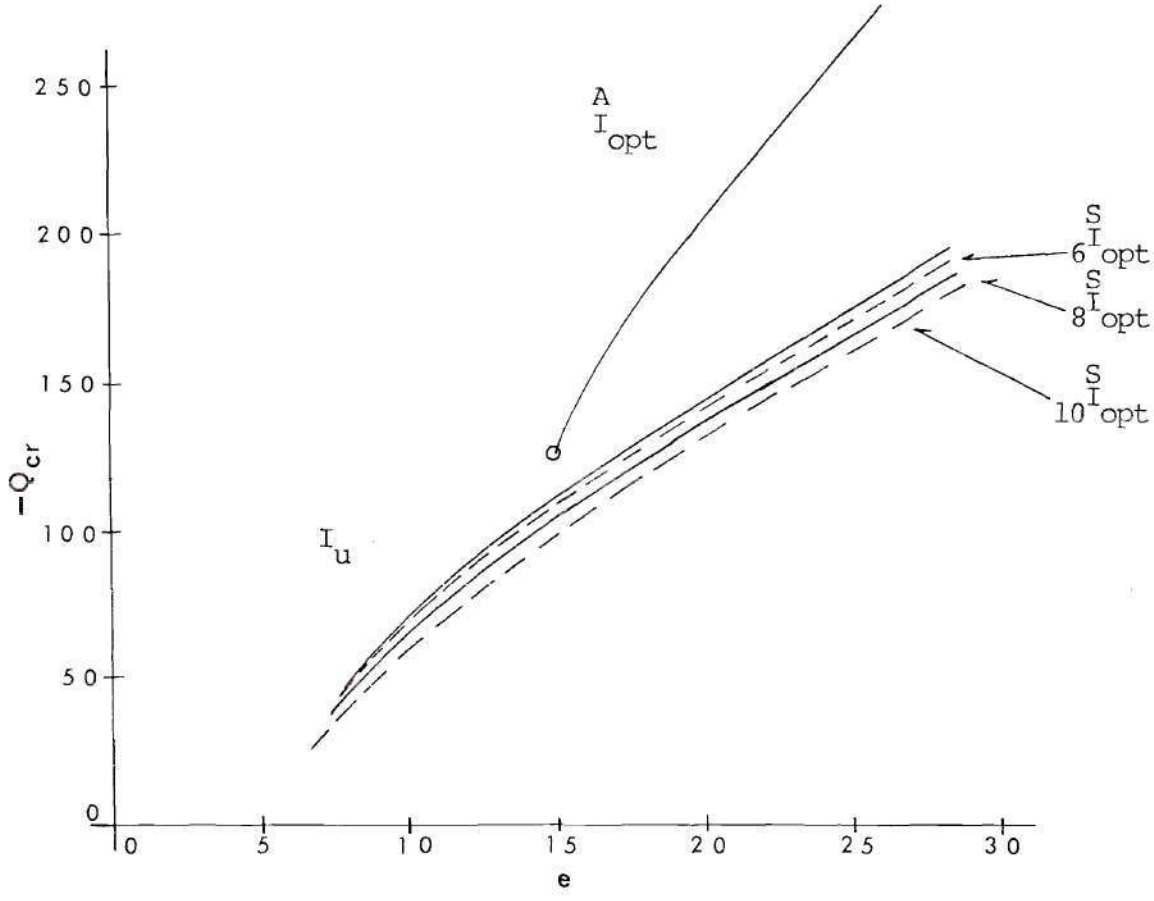

Fig. 9a. Anti-Symmetric Response, Different Designs, $\beta_o = \infty$, n = 2.

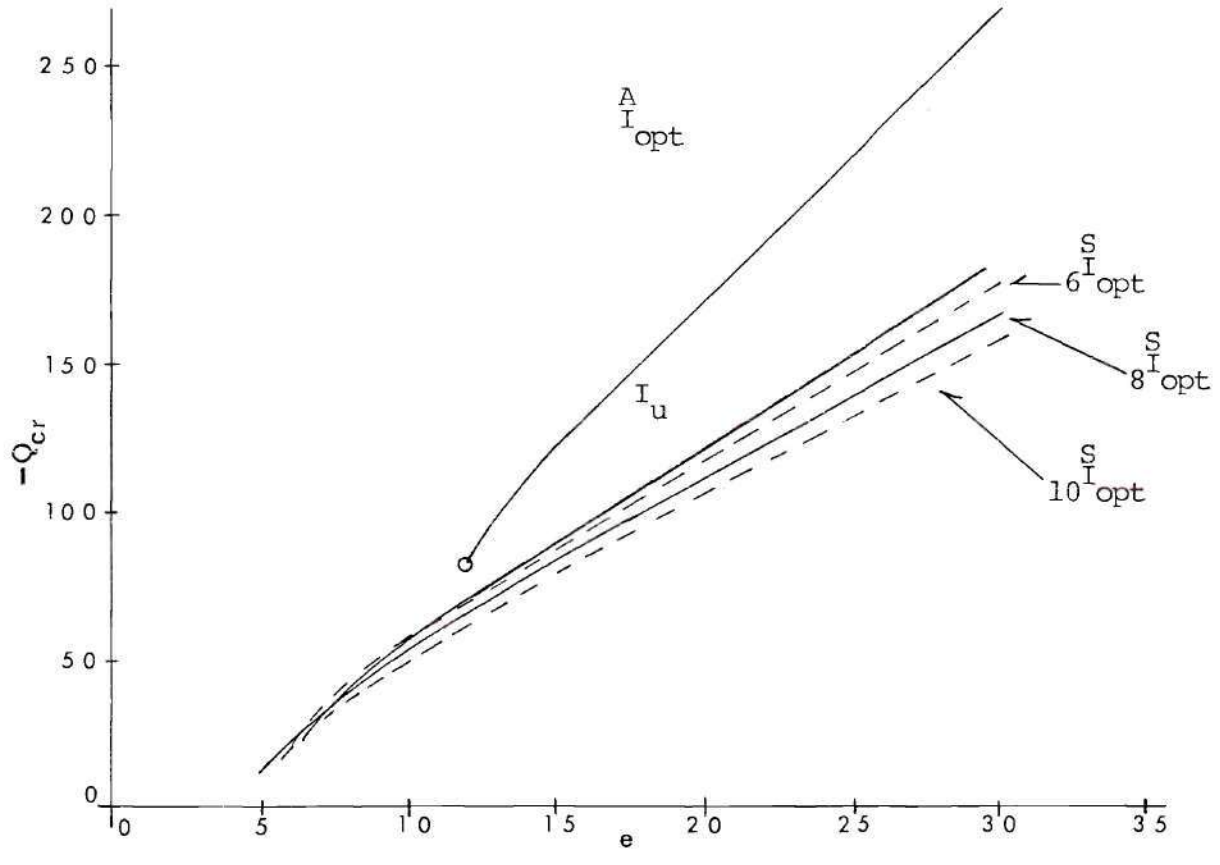

Fig. 9b. Anti-Symmetric Response, Different Designs, $\beta_o = 10$, $n = 2$.

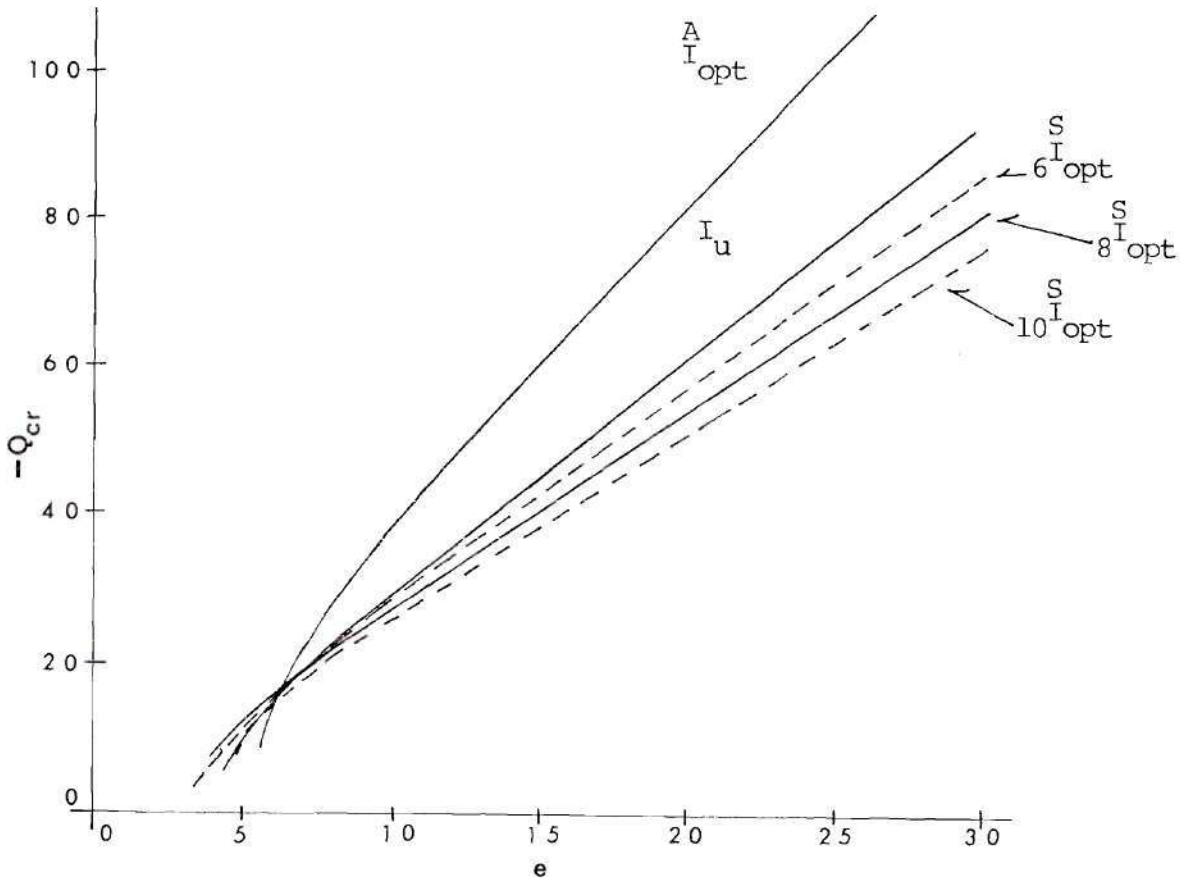

Fig. 9c. Anti-Symmetric Response, Different Designs, $\beta_o = 0$, n = 2.

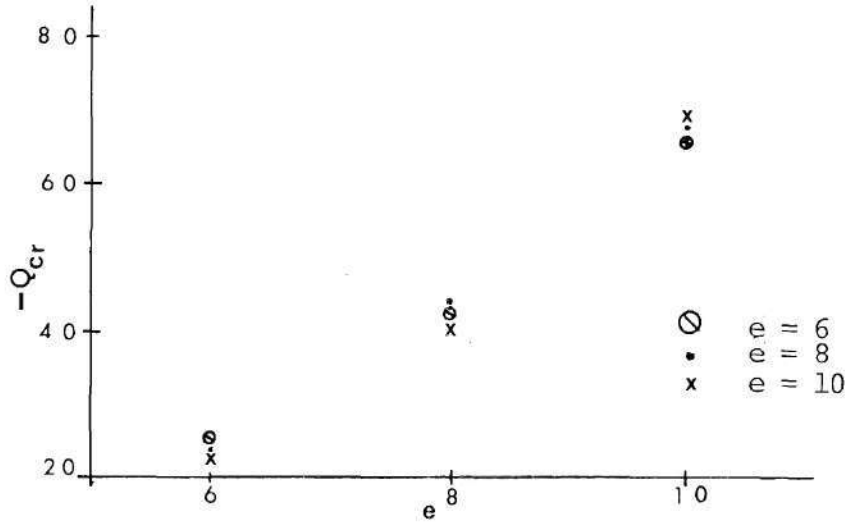

Fig. 9d. Limit Point Load Versus Rise Parameter for Symmetric Optimum Designs at e=6,8, 10, $\beta_o = \infty$, n=2.

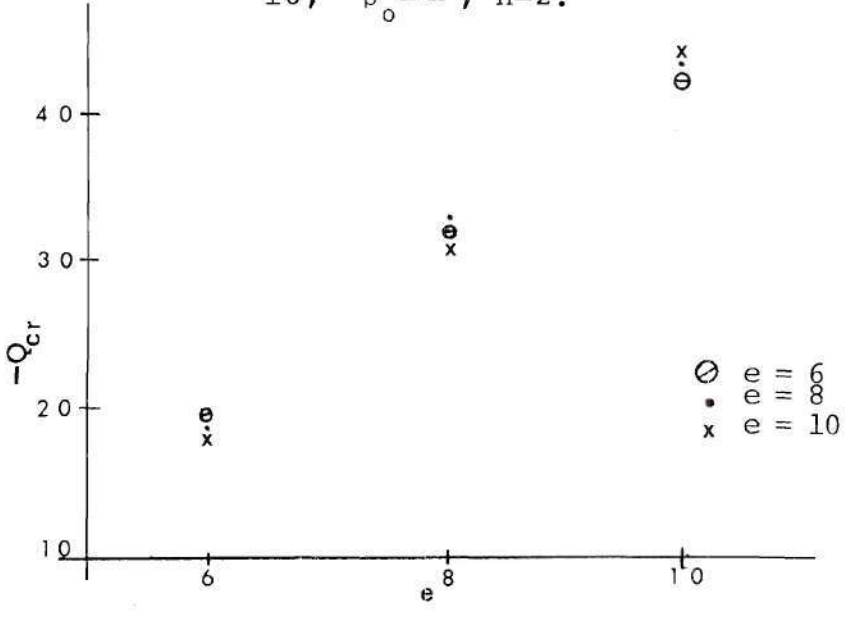

Fig. 9e. Limit Point Load Versus Rise Parameter for Symmetric Optimum Designs at e=6, 8, and 10, $\beta_o = 0$, n=2.

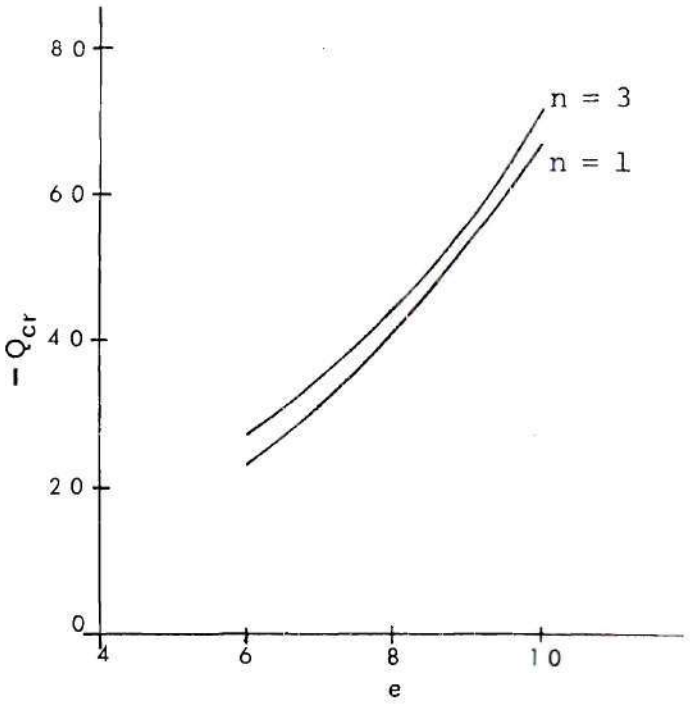

Fig. 10. Symmetric Critical Response, Symmetric Optimum Designs at e=6, 8, 10, $\beta_o = \infty$, n=1, 3.

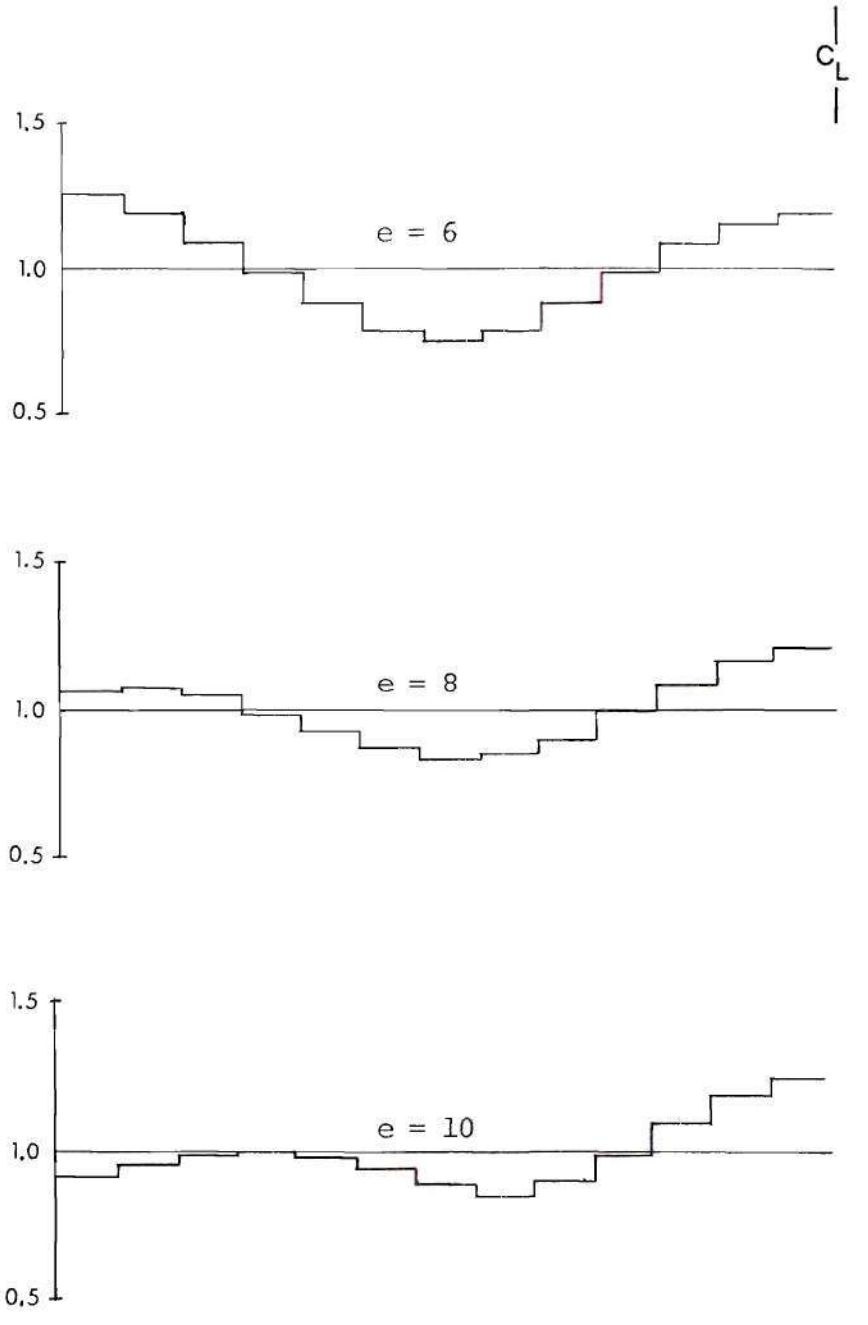

Fig. 11. Variation in Symmetric Optimum Designs with Rise Parameter, $\beta_o = \infty$, n=2.

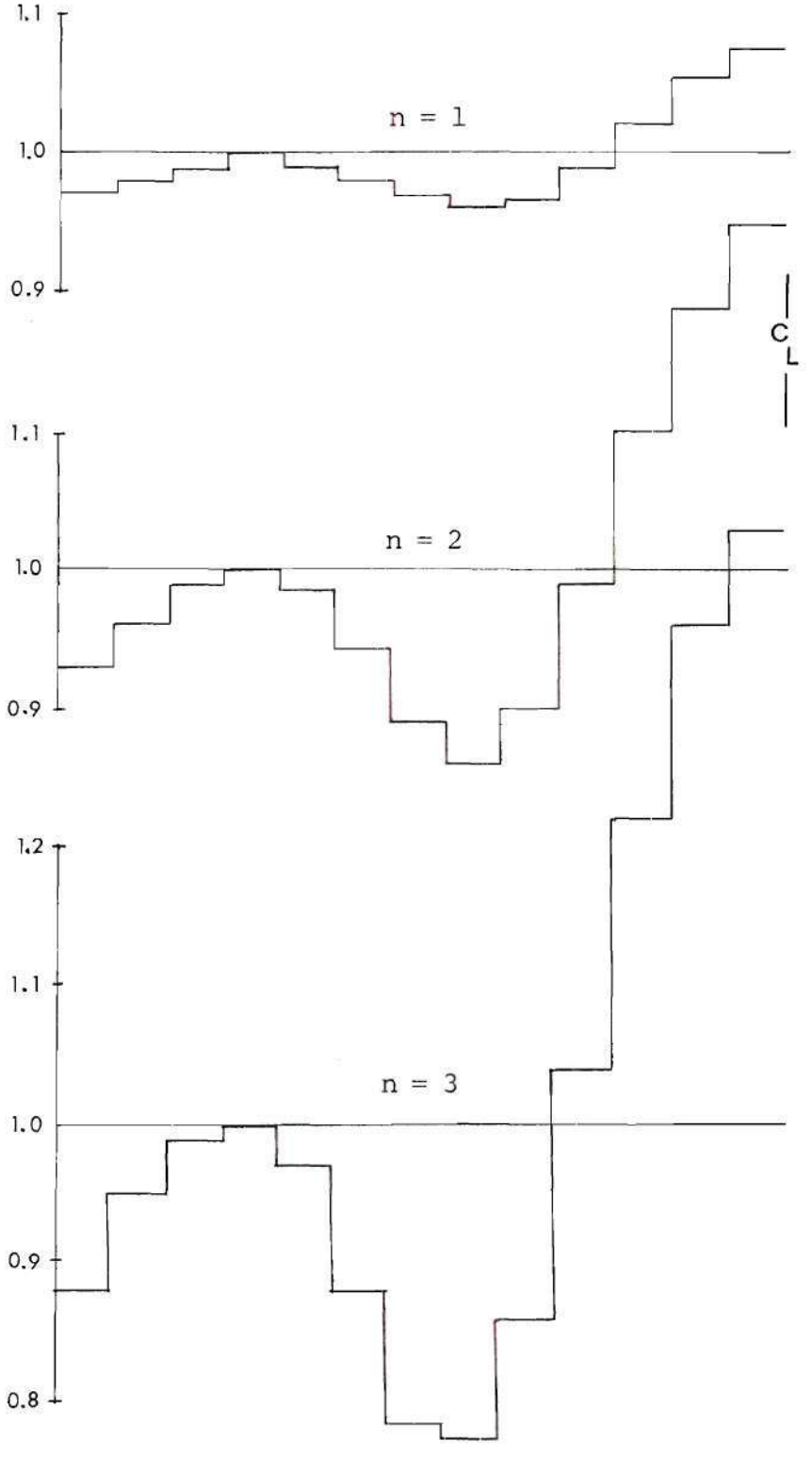

Fig. 12. Variation in Symmetric Optimum Designs with n, $\beta_o = \infty$, e=10.0.

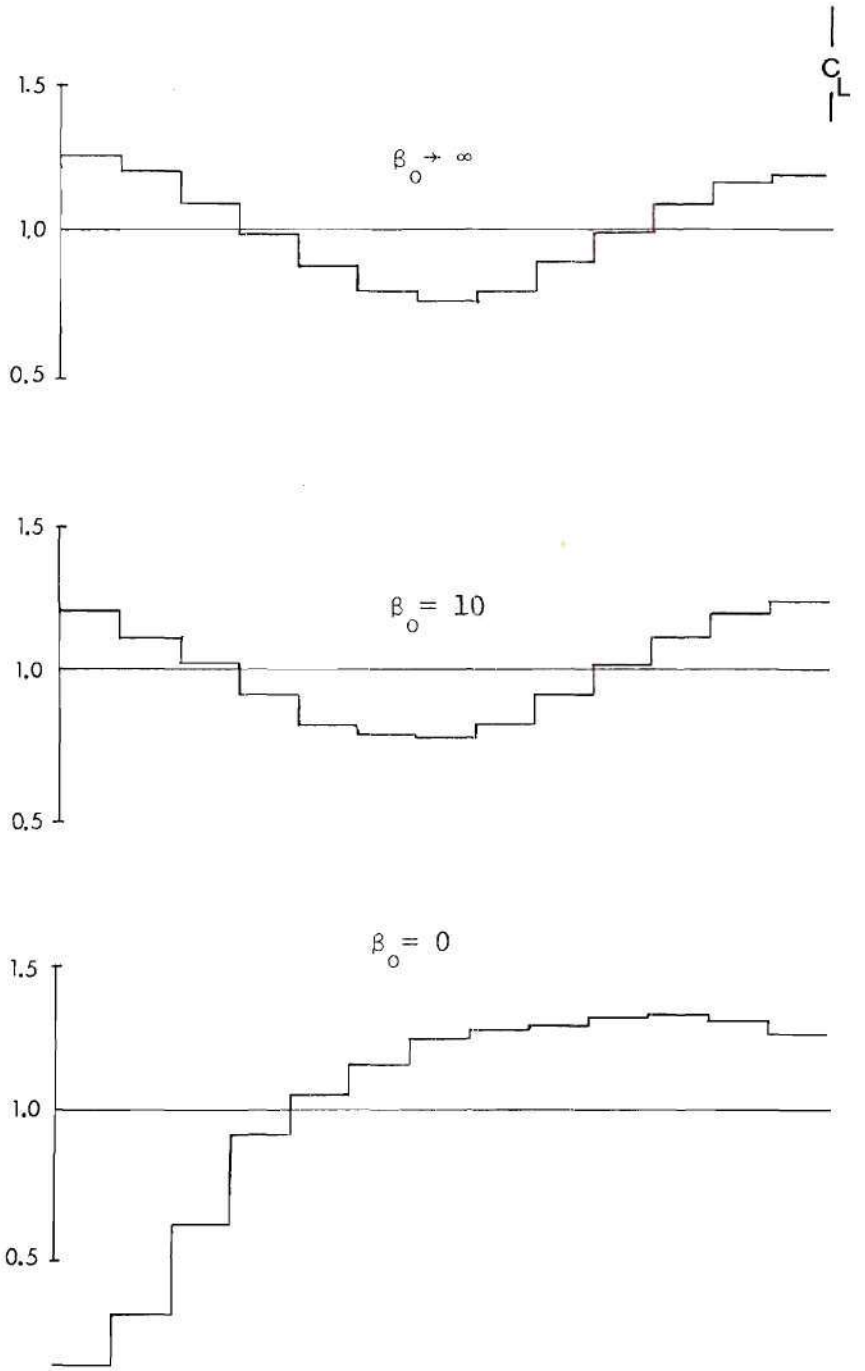

Fig. 13. Variation in Symmetric Optimum Designs with Boundary Conditions, e=6, n=2.

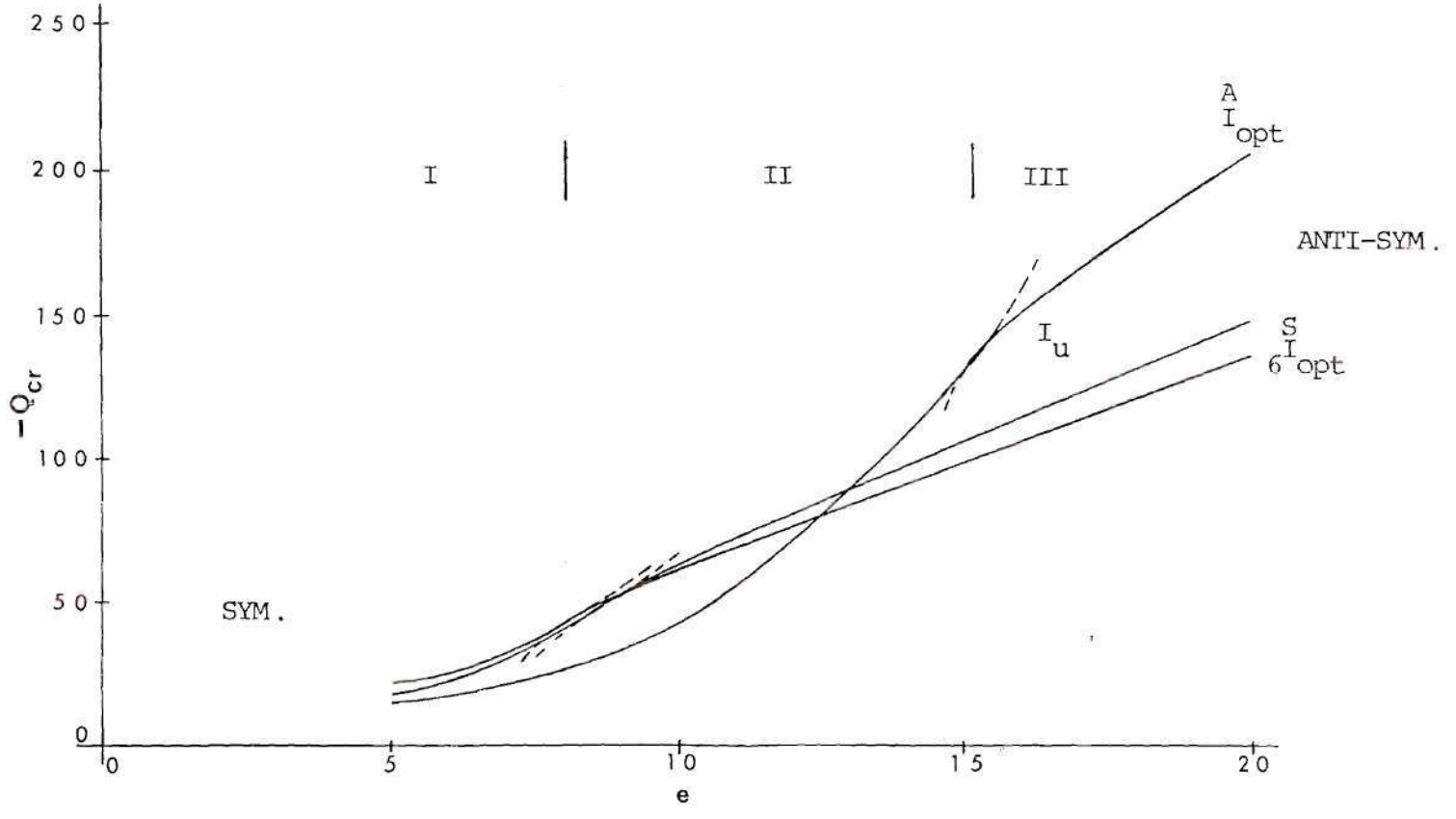

Fig. 14. Critical Response of I_u, I^A_{opt}, and $6I^A_{opt}$, $\beta_o = \infty$, n=2.

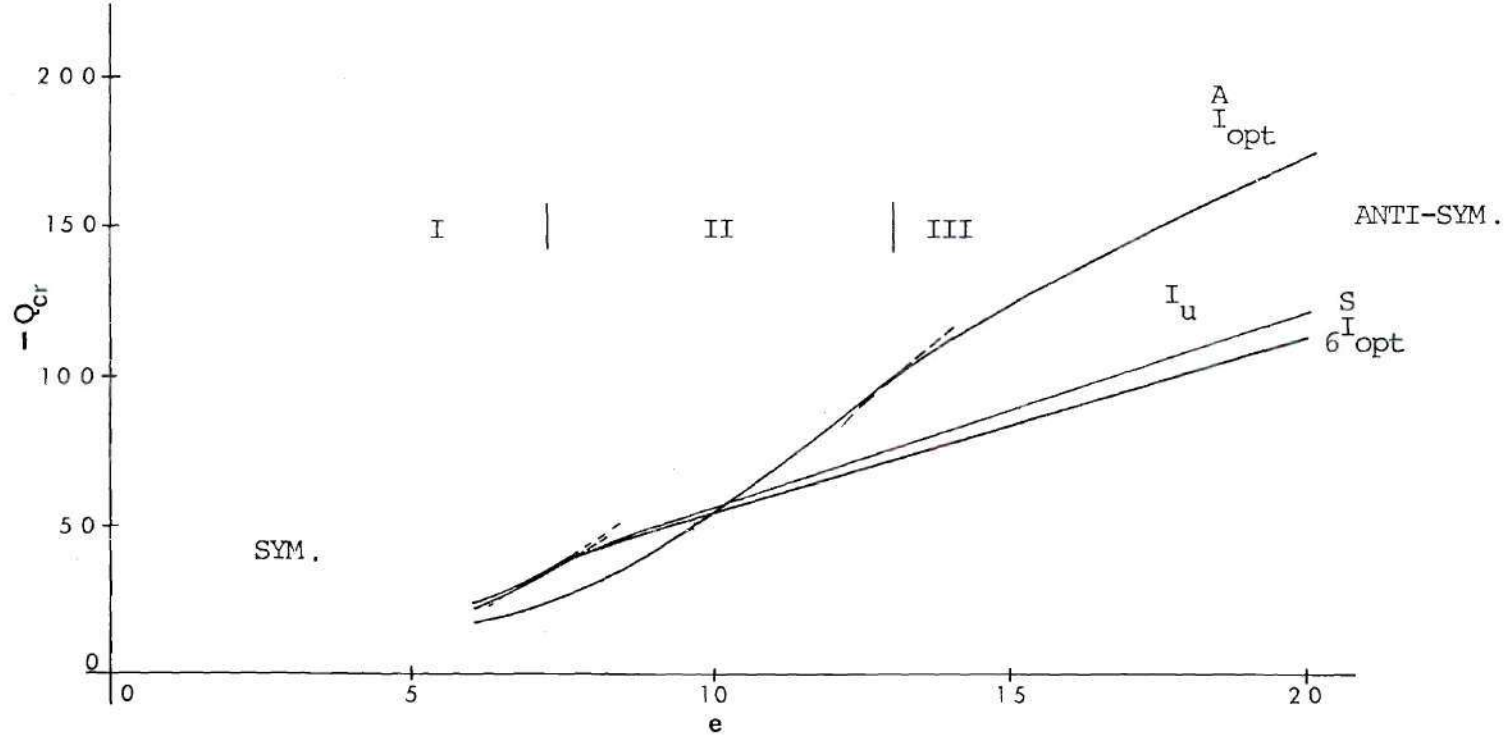

Fig. 15. Critical Response of I_u, I^A_{opt}, and $6I^S_{opt}$, $\beta_o=10, n=2$.

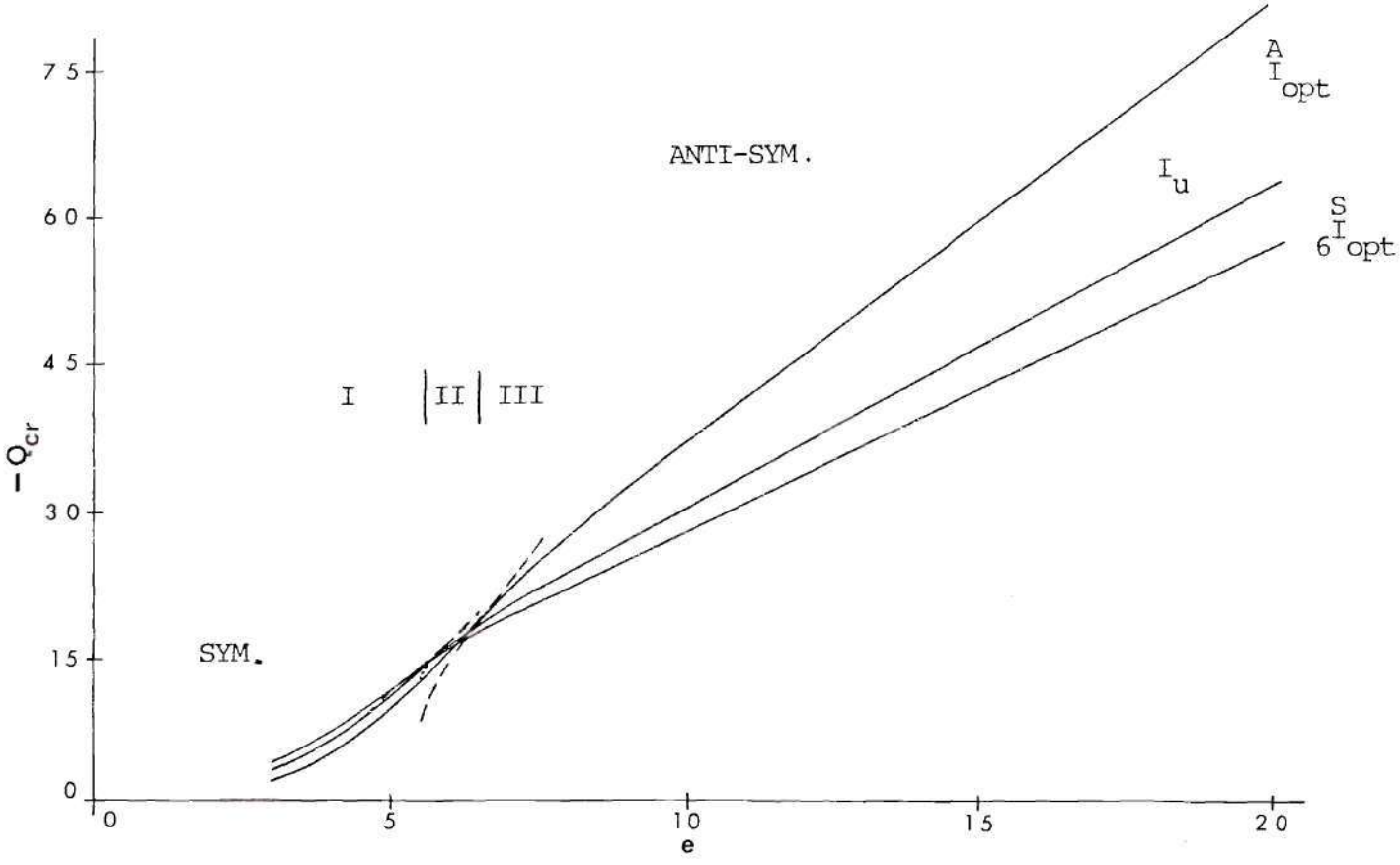

Fig. 16. Critical Response of I_u, I^A_{opt}, and $6I^S_{opt}$. $\beta_o=0$, n=2.

APPENDIX A

ANALYTICAL SOLUTION FOR UNIFORM ARCH BUCKLING

In Ref. (10), the author reports a methodology developed herein whereby critical conditions are obtained for a uniform arch subjected to arbitrary load distributions and with varying degrees of rotational restraint at the boundaries. The analytical solution is made tractable by the assumption of uniform inertia distribution; however, by the use of the finite element discretization of Chapter II, the methodology can be extended to arbitrary nonuniform geometries. For the case of snapping through the existence of a limit point, solution procedures are outlined utilizing either the buckling equation, Eq. (32), or the second variation of the total potential, Eq. (29) with the requirement that the buckling mode (at the limit point) resembles the primary path equilibrium response.

In the illustrations, the geometry is assumed to be uniform, $\bar{I} = 1$, $\bar{A} = 1$, and there is no elastic foundation, $\beta = 0$. The six particular examples, for which critical conditions are presented, are:

1) A simply supported low arch with half sine initial shape under a half sine transverse load distribution,

2) A clamped low arch with a half sine initial shape under a half sine load distribution,

3) A simply supported parabolic low arch under a uniform transverse loading,

4) A rotationally restrained low arch with a half sine initial shape under a half sine transverse loading,

5) A simply supported half sine low arch under a uniform transverse loading, and

6) A clamped half sine low arch under a uniform transverse loading.

Example 1: Simply Supported Half Sine Arch, Half Sine Loading

The initial shape and the loading are characterized by the following equations:

$$q(\xi) = q_o \sin\xi \quad F=0 \tag{A-1}$$

$$\eta_o(\xi) = e \sin\xi$$

The equilibrium equation and the boundary conditions for the primary path which is symmetric are given below

$$\eta^{(IV)} + \bar{p}\eta'' = Q \sin \xi \tag{A-2}$$

where

$$\bar{p} = -p, \text{ and } Q = q_o + e$$

$$\eta(0) = \eta''(0) = \eta' \left\{\frac{\pi}{2}\right\} = \eta''' \left\{\frac{\pi}{2}\right\} = 0 \tag{A-3}$$

The solution for η is given by

$$\eta(\xi) = - \frac{Q \sin \xi}{\bar{p}-1} \tag{A-4}$$

Substitution into Eq. (25) yields the $(\bar{p},Q,e)$ relation

$$\left[\frac{Q}{\bar{p}-1}\right]^2 = e^2 - 4\bar{p} \tag{A-5}$$

These two equations, Eqs. (A-4) and (A-5), hold true at every primary path equilibrium point. At a critical condition the equilibrium becomes unstable either through a bifurcation point (antisymmetric buckling mode) or through a limit point (top-of-the-knee symmetric buckling mode). Thus these two cases are considered separately and from the buckling equation, Eq. (32) the critical conditions are obtained.

a) Limit Point Analysis

For this particular example, the buckling equation becomes

$$\gamma^{(IV)} + \bar{p}\gamma'' + \frac{2\eta''}{\pi} \int_0^{\pi/2} \eta''\gamma d\xi = 0 \tag{A-6}$$

Since the primary path equilibrium is given by $\eta-\eta_o$ and since one is interested in a limit point instability, the buckling mode, γ, can be approximated by $\gamma = c(\eta-\eta_o)$, where c is some arbitrary constant. Note that this expression for

γ satisfies the buckling boundary conditions, Eq. (33). Substitution of this expression for γ into the buckling equation, Eq. (A-6) and performing the indicated operations yield

$$\left[\frac{Q_{cr}}{\bar{p}_{cr}-1} + e\right]\left[\left(\frac{Q_{cr}}{\bar{p}_{cr}-1}\right)^2 - 2(\bar{p}-1)\right] \sin\xi = 0 \quad \text{(A-7)}$$

where Q_{cr} and $\bar{p}_{cr}$ refer to values of Q and $\bar{p}$ at the limit point. Since the limit point is also an equilibrium point, the simultaneous satisfaction of Eqs. (A-7) and (A-5) yields

$$Q_{cr} = -\tfrac{1}{2}\left\{\frac{e^2-4}{3}\right\}^{3/2} \qquad e > 2 \quad \text{(A-8)}$$

$$\bar{p}_{cr} = \frac{e^2+2}{6}$$

and the position of the limit point at the midpoint of the arch $\eta(\frac{\pi}{2})$ is given by Eq. (A-4)

$$\eta_{L_p}(\tfrac{\pi}{2}) = \frac{e^2-4}{3} \quad \text{(A-9)}$$

Note that in Eq. (A-8) the negative Q is taken, which yields a positive $\eta_{L_p}(\frac{\pi}{2})$, because the unloaded position of the arch is characterized by $Q = e$, $\eta(\frac{\pi}{2}) = e$ and the first limit point is given by Q_{cr} and η_{L_p} as denoted by Eqs. (A-8) and

(A-9). The second limit point is characterized by

$$Q_{cr} = \tfrac{1}{2}\left(\frac{e^2-4}{3}\right)^{3/2} \quad \text{and} \quad \eta_{\bar{p}}\left(\frac{\pi}{2}\right) = \frac{e^2-4}{3} \qquad \text{(A-10)}$$

These results are in complete agreement with those reported in Refs. (29) and (33).

An alternative approach is demonstrated for the limit point analysis by utilizing the fact that the second variation of the total potential vanishes at the critical point, namely when there exists a non-trivial solution to the buckling equations and the equilibrium conditions are simultaneously satisfied. Substituting the equilibrium solution Eq. (A-4) into the second variation, Eq. (29), one obtains

$$V[Q,\bar{p},e] = \left\{\frac{Q}{\bar{p}-1} + e\right\}^2 \left[-\bar{p}\int_o^\pi \cos^2\xi d\xi + \int_o^\pi \sin^2\xi d\xi + \frac{1}{\pi}\left\{\frac{Q}{\bar{p}-1}\right\}^2 \int_o^\pi \cos^2\xi d\xi\right]$$

which becomes, after performing the integrations,

$$\left(\frac{Q}{\bar{p}-1} + e\right)^2 \left(\left\{\frac{Q}{\bar{p}-1}\right\}^2 - 2(\bar{p}-1)\right) = 0$$

Now the first term cannot vanish since this implies when solved with Eq. (A-5) the trivial solution $\bar{p} = Q = 0$; thus, to obtain the critical conditions for the limit point, one must solve

together the following:

$$\left(\frac{Q}{\bar{p}-1}\right)^2 = 2(\bar{p} - 1)$$

and

$$\left(\frac{Q}{\bar{p}-1}\right)^2 = e^2 - 4\bar{p} \qquad \text{(A-5)}$$

The results of this approach are identical to those reflected by Eq. (A-8) for this case. Note that either of the approaches depends upon being able to form an explicit solution for the equilibrium equation. The limit point analysis approach can be utilized for any of the examples presented here, but the simultaneous solution of the resulting algebraic equations cannot be effected in closed form as was done for example one; hence, one must resort to numerical techniques to obtain the critical conditions.

b) Bifurcation Point Analysis

For the case of instability through an anti-symmetric mode (bifurcation) γ, which is orthogonal to the symmetric primary path $\eta(\xi)$, the integral in Eq. (A-6) vanishes and the buckling condition becomes

$$\gamma'''' + \bar{p}\gamma'' = 0 \qquad \text{(A-11)}$$

subject to the conditions

$$\gamma(0) = \gamma''(0) = \gamma\left[\frac{\pi}{2}\right] = \gamma''\left[\frac{\pi}{2}\right] = 0 \qquad \text{(A-12)}$$

The solution to this equation is

$$\gamma = A \sin 2m\xi \qquad m = 1,2,\ldots 3 \tag{A-13}$$

$$\bar{p} = 4m^2$$

$$Q = -(4m^2 - 1)(e^2 - 16m^2)^{\frac{1}{2}} \tag{A-14}$$

The smallest $Q(Q_{cr})$ occurs at $m = 1$, therefore

$$\bar{p}_{cr} = 4, \quad Q_{cr} = -3(e^2 - 16)^{\frac{1}{2}}, \quad e > 4 \tag{A-15}$$

and

$$\eta_{L_p}\left(\frac{\pi}{2}\right) = (e^2 - 16)^{\frac{1}{2}} \tag{A-16}$$

These results also agree with those reported in Refs. (29) and (33).

The results are graphically presented in Fig. A1 as Q_{cr} versus the rise parameter, e. Note that although anti-symmetric bifurcation is possible for $e > 4$, snapping occurs through a limit point as long as $e \leq \sqrt{22}$ and thus Q_{cr} is given by Eq. (A-8) for $2 < e < \sqrt{22}$.

Example 2: Clamped Half Sine Arch, Half Sine Loading

For this particular case, the initial shape and the loading are also characterized by Eqs. (A-1).

Following the same procedure as in Example 1, the primary path equilibrium points are characterized by

$$\eta(\xi) = \bar{A}\left[\cos\sqrt{\bar{p}}\left\{\xi - \frac{\pi}{2}\right\} - \cos\sqrt{\bar{p}}\frac{\pi}{2}\right] - \frac{Q\sin\xi}{\bar{p}-1} \quad \text{(A-17)}$$

where

$$\bar{A} = \left(e + \frac{Q}{\bar{p}-1}\right)\sqrt{\bar{p}}\ \sin\sqrt{\bar{p}}\ \frac{\pi}{2} \quad \text{(A-18)}$$

Substitution of this expression for η, Eq. (A-17), into Eq. (25), yields the following $(\bar{p},Q,e)$ relation

$$B_1Q^2 + B_2Q + (B_3 - B_4) = 0 \quad \text{(A-19)}$$

where

$$B_1 = \left\{\frac{1}{\bar{p}-1}\right\}^2\left\{\frac{\sqrt{\bar{p}}\pi - \sin\sqrt{\bar{p}}\pi}{4\sqrt{\bar{p}}\sin^2\sqrt{\bar{p}}\frac{\pi}{2}} + \frac{2\sqrt{\bar{p}}\cot\sqrt{\bar{p}}\frac{\pi}{2}}{\bar{p}-1} + \frac{\pi}{4}\right\} \quad \text{(A-20)}$$

$$B_2 = \left\{\frac{2e}{\bar{p}-1}\right\}\left\{\frac{\sqrt{\bar{p}}\pi - \sin\bar{p}\pi}{4\sqrt{\bar{p}}\sin^2\bar{p}\frac{\pi}{2}} + \frac{\sqrt{\bar{p}}\cot\sqrt{\bar{p}}\frac{\pi}{2}}{\bar{p}-1}\right\}$$

$$B_3 = e^2\left\{\frac{\sqrt{\bar{p}}\pi - \sin\sqrt{\bar{p}}\pi}{4\sqrt{\bar{p}}\sin^2\sqrt{\bar{p}}\frac{\pi}{2}}\right\}$$

$$B_4 = \frac{\pi}{4}\left[e^2 - 4\bar{p}\right]$$

a) Limit Point Analysis

As before, characterizing the buckling mode γ by $\gamma = c(\eta - \eta_o)$, substituting this and the expression for η into the buckling equation, Eq. (A-6), performing the indicated operations and evaluating this equation at $\xi = \frac{\pi}{2}$ (midpoint of the arch), the following relationship is obtained between $\bar{p}_{cr}$ and Q_{cr} for every e value, at the limit point.

$$[B_5 Q_{cr} + B_6]\ [B_1 Q_{cr}^2 + B_2 Q_{cr} + B_3 + B_7 Q_{cr} + B_8] \qquad \text{(A-21)}$$

$$= B_9 Q_{cr} + B_{10}$$

where B_1, B_2, and B_3 are given by Eqs. (A-20), and

$$B_5 = \left\{\frac{1}{\bar{p}_{cr}-1}\right\} \left\{1 - \frac{\sqrt{\bar{p}_{cr}}}{\sin \sqrt{\bar{p}_{cr}}\ \frac{\pi}{2}}\right\} \qquad \text{(A-22)}$$

$$B_6 = - \frac{e \sqrt{\bar{p}_{cr}}}{\sin \sqrt{\bar{p}_{cr}}\ \frac{\pi}{2}}$$

$$B_7 = \left[\frac{e}{\bar{p}_{cr}-1}\right] \left\{\frac{\sqrt{\bar{p}_{cr}}\ \cot \sqrt{\bar{p}_{cr}}\ \frac{\pi}{2}}{\bar{p}_{cr}-1} + \frac{\pi}{4}\right\}$$

$$B_8 = e^2 \left\{\frac{\sqrt{\bar{p}_{cr}}\ \cot \sqrt{\bar{p}_{cr}}\ \frac{\pi}{2}}{\bar{p}_{cr}-1}\right\}$$

$$B_9 = \frac{\pi}{2} \quad \text{and} \quad B_{10} = \frac{\pi}{2}\, e(\bar{p}_{cr}-1)$$

A computer program is written to solve the two equations, Eqs. (A-19) and (A-21), simultaneously in order to obtain $\bar{p}_{cr}$ and $\bar{Q}_{cr}$. If these values are known, then $\eta_{L_p}\left[\frac{\pi}{2}\right]$ can easily be computed from Eqs. (A-17) for every value of the rise parameter, e.

The results are shown graphically in Fig.(A2) as Q_{cr} versus the rise parameter.

b) Bifurcation Analysis

For this particular example the buckling equation is still given by Eq. (A-11), but the boundary conditions are

$$\gamma(0) = \gamma'(0) = 0 \qquad \text{(A-23)}$$

$$\gamma\left[\frac{\pi}{2}\right] = \gamma''\left[\frac{\pi}{2}\right] = 0$$

The lowest positive root of the following transcendental equation denotes $\bar{p}_{cr}$:

$$\sqrt{\bar{p}}\,\frac{\pi}{2} = \tan\sqrt{\bar{p}}\,\frac{\pi}{2} \qquad \text{(A-24)}$$

Thus

$$\bar{p}_{cr} = 8.1842$$

With this value for $\bar{p}_{cr}$, substitution into Eq. (A-19) yields

$$Q_{cr} = 3.5914[-e - (e^2 - 58.8297)^{\frac{1}{2}}] \qquad \text{(A-25)}$$

for $e > 7.67$

Again as before, although it is possible to have anti-symmetric bifurcation for $e > 7.67$, snapping takes place through the existence of a limit point (symmetric snapping) for $e \leq 9.00$ (see Fig. A2).

Example 3: Simply Supported Parabolic Arch, Uniform Loading

The initial shape and loading for this example are characterized by the following:

$$q(\xi) = q; \qquad F = 0 \tag{A-26}$$

$$\eta_o(\xi) = \frac{4e}{\pi^2}\,\xi\,(\pi-\xi)$$

The primary path equilibrium points are characterized by

$$\eta(\xi) = \frac{C_1}{\cos\sqrt{\bar{p}}\,\frac{\pi}{2}}\left\{\cos\sqrt{\bar{p}}\,\left[\xi - \frac{\pi}{2}\right] - \cos\sqrt{\bar{p}}\frac{\pi}{2}\right\} + \frac{q}{2\bar{p}}\,\xi(\xi-\pi) \tag{A-27}$$

where

$$C_1 = \frac{q}{\bar{p}^2} + \frac{8e}{\bar{p}\pi^2}$$

Substitution of this expression for η, Eq. (A-27), into Eq. (25) yields the following $(\bar{p},Q,e)$ relation which holds true at every point on the equilibrium primary path.

$$q^2 C_2 + qC_3 + C_4 = C_5 \tag{A-28}$$

where

$$C_2 = \frac{1}{\bar{p}^2} \left[\frac{\sqrt{\bar{p}}\pi - \sin\sqrt{\bar{p}}\pi}{4\bar{p}\sqrt{\bar{p}}\cos^2\sqrt{\bar{p}}\frac{\pi}{2}} + \frac{\pi^3}{24} - \frac{2}{\bar{p}\sqrt{\bar{p}}} \left(\tan\sqrt{\bar{p}}\frac{\pi}{2} - \sqrt{\bar{p}}\frac{\pi}{2} \right) \right] \tag{A-29}$$

$$C_3 = \frac{16e}{\bar{p}\pi^2} \left[\frac{\sqrt{\bar{p}}\pi - \sin\sqrt{\bar{p}}\pi}{4\bar{p}\sqrt{\bar{p}}\cos^2\sqrt{\bar{p}}\frac{\pi}{2}} - \frac{1}{\bar{p}\sqrt{\bar{p}}} \left(\tan\sqrt{\bar{p}}\frac{\pi}{2} - \sqrt{\bar{p}}\frac{\pi}{2} \right) \right]$$

$$C_4 = \frac{64e^2}{\pi^4} \left[\frac{\sqrt{\bar{p}}\pi - \sin\sqrt{\bar{p}}\pi}{4\bar{p}\sqrt{\bar{p}}\cos^2\sqrt{\bar{p}}\frac{\pi}{2}} \right]$$

$$C_5 = \frac{8}{3\pi} \left(e^2 - \frac{3\bar{p}\pi^2}{8} \right)$$

a) Limit Point Analysis

Characterizing the buckling mode γ by $\gamma = c(\eta - \eta_o)$ and following all the steps as in the two previous examples, the following relation is obtained for $\bar{p}_{cr}$ and $\bar{q}_{cr}$ for every e value at the limit point.

$$(c_6 q_{cr} + c_7)[c_2 q_{cr}^2 + c_3 q_{cr} + c_4 + c_8 q_{cr} + c_9] = c_{10} q_{cr} + c_{11} \tag{A-30}$$

where c_2, c_3, c_4 and c_5 are given by Eqs. (A-29) and

$$C_6 = \frac{1}{\bar{p}} \left(1 - \frac{1}{\cos\sqrt{\bar{p}}\frac{\pi}{2}} \right) \tag{A-31}$$

$$C_7 = \frac{8e}{\pi^2 \cos \sqrt{\bar{p}}\ \frac{\pi}{2}} \qquad \text{(A-31)}$$

$$C_8 = \frac{8e}{\bar{p}\ \pi^2} \left[\frac{\pi^3}{24} - \frac{1}{\bar{p}\sqrt{\bar{p}}} \left(\tan \sqrt{\bar{p}}\ \frac{\pi}{2} - \sqrt{\bar{p}}\ \frac{\pi}{2} \right) \right]$$

$$C_9 = - \frac{64e^2}{\pi^4 \bar{p} \sqrt{\bar{p}}} \left(\tan \sqrt{\bar{p}}\ \frac{\pi}{2} - \sqrt{\bar{p}}\ \frac{\pi}{2} \right)$$

$$C_{10} = \frac{\pi}{2} \text{ and } C_{11} = 4\bar{p}\ e/\pi$$

The simultaneous solution of Eqs. (A-28) and (A-30) yields q_{cr} and the corresponding $\bar{p}_{cr}$ for each e value. The results are presented graphically in Fig. (A3).

b) Bifurcation Analysis

The buckling equation and boundary conditions for anti-symmetric modes are identical to those for Example 1, Eqs. (A-11) and (A-12). Therefore

$$\bar{p}_{cr} = 4 \quad \text{and} \quad \gamma(\xi) = A \sin 2\xi.$$

Following the same procedure as in Example 1, one obtains the following expression for q_{cr}.

$$q_{cr} = 0.83998\ [-e - 2.8598(e^2 - 15.3231)^{\frac{1}{2}}] \qquad \text{(A-32)}$$

$$e > 3.9144$$

Note that although antisymmetric modes are possible for $e > 3.9144$, q_{cr} corresponds to a symmetric mode for $e < 5.105$. Therefore the expression for q_{cr} given by Eq. (A-32) is applicable only to $e > 5.105$. The reasons are clearly stated in the discussion of Example 1.

Example 4: Rotationally Restrained Half Sine Arch, Half Sine Loading

The initial shape and the loading for this case are characterized by

$$\eta_o(\xi) = e \sin \xi \tag{A-1}$$

$$q(\xi) = q_o \sin \xi, \qquad F = 0$$

The equilibrium equations becomes

$$\eta^{(IV)} + \bar{p}\,\eta'' = Q \sin \xi; \quad Q = q_o + e \tag{A-2}$$

The boundary conditions for this case are

$$\eta(0) = 0; \quad \eta''(0) = \beta_o[\eta'(0) - e] \tag{A-33}$$

$$\eta' \left\{\frac{\pi}{2}\right\} = \eta''' \left\{\frac{\pi}{2}\right\} = 0$$

Note that only half of the arch is considered and one seeks symmetric responses for $\eta(\xi)$ (primary equilibrium path).

The solution for η is given by

$$\eta(\xi) = R\bar{A}\left[\cos\sqrt{\bar{p}}\ \left(\xi - \frac{\pi}{2}\right) - \cos\sqrt{\bar{p}}\ \frac{\pi}{2}\right] - \frac{Q \sin \xi}{\bar{p} - 1} \qquad \text{(A-34)}$$

where $\bar{A}$ is given by Eq. (A-18) and

$$R = \frac{\beta_o \tan\sqrt{\bar{p}}\ \frac{\pi}{2}}{\beta_o \tan\sqrt{\bar{p}}\ \frac{\pi}{2} + \sqrt{\bar{p}}} \qquad \text{(A-35)}$$

Note that as $\beta_o \to 0$, Eq. (A-34) becomes identical to the solution of Example 1, as expected, and as $\beta_o \to \infty$, $R \to 1$ and this solution becomes identical to that for Example 2.

Proceeding as before, the $(\bar{p},Q,e)$ relation on the primary equilibrium path is obtained from Eq. (25).

$$D_1 Q^2 + D_2 Q + D_3 - D_4 = 0 \qquad \text{(A-36)}$$

where

$$D_1 = \left[\frac{1}{\bar{p}-1}\right]^2 \left\{R^2 \frac{\sqrt{\bar{p}}\pi - \sin\sqrt{\bar{p}}\ \pi}{4\sqrt{\bar{p}}\ \sin^2\sqrt{\bar{p}}\ \frac{\pi}{2}} + R\,\frac{2\sqrt{\bar{p}}\ \cot\sqrt{\bar{p}}\ \frac{\pi}{2}}{\bar{p} - 1} + \frac{\pi}{4}\right\}$$

$$D_2 = \frac{2e}{\bar{p}-1} \left\{R^2 \frac{\sqrt{\bar{p}}\pi - \sin\sqrt{\bar{p}}\pi}{4\sqrt{\bar{p}}\ \sin^2\sqrt{\bar{p}}\ \frac{\pi}{2}} + \frac{R\sqrt{\bar{p}}\ \cot\sqrt{\bar{p}}\ \frac{\pi}{2}}{\bar{p} - 1}\right\} \qquad \text{(A-37)}$$

$$D_3 = [R^2 e^2]\ \frac{\sqrt{\bar{p}}\pi - \sin\sqrt{\bar{p}}\ \pi}{4\sqrt{\bar{p}}\ \sin^2\sqrt{\bar{p}}\ \frac{\pi}{2}}$$

$$D_4 = \frac{\pi}{4}\ (e^2 - 4\bar{p})$$

The buckling equation is solved for the limit point and bifurcation point independently, as before.

a) Limit Point Analysis

Following the steps outlined previously the buckling equation yields the following equation that related $\bar{p}_{cr}$ to Q_{cr} for each e value.

$$(D_5Q + D_6)(D_1Q^2 + D_2Q + D_3 + D_7Q + D_8) = D_9Q + D_{10} \qquad \text{(A-38)}$$

where D_1, D_2, and D_3 are given by Eqs. (A-37), D_9 and D_{10} are the same as B_9 and B_{10} respectively, given by Eqs. (A-22), and

$$D_5 = \frac{1}{\bar{p}-1}\left\{1 - \frac{R\sqrt{\bar{p}}}{\sin\sqrt{\bar{p}}\,\frac{\pi}{2}}\right\}; \quad D_6 = -\frac{Re\sqrt{\bar{p}}}{\sin\sqrt{\bar{p}}\,\frac{\pi}{2}} \qquad \text{(A-39)}$$

$$D_7 = \frac{e}{\bar{p}-1}\left\{\frac{R\sqrt{\bar{p}}\cot\sqrt{\bar{p}}\,\frac{\pi}{2}}{\bar{p}-1} + \frac{\pi}{4}\right\}$$

$$D_8 = Re^2\,\frac{\sqrt{\bar{p}}\cot\sqrt{\bar{p}}\,\frac{\pi}{2}}{\bar{p}-1}$$

The results for this case are presented graphically in Fig. (A4) for β_o values of 0, 1, 10, 100, and ∞. Note that the results for the two extreme cases $\beta_o = 0$ and ∞ are in complete agreement with those of Examples 1 and 2 respectively.

b) Bifurcation Analysis

The buckling equation and the boundary conditions (antisymmetric buckling) for this case are

$$\gamma^{(IV)} + \bar{p}\,\gamma'' = 0 \qquad \text{(A-40)}$$

$$\gamma(0) = 0; \qquad \gamma''(0) = \beta_o \gamma'(0)$$

$$\gamma\left[\frac{\pi}{2}\right] = \gamma''\left[\frac{\pi}{2}\right] = 0$$

The characteristic equation for this eigenboundary value problem is given by

$$\sqrt{\bar{p}}\,\frac{\pi}{2} = \left[1 + \frac{\bar{p}\,\pi}{2\beta_o}\right] \tan \sqrt{\bar{p}}\,\frac{\pi}{2} \qquad \text{(A-41)}$$

This transcendental equation, Eq. (A-41), is solved for a number of β_o values. The corresponding value of $\bar{p}_{cr}$ (lowest eigenvalue) and the corresponding lowest value of e for which an antisymmetric mode is possible, e_{min}, are presented in Table A1. (For final results, see Fig. A5).

Note that the first and last rows of Table A1, are in complete agreement with the results of Examples 1 and 2 respectively.

Table A1. Effect of Rotational Restraint on the Critical Axial Stress, $\bar{p}$, and Lowest Rise Parameter for Antisymmetric Buckling.

β_o	$\bar{p}$	e_{min}
0	4.0000	4.000
1	5.0181	4.587
10	7.3002	6.686
100	8.0805	7.558
∞	8.1842	7.670

Examples 5 and 6: Simply Supported and Clamped Half Sine Arch, Uniform Loading

The initial shape and the loading for both examples are characterized by

$$q(\xi) = q; \qquad F = 0$$

$$\eta_o(\xi) = e \sin \xi$$

For the sake of brevity, only the final equations are listed. The procedure employed is the same as for all previous examples.

Equilibrium Solution

Simply Supported

$$\eta(\xi) = \frac{q}{\bar{p}^2 \cos \sqrt{\bar{p}}\frac{\pi}{2}} \left\{ \cos \sqrt{\bar{p}}\left(\xi - \frac{\pi}{2}\right) - \cos \sqrt{\bar{p}}\frac{\pi}{2} \right\} + \frac{q\xi(\xi - \pi)}{2\bar{p}} - \frac{e \sin \xi}{\bar{p} - 1} \tag{A-42}$$

Clamped

$$\eta(\xi) = \frac{\sqrt{\bar{p}}}{\sin \sqrt{\bar{p}}\frac{\pi}{2}} \left\{ \frac{e}{\bar{p}-1} + \frac{q}{2\bar{p}^2} \right\} \left\{ \cos \sqrt{\bar{p}}\left(\xi - \frac{\pi}{2}\right) - \cos \sqrt{\bar{p}}\,\frac{\pi}{2} \right\} + \frac{q\xi(\xi-\pi)}{2\bar{p}} - \frac{e \sin \xi}{\bar{p} - 1} \tag{A-43}$$

($\bar{p}$, q, e) Relation on Primary Equilibrium Path

$$E_1 q^2 + E_2 q + E_3 - E_4 = 0 \qquad \text{(A-44)}$$

where the constants for these two examples are Simply Supported

$$E_1 = \frac{1}{\bar{p}^2}\left\{\frac{\sqrt{\bar{p}}\pi - \sin\sqrt{\bar{p}}\pi}{4\bar{p}\sqrt{\bar{p}}\cos^2\sqrt{\bar{p}}\frac{\pi}{2}} + \frac{\pi^3}{24} - \frac{2}{\bar{p}\sqrt{\bar{p}}}\left[\tan\sqrt{\bar{p}}\frac{\pi}{2} - \sqrt{\bar{p}}\,\frac{\pi}{2}\right]\right\} \qquad \text{(A-45)}$$

$$E_2 = \frac{2e}{(\bar{p}-1)^2} \; ; \quad E_3 = \left(\frac{e}{\bar{p}-1}\right)^2\frac{\pi}{4} \; ; \quad E_4 = \frac{\pi}{4}(e^2 - 4\bar{p})$$

Clamped

$$E_1 = \frac{1}{\bar{p}^2}\left\{\frac{\pi^2}{4}\cdot\frac{\sqrt{\bar{p}}\pi - \sin\sqrt{\bar{p}}\pi}{4\sqrt{\bar{p}}\sin^2\sqrt{\bar{p}}\frac{\pi}{2}} + \frac{\pi^3}{24} - \frac{\pi}{\bar{p}}\left[1 - \sqrt{\bar{p}}\frac{\pi}{2}\cot\sqrt{\bar{p}}\frac{\pi}{2}\right]\right\} \qquad \text{(A-46)}$$

$$E_2 = \frac{e\pi}{\bar{p}-1}\left\{\frac{\sqrt{\bar{p}}\pi - \sin\sqrt{\bar{p}}\pi}{4\sqrt{\bar{p}}\sin^2\sqrt{\bar{p}}\,\frac{\pi}{2}} + \frac{\sqrt{\bar{p}}}{\bar{p}-1}\cot\sqrt{\bar{p}}\,\frac{\pi}{2}\right\}$$

$$E_3 = \left(\frac{e}{\bar{p}-1}\right)^2\left\{\bar{p}^2\,\frac{\sqrt{\bar{p}}\pi - \sin\sqrt{\bar{p}}\pi}{4\;\bar{p}\sin^2\sqrt{\bar{p}}\,\frac{\pi}{2}} + \frac{2\bar{p}\sqrt{\bar{p}}\cot\sqrt{\bar{p}}\frac{\pi}{2}}{\bar{p}-1} + \frac{\pi}{4}\right\}$$

$$E_4 = \frac{\pi}{4}(e^2 - 4\bar{p})$$

Symmetric Buckling Equation [Limit Point $\bar{p}_{cr}$, q_{cr}, e relation.

$$(E_5 q + E_6)[E_1 q^2 + E_2 q + E_3 + E_7 q + E_8] = E_9 q + E_{10} \qquad \text{(A-47)}$$

where constants E_1, E_2 and E_3 are given by Eqs. (A-45) and (A-46) for the simply supported and clamped cases respectively, and Simply Supported Case

$$E_5 = \frac{1}{\bar{p}} \left\{ 1 - \frac{1}{\cos \sqrt{\bar{p}}\, \frac{\pi}{2}} \right\}; \quad E_6 = \frac{e}{\bar{p}-1} \tag{A-48}$$

$$E_7 = E_6 = \frac{e}{\bar{p}-1}; \quad E_8 = \frac{e^2 \pi}{4(\bar{p}-1)}$$

$$E_9 = \frac{\pi}{2}, \quad E_{10} = \bar{p} e\, \frac{\pi}{2}$$

Clamped

$$E_5 = \frac{1}{\bar{p}} \left\{ 1 - \frac{\sqrt{\bar{p}}\, \frac{\pi}{2}}{\sin \sqrt{\bar{p}}\, \frac{\pi}{2}} \right\}; \quad E_6 = \frac{e}{\bar{p}-1} \left\{ 1 - \frac{\bar{p}\sqrt{\bar{p}}}{\sin \sqrt{\bar{p}} \frac{\pi}{2}} \right\} \tag{A-49}$$

$$E_7 = \frac{e}{\bar{p}} \left\{ 1 + \frac{\sqrt{\bar{p}} \frac{\pi}{2}}{\bar{p} - 1} \cot \sqrt{\bar{p}}\, \frac{\pi}{2} \right\}; \quad E_9 = \frac{\pi}{2}$$

$$E_8 = \frac{e^2}{\bar{p}-1} \left\{ \frac{\pi}{4} + \frac{\bar{p}\sqrt{\bar{p}}}{\bar{p} - 1} \cot \sqrt{\bar{p}}\, \frac{\pi}{2} \right\}; \quad E_{10} = \bar{p} e\, \frac{\pi}{2}$$

Antisymmetric Critical Load Expression

Simply Supported

$$q_{cr} = - 0.7819e - 2.262\, (e^2 - 17.2705)^{\frac{1}{2}} \tag{A-50}$$

$$e > 4.15$$

Clamped

$$q_{cr} = - 3.9632e - 3.1554 \ (e^2 - 53.5015)^{\frac{1}{2}} \qquad \text{(A-51)}$$

$$e > 7.3144$$

The results for these two examples are presented graphically in Fig. (A6) and (A7).

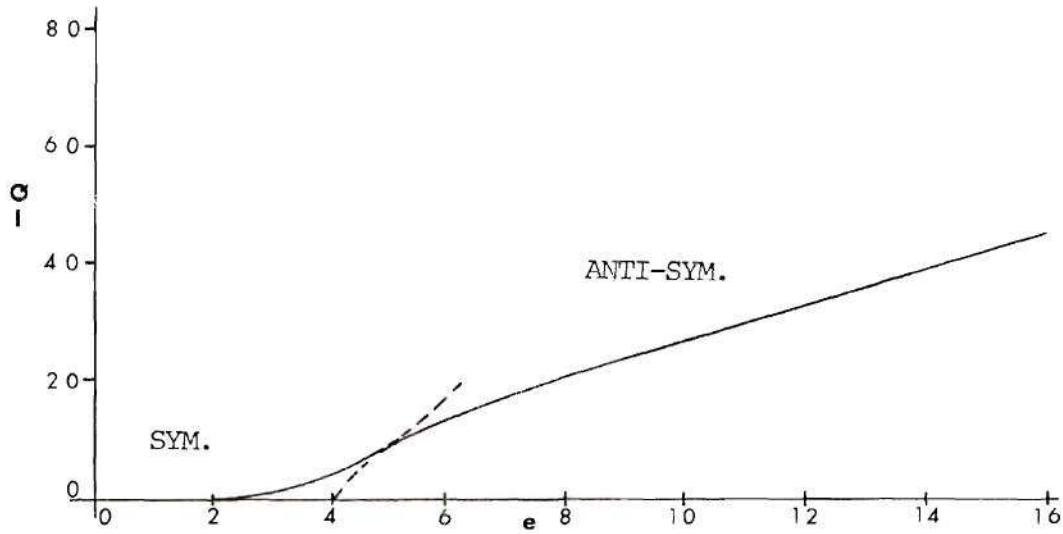

Fig. A1. Critical Load Vs. Rise Parameter, Simply Supported, Half Sine Load, Half Sine Arch.

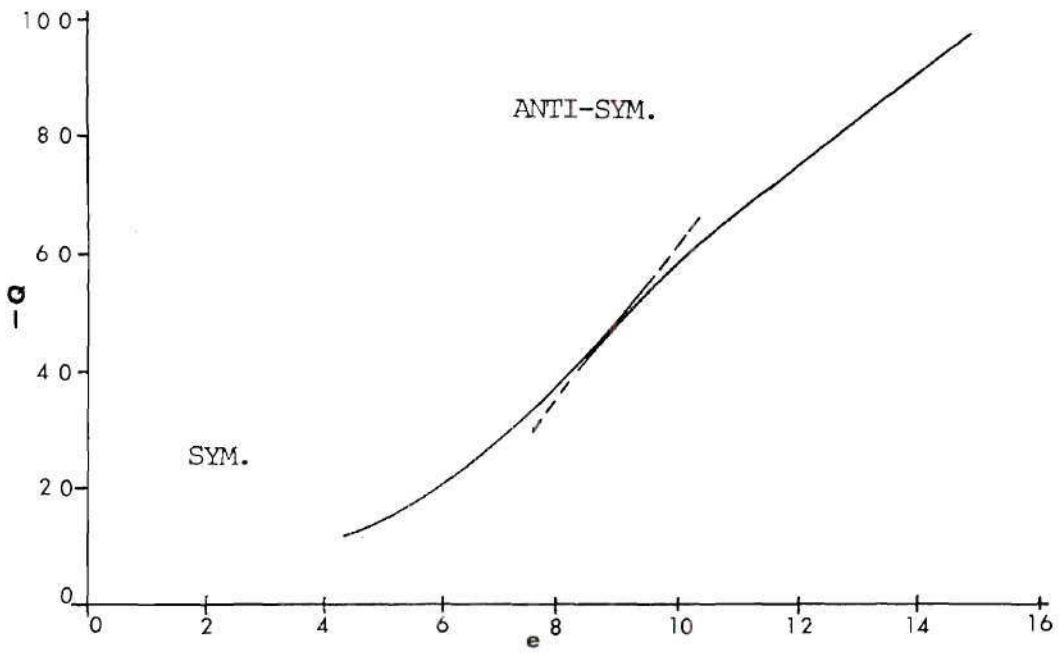

Fig. A2. Critical Load Vs. Rise Parameter, Clamped, Half Sine Load, Half Sine Arch.

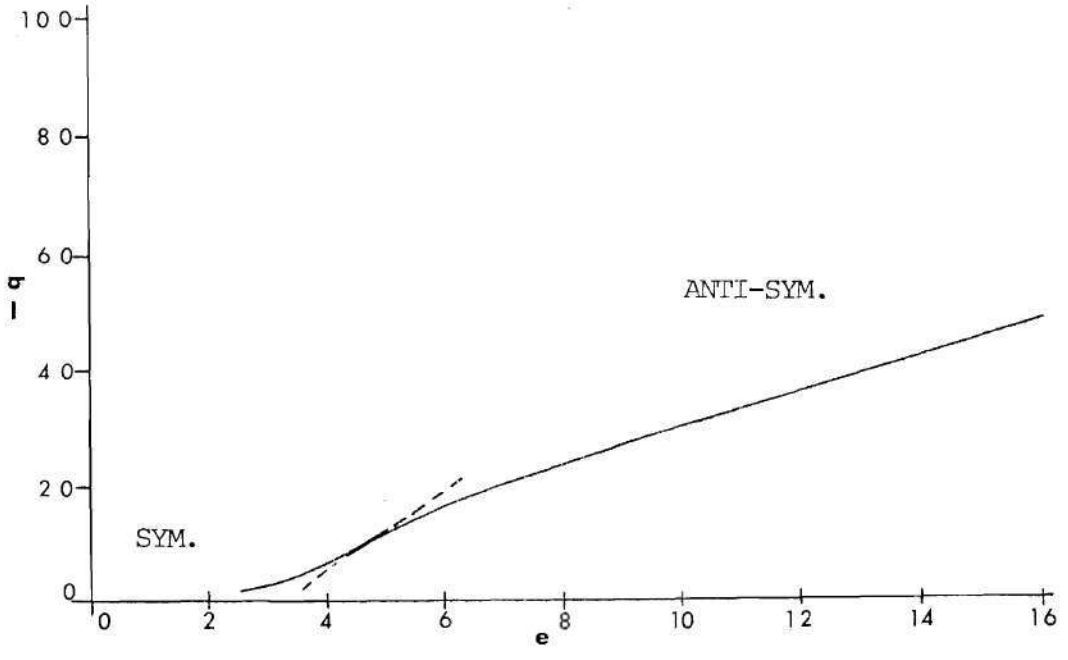

Fig. A3. Critical Load Vs. Rise Parameter, Simply Supported, Uniform Load, Parabolic Arch.

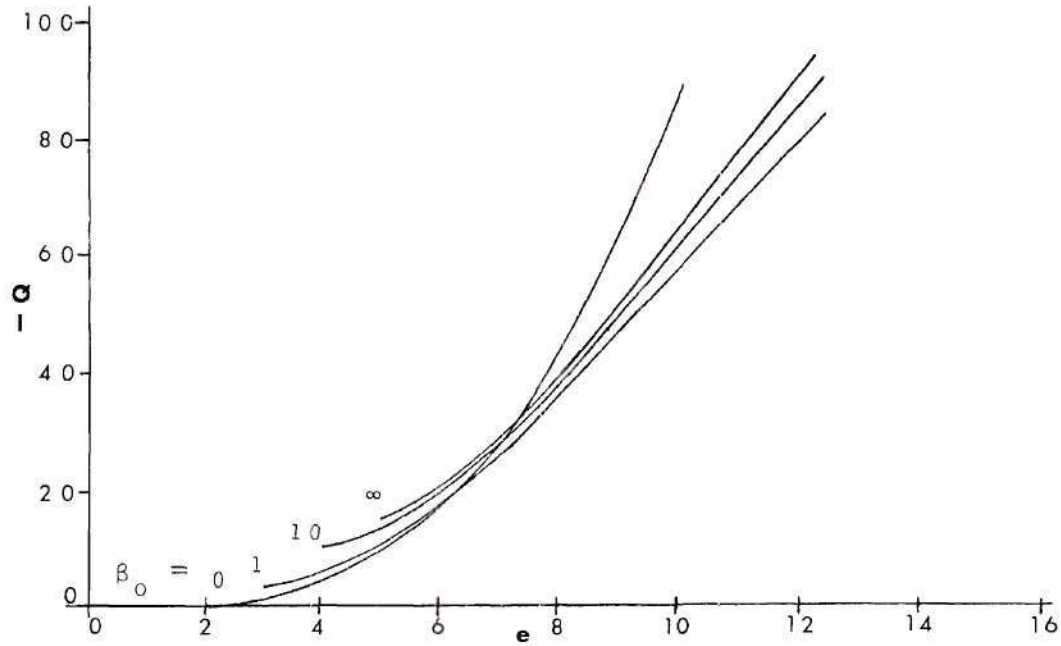

Fig. A4. Effect of Rotational Restraint, Symmetric Response.

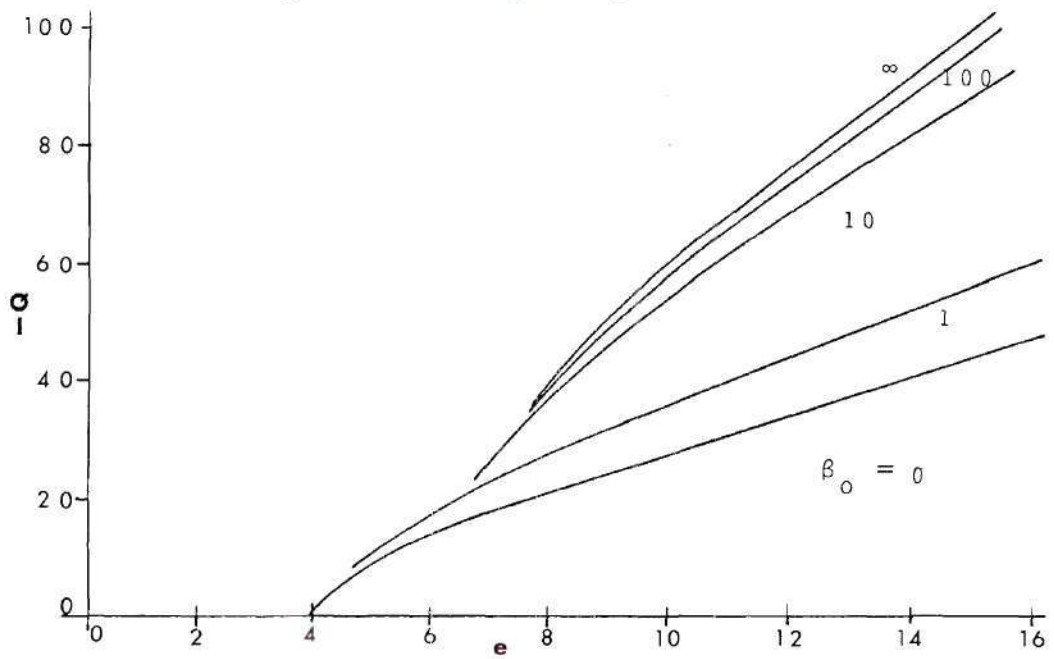

Fig. A5. Effect of Rotational Restraint, Anti-Symmetric Response, Half Sine Load, Half Sine Arch.

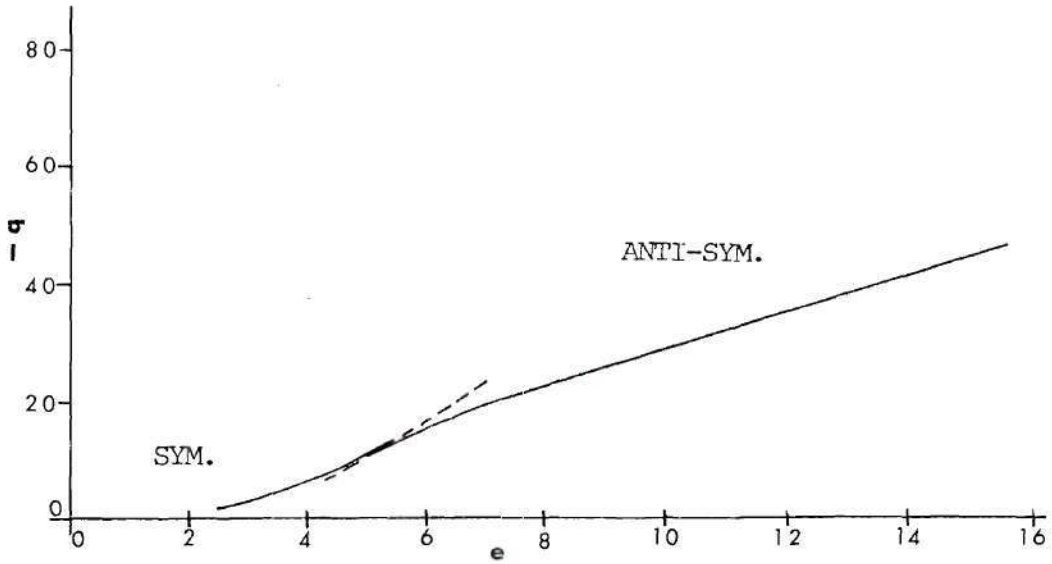

Fig. A6. Critical Load Vs. Rise Parameter, Simply Supported, Uniform Load, Half Sine Arch.

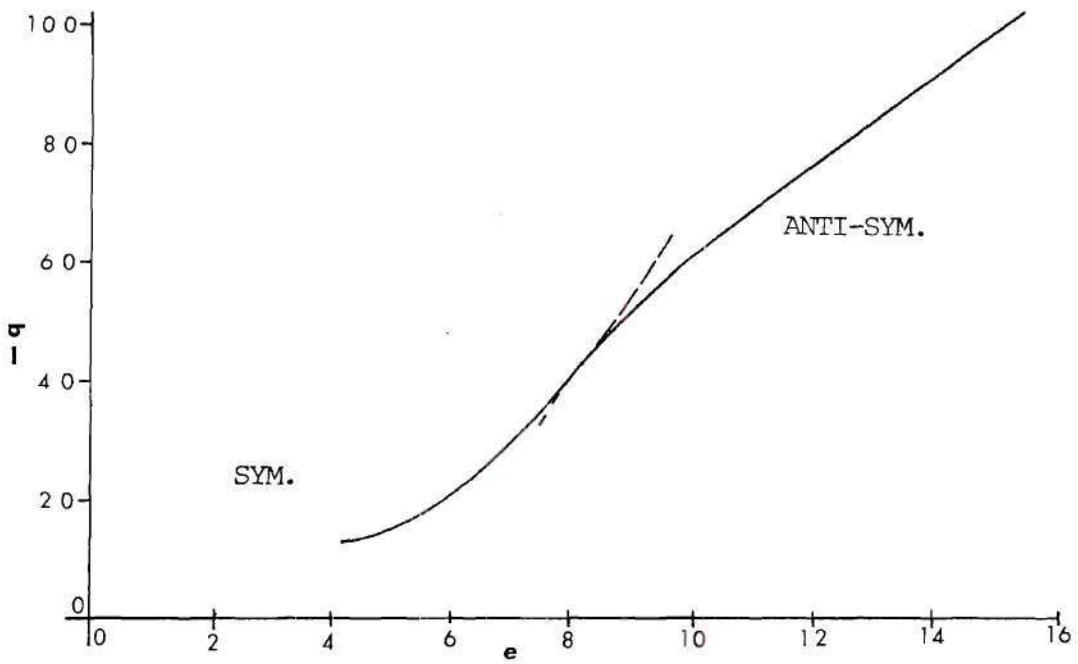

Fig. A7. Critical Load Vs. Rise Parameter, Clamped, Uniform Load, Half Sine Arch.

APPENDIX B

FINITE ELEMENT METHOD APPLIED TO BUCKLING OF SHALLOW ARCHES

In order to solve the nonlinear governing equations of Chapter II for the optimum design, it is essential to employ a numerical approach. The finite element displacement approach is chosen for the shallow arch problem because of its simplicity and high degree of reliability when applied to structural problems. Kamat (Ref. 49) employs a similar approach for his formulation of beam and plate optimization problems.

By discretizing the shallow arch along the ξ-axis into m finite elements as follows and considering the $i^{\underline{th}}$ such element,

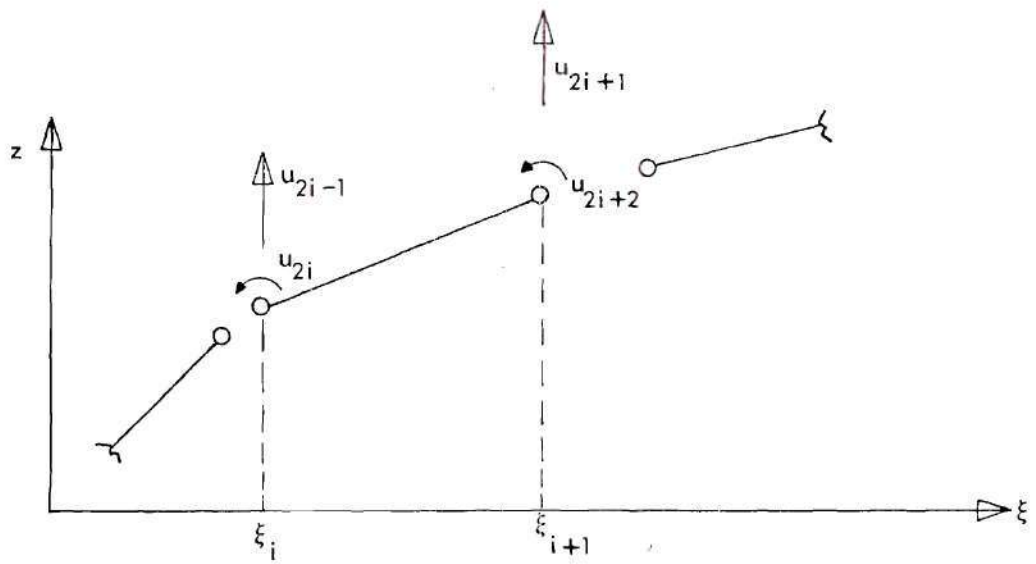

one may express the degrees of freedom of the arch in terms of its nodal displacements and rotations as,

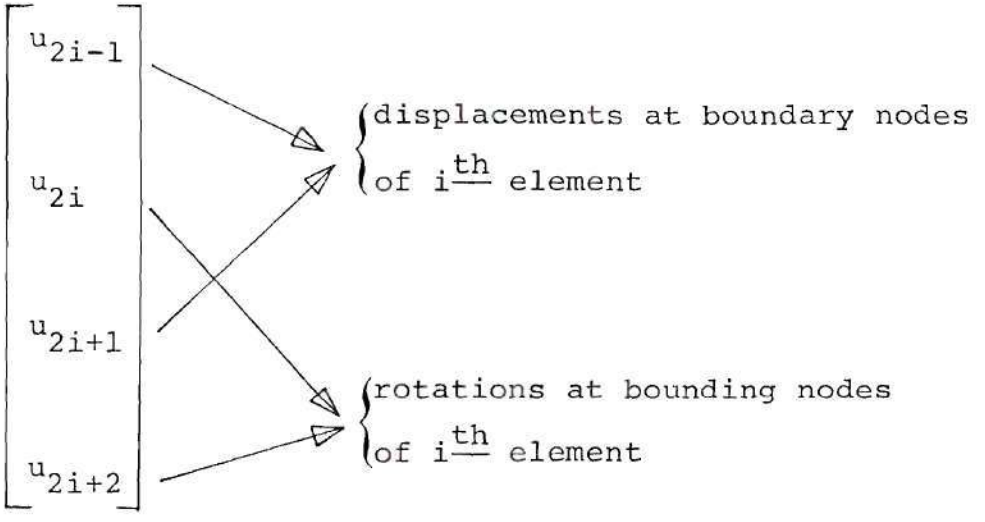

The displacement function $y(\xi)$ in Eq. (34) can be approximated in the $i^{\underline{th}}$ element in terms of a complete cubic. Such an approximation for the displacement is made on the grounds of compatibility and completeness which is necessary for convergence to the true solution as the element size shrinks to zero. Compatibility implies continuity of displacements at the boundaries (nodes) while the completeness requirement assures that the representation allows for rigid body motion and constant strain states within the element. Thus,

$$y^i(\xi) = a_o + a_1\xi + a_2\xi^2 + a_3\xi^3 \qquad \xi_i \leq \xi \leq \xi_{i+1} \tag{B-1}$$

$$= \underline{L}^T\underline{a}$$

where

$$\underline{L}^T = \begin{bmatrix} 1 & \xi & \xi^2 & \xi^3 \end{bmatrix}$$

and

$$\underline{a} = \begin{bmatrix} a_1 \\ a_2 \\ a_3 \\ a_4 \end{bmatrix}$$

By interpolating (B-1) in terms of its nodal values as follows:

$$y(\xi_i) = u_{2i-1} = \underline{L}^T(\xi_i)\ \underline{a}$$

$$y'(\xi_i) = u_{2i} = [\underline{L}^T(\xi_i)]'\ \underline{a}$$

$$y(\xi_{i+1}) = u_{2i+1} = \underline{L}^T(\xi_{i+1})\ \underline{a}$$

$$y'(\xi_{i+1}) = u_{2i+2} = [\underline{L}^T(\xi_{i+1})]'\ \underline{a}$$

for the $i^{\underline{th}}$ element, then (B-2) becomes,

$$\underline{u}^{(i)} = \begin{bmatrix} u_{2i-1} \\ u_{2i} \\ u_{2i+1} \\ u_{2i+2} \end{bmatrix} = [\underline{\underline{B}}]^{(i)}\ \underline{a} \qquad \text{(B-3)}$$

where matrix B for the $i^{\underline{th}}$ element is,

$$\underline{\underline{B}} \equiv \begin{bmatrix} 1 & \xi_i & \xi_i^2 & \xi_i^3 \\ 0 & 1 & 2\xi_i & 3\xi_i^2 \\ 1 & \xi_{i+1} & \xi_{i+1}^2 & \xi_{i+1}^3 \\ 0 & 1 & 2\xi_{i+1} & 3\xi_{i+1}^2 \end{bmatrix}$$

and relates the $\underline{a}_i$ to the $\underline{u}_i$.

From Eq. (B-3), vector $\underline{a}$ is given by

$$\underline{a} = \underline{\underline{B}}_i^{-1} \underline{u}_i$$

Substitution of this expression into Eq. (B-1) yields the displacement function for the $i^{\underline{th}}$ element,

$$y_i(\xi) = \underline{L}^T \quad \underline{\underline{B}}_i^{-1} \quad \underline{u}_i \qquad \xi_i \leq \xi \leq \xi_{i+1} \tag{B-4}$$

$i = 1,...m$

m = total number elements

The total potential $U_T(y)$, Eq. (34) is reproduced as follows:

$$U_T(y) = J\left[\int_o^\pi (y'^2 + 2y'\eta_o')d\xi\right]^2 + 2\beta\int_o^\pi y^2 d\xi \qquad \text{(B-5)}$$

$$+ 2\int_o^\pi \bar{I}(\xi)y''^2 d\xi - 4Q\int_o^\pi yN(\xi)d\xi$$

$$+ 2\beta_o[y'(0)^2 + y'(\pi)^2]$$

where

$$J = \frac{1}{2\int_o^\pi \frac{d\xi}{A}}$$

Note that the concentrated load term $4\int_o^\pi F\delta(\xi-\bar{\xi})d\xi$ has been omitted since it is not considered in the formulation of Chapter II. Furthermore, the continuous load function is expressed as $q_o(\xi) = QN(\xi)$ where $N(\xi)$ is given and the magnitude Q is unknown. The definition of J, Eq. (28) has been modified by elimination of the axial elastic restraint α_o at the boundaries. From Eq. (B-4) one may construct the following:

$$[y_i(\xi)]^2 = \underline{u}_i^T \underline{\underline{B}}_i^{-T} \underline{\underline{L}}\underline{\underline{L}}^T \underline{\underline{B}}_i^{-1} \underline{u}_i \qquad \text{(B-6)}$$

$$[y_i'(\xi)]^2 = \underline{u}_i^T \underline{\underline{B}}_i^{-T} \underline{\underline{L}}'\underline{\underline{L}}'^T \underline{\underline{B}}_i^{-1} \underline{u}_i$$

$$[y_i''(\xi)]^2 = \underline{u}_i^T \underline{\underline{B}}_i^{-T} \underline{\underline{L}}''\underline{\underline{L}}''^T \underline{\underline{B}}_i^{-1} \underline{u}_i$$

Substitution of Eqs. (B-4) and (B-6) into Eq. (B-5) yields the potential for the $i^{\underline{th}}$ element,

$$
\begin{aligned}
U_T^{(i)}(\underline{u}_i) = J\Big[&\underline{u}_i^T \left\{ \underline{\underline{B}}_i^{-T} \int_{\xi_i}^{\xi_{i+1}} \underline{L}'\underline{L}'^T d\xi \underline{\underline{B}}_i^{-1} \right\} \underline{u}_i \\
&+ 2\left\{ \int_{\xi_i}^{\xi_{i+1}} \eta_o'(\xi)\underline{L}'^T d\xi B_i^{-1} \right\} \underline{u}_i \Big]^2 \\
&+ 2\beta\, \underline{u}_i^T \left\{ \underline{\underline{B}}_i^{-T} \int_{\xi_i}^{\xi_{i+1}} \underline{L}\underline{L}^T d\xi \underline{\underline{B}}_i^{-1} \right\} \underline{u}_i \\
&+ 2\underline{u}_i^T \left\{ \underline{\underline{B}}_i^{-T} \int_{\xi_i}^{\xi_{i+1}} I^{(i)} \underline{L}''\underline{L}''^T d\xi \underline{\underline{B}}_i^{-1} \right\} \underline{u}_i \\
&- 4Q\left\{ \int_{\xi_i}^{\xi_{i+1}} N(\xi)\underline{L}^T d\xi \underline{\underline{B}}_i^{-1} \right\} \underline{u}_i \\
&+ 4\beta_o\, \underline{u}_1^T \left\{ \underline{\underline{B}}_1^{-T}\, \underline{L}_o'\underline{L}_o'^T \underline{\underline{B}}_1^{-1} \right\} \underline{u}_1
\end{aligned}
\tag{B-7}
$$

The total potential for the entire system is

$$
U_T(\underline{u}_i) = \sum_{i=1}^{m} U_T^{(i)}
$$

The summation and assembly process yields the following representation for the total potential

$$
\begin{aligned}
U_T(\underline{u}) = J[\underline{u}^T \underline{\underline{K}}_2 \underline{u} + 2\underline{V}_6^T \underline{u}]^2 \;+\; 2\,\underline{u}^T \underline{\underline{K}}_3\, \underline{u} \\
+ 2\underline{u}^T\, \underline{\underline{K}}_1\, \underline{u} - 4Q\, \underline{V}_5^T \underline{u} + 4\beta_o\, \underline{u}^T\, \underline{\bar{R}}\, \underline{\bar{R}}^T\, \underline{u}
\end{aligned}
\tag{B-8}
$$

where the following global terms are defined;

$$\underline{\underline{K}}_1 = \sum_{i=1}^{m} \underline{\underline{B}}_i^{-T} \left[I_i \int_{el} \underline{L}''\underline{L}''^T d\xi \right] \underline{\underline{B}}_i^{-1} \qquad \text{(B-9)}$$

$$\underline{\underline{K}}_2 = \sum_{i=1}^{m} \underline{\underline{B}}_i^{-T} \left[\int_{el} L'L'^T d\xi \right] \underline{\underline{B}}_i^{-1}$$

$$\underline{\underline{K}}_3 = \sum_{i=1}^{m} \underline{\underline{B}}_i^{-T} \left[\int_{el} LL^T d\xi \right] \underline{\underline{B}}_i^{-1}$$

$$\underline{V}_5 = \sum_{i=1}^{m} \left[\int_{el} N(\xi)\ \underline{L}^T d \right] \underline{\underline{B}}_i^{-1}$$

$$\underline{V}_6 = \sum_{i=1}^{m} \left[\int_{el} \eta_o'(\xi)\ \underline{L}'^T d\xi \right] B_i^{-1}$$

$$\underline{\bar{R}} = \left[\underline{\underline{B}}_{(1)}^{-T} \quad \underline{L}' \right]_{\xi=0} \qquad \xi_i \leq \xi \leq \xi_{i+1}$$

The above quantities in global form are of order (2m+2). The rotational restraint matrix $\underline{\bar{R}}\underline{\bar{R}}^T$ is assembled on the basis that $[y'(0)]^2 = [y'(\pi)]^2$. This is true for both symmetric and antisymmetric modes. In other words, under the action of symmetric loading, initial configuration and boundary conditions, the rotations at the boundary nodes are equal in magnitude. During the assembly of the stiffness matrix, $\underline{\underline{K}}_1$, for a given element the inertia I_i is constant and thus outside the integral. Furthermore, for simplicity, the length of each element is the same.

The total potential, Eq. (B-8), will now be used to amplify the development of the governing equations of Chapter II as well as the solution methodology of Chapter III. The displacement $\underline{u}$ of order (2m+2) gives the displacement and rotation at the (m+1) nodal points in the space $[0,\pi]$, under the action of the lateral load $QN(\xi)$ with the resultant axial thrust being that obtained by Eq. (38). The condition of symmetry for $\underline{u}$ can be given a physical interpretation. Assuming a node at the apex (i.e., the midpoint of the arch), for symmetry we require that the nodal displacements to the left of the apex be equal in magnitude and direction (sign) to those on the right (equidistant points); and the nodal rotations on the left be equal to and of opposite sign to those on the right. In addition, the apex rotation is zero while the apex displacement is arbitrary. Symbolically,

$$\underline{u}_R = \bar{\underline{\underline{T}}}_S \, \underline{u}_L$$

and

$$\underline{u} = \begin{bmatrix} \underline{u}_L \\ \underline{u}_R \end{bmatrix} \tag{B-10}$$

thus

$$\underline{u} = \begin{bmatrix} I \\ \bar{\underline{\underline{T}}}_S \end{bmatrix} \underline{u}_L = \underline{\underline{T}}_S \underline{u}_L$$

where $\underline{u}$ is of order (2m+2) x (1), $\bar{\underline{\underline{T}}}_S$ is (m) x (m+2) and $\underline{\underline{T}}_S$ is (2m+2) x (m+2).

For a simple 2 element model (m = 2), we can construct the following. (Note that $\underline{u}_L$ contains the apex):

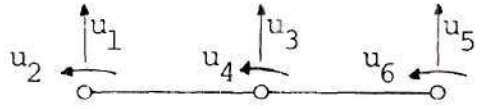

$$\underline{u} = \begin{bmatrix} u_1 \\ u_2 \\ u_3 \\ u_4 \\ u_5 \\ u_6 \end{bmatrix} = \begin{bmatrix} \underline{u}_L \\ \underline{u}_R \end{bmatrix}$$

For symmetry we must have $u_1 = u_5$

$u_2 = -u_6$

(The additional requirement that $u_4 = 0$ is imposed directly in the execution of the program and not through the assembly of the transformation matrix $\underline{T}_S$.) For this case

$$\begin{bmatrix} u_5 \\ u_6 \end{bmatrix} = \begin{bmatrix} -1 & 0 & 0 & 0 \\ 0 & -1 & 0 & 0 \end{bmatrix} \begin{bmatrix} u_1 \\ u_2 \\ u_3 \\ u_4 \end{bmatrix}$$

for $\underline{u}_R = \underline{\bar{T}}_S \underline{u}_L$

and

$$\underline{\underline{T}}_S = \left[\begin{array}{cccc} 1 & 0 & 0 & 0 \\ 0 & 1 & 0 & 0 \\ 0 & 0 & 1 & 0 \\ 0 & 0 & 0 & 1 \\ \hline -1 & 0 & 0 & 0 \\ 0 & -1 & 0 & 0 \end{array}\right] = \left[\begin{array}{c} \underline{\underline{I}} \\ \hline \\ \bar{\underline{\underline{T}}}_S \end{array}\right]$$

for $$\underline{u} = \underline{\underline{T}}_S \, \underline{u}_L$$

Substitution of Eq. (B-10) into Eq. (B-8) has the effect of reducing the order of all matrices and vectors from (2m+2) to (m+2) and thus promotes efficient use of computer storage and execution time. This transformation is carried out, where appropriate, during the assembly of the relevant quantities. The total potential becomes

$$U_T(\underline{u}_L) = J[\underline{u}_L^T \, \underline{\underline{K}}_2^* \, \underline{u}_L + 2\underline{V}_6^{*T} \, \underline{u}_L]^2 + 2\beta \underline{u}_L^T \, \underline{\underline{K}}_3^* \, \underline{u}_L \qquad \text{(B-11)}$$

$$+ 2\underline{u}_L^T \, \underline{\underline{K}}_1^* \, \underline{u}_L - 4Q\underline{V}_5^{*T} \, \underline{u}_L + 4\beta_o \underline{u}_L^T \, \bar{\underline{\underline{R}}}^* \bar{\underline{\underline{R}}}^{*T} \underline{u}_L$$

where

$$\underline{\underline{K}}_1^* = \underline{\underline{T}}_S^T \, \underline{\underline{K}}_1 \, \underline{\underline{T}}_S; \qquad \underline{\underline{K}}_2^* = \underline{\underline{T}}_S^T \, \underline{\underline{K}}_2 \, \underline{\underline{T}}_S, \quad \text{etc.}$$

During the solution process for symmetric snapping, the governing equations [Eqs. (38) (39) (42)] utilize the symmetry property of the equilibrium solution $\underline{u}$ as well as the buckling modes $\underline{v}$; hence, one need not be concerned with antisymmetry at all. On the other hand, for unstable bifurcation, the orthogonality of the buckling mode with respect to the symmetric primary path equilibrium configuration is crucial in formulating the eigenvalue problem for the critical conditions expressed by Eq. (41). In solving Eq. (41), one must impose antisymmetry on the buckling mode $\underline{v}$ first. This means that matrices $\underline{\underline{K}}_1$, $\underline{\underline{K}}_2$, $\underline{\underline{K}}_3$ and $\underline{\underline{R}}$ will be subjected to an anti-symmetric transformation to determine $\bar{p}_{cr}$ from Eq. (41) then must be symmetrically transformed to form the coefficients in Eq. (39) which reflect the required symmetry property of the equilibrium solutions $\underline{u}$. Such manipulations are easily carried out by the computer and for further details, one is referred to Appendix D.

In order to effect a solution, whether antisymmetric or symmetric, one must further specify the boundary conditions. (In effect, the apex becomes a boundary under the symmetry transformations). At the left boundary or support, we require that the vertical displacement be zero for all degrees of rotational restraint. The boundary and apex conditions are summarized as follows:

$$u_1 = 0 \qquad \text{vertical displacement at } \xi = 0$$

and either $u_2 = 0$ ($\beta_o \to \infty$), clamped case;

or u_2 arbitrary ($0 < \beta_o < \infty$), restrained case;

or u_2 arbitrary ($\beta_o = 0$), simply supported case;

with $u_{m+1} = 0$, apex displacement for anti-symmetry;

or $u_{m+2} = 0$, apex rotation for symmetry.

In practical application of the computer program, one specifies β_o. If β_o is set greater than 100, the program automatically imposes clamped boundary conditions ($u_1 = 0$, $u_2 = 0$). The value of 100 is arbitrary, but based upon some experience (see Appendix A) for uniform arch buckling with rotationally restrained boundaries. If β_o is set equal to zero, the program automatically imposes $u_1 = 0$ without any requirement on the boundary rotation. For the intermediate cases of β_o, one must examine the boundary restraint matrix $\underline{\underline{R}} = \bar{R}\bar{R}^T$ after it has been transformed by either symmetric or anti-symmetric transformations. As an example, consider the equilibrium equation, Eq. (39) which, by the principle of stationary value of total potential, is obtained from Eq. (34) or Eq. (B-11).

$$[\underline{\underline{K}}_1 - \bar{p}\underline{\underline{K}}_2 + \beta\underline{\underline{K}}_3 + \beta_o\underline{\underline{R}}]\underline{u} = \bar{p}\underline{V}_6 + Q\underline{V}_5 \qquad (39)$$

Matrix $\underline{\underline{R}}$, after transformation, is of the form

$$\underline{\underline{R}} = \begin{bmatrix} 0 & 0 & 0 & \cdots & 0 \\ 0 & 2 & 0 & \cdots & 0 \\ 0 & 0 & 0 & \cdots & 0 \\ \cdots & \cdots & \cdots & \cdots & \cdots \\ \cdots & \cdots & \cdots & \cdots & \cdots \\ \cdots & \cdots & \cdots & \cdots & \cdots \\ 0 & 0 & 0 & \cdots & 0 \end{bmatrix}$$

so that for finite non-zero values of β_o, one simply adds the quantity $2\beta_o$ to the appropriate element of the stiffness matrix $\underline{\underline{K}}_1$. This is readily seen to be an additional stiffness at the boundary and effectively restrains the change in rotation u_2 at the support. To impose the homogeneous boundary conditions at the support and the apex, the standard technique of zeroing out the appropriate rows and columns of all matrices and vectors is used (see Ref. (50) pp. 8-9). The imposition of boundary conditions could also be made mathematically by construction of some non-square transformation matrix relating the arbitrary vector $\underline{u}$ to the unrestrained degrees of freedom $\underline{u}_u$ in much the same way that the symmetry transformation matrix $\underline{\underline{\bar{T}}}_S$ is constructed. In either case, the system of equations is further reduced by the specification of 2 or 3 homogeneous conditions.

APPENDIX C

ANALYTIC APPROACH FOR ANTI-SYMMETRIC OPTIMIZATION

In Ref. 3 Tadjbakhsh and Kellar expand the earlier solution for the simply supported optimum column (Ref. 1) by including the cases for clamped at one end and clamped, hinged or free at the other. Since the buckling analysis for the column and the anti-symmetric buckling analysis for the critical thrust $\bar{p}_{cr}$ for the shallow arch are both governed by an eigenvalue problem, their solution procedure for the optimum shape is applicable. It will be shown that, for the simply supported case and n = 2 in the inertia area relation, a closed form solution can be obtained and approaches that obtained by the energy optimization methods depicted graphically in Fig.(5b). In addition to those boundary conditions considered in Ref. (3), an analytic solution procedure will be outlined which will allow for rotational restraint at the boundary.

Recalling the equations and relations governing the anti-symmetric optimization problem from Chapter II:

Optimality Condition:

$$\bar{\rho} n A(\xi)^{n-1} [\gamma''(\xi)]^2 = \lambda \qquad \text{(C-1)}$$

Definition of $\bar{p}$

$$\bar{p} = J \int_o^{\pi} \{(\eta_o')^2 - (\eta')^2\} d\xi \qquad (C\text{-}2)$$

Inertia/Area relation

$$I(\xi) = \bar{\rho} A^n(\xi) \qquad (C\text{-}3)$$

Constant Volume Condition

$$\int_o^{\pi} A(\xi) d\xi = \bar{v} \qquad (C\text{-}4)$$

and

$$J = 1 \div 2 \left[\int_o^{\pi} \frac{d\xi}{A(\xi)} + \hat{\alpha} \right] \qquad (C\text{-}5)$$

Solution for Asymmetric Buckling:

Consider the case without elastic foundation ($\beta \equiv 0$). The buckling Eq. (32) becomes,

$$[I(\xi)\gamma''(\xi)]'' + \bar{p}\gamma''(\xi) = 0 \qquad (C\text{-}6)$$

Following the solution procedure for the column eigenvalue problem (Ref. 3) let $\phi(\xi) = I(\xi)\gamma''(\xi)$ in (C-6) and obtain

$$\phi''(\xi) + \frac{\bar{p}}{I(\xi)} \phi(\xi) = 0 \qquad (C\text{-}7)$$

with boundary conditions

(a) $\phi(0) = 0$ simply supported

$\phi(\frac{\pi}{2}) = 0$

(b) $\phi(0) + \phi'(0)\ \frac{\pi}{2} = 0$ clamped

$\phi(\frac{\pi}{2}) = 0$

(c) $\phi(0)\left[1 + \frac{(\frac{\pi}{2})\bar{p}}{\beta_o}\right] + \frac{\pi}{2}\ \phi'(0) = 0$ rotationally restrained

$\phi(\frac{\pi}{2}) = 0$

Using the optimality criterion (C-1) we obtain a relation between $\phi(\xi)$ and $\bar{I}(\xi)$, namely

$$\bar{I}(\xi) = c\phi(\xi)^{\frac{2n}{n+1}} \qquad \text{(C-8)}$$

The constant c can be taken as one owing to the linearity and homogeneity of Eq. (C-6) which upon substitution of the above becomes:

$$\phi''(\xi) + \bar{p}\phi^{\frac{1-n}{1+n}} = 0$$

multiply by $\phi'(\xi)$ and obtain

$$\{\phi'(\xi)^2\}' + \bar{p}(n+1)\left\{\phi^{\frac{2}{n+1}}\right\}' = 0$$

Integration yields

$$\phi'^2(\xi) + \bar{p}(n+1)\phi^{\frac{2}{n+1}} = \bar{p}(n+1)\phi_o^{\frac{2}{n+1}} \qquad \text{(C-9)}$$

where ϕ_o is constant.

To solve (C-9), introduce the following new dependent variable $\theta(\xi)$ defined by

$$\phi(\xi) = \phi_o[\sin\,\theta(\xi)]^{n+1} \qquad \text{(C-10)}$$

Substitution of (C-10) into (C-9) yields the following equation for the determination of $\theta(\xi)$

$$[\sin\,\theta(\xi)]^n\theta'(\xi) = \left[\frac{\bar{p}}{n+1}\right]^{\frac{1}{2}}\phi_o^{\frac{-n}{n+1}} \qquad \text{(C-11)}$$

Integrating (C-11) from $\xi = 0$, obtain

$$\int_{\theta(0)}^{\theta(\xi)} (\sin\,t)^n dt = \left[\frac{\bar{p}}{n+1}\right]^{\frac{1}{2}}\phi_o^{\frac{-n}{n+1}}\xi \qquad \text{(C-12)}$$

At this stage we have three unknowns $\theta(0)$, $\bar{p}_{cr}$, and ϕ_o to be determined by the boundary conditions and the constant volume constraint.

Considering the simply supported case

With boundary conditions,

$$\phi(0) = 0 \quad ; \quad \phi(\tfrac{\pi}{2}) = 0$$

and using (C-10), we obtain

$$\sin\theta(0) = 0 \rightarrow \theta(0) = m\pi \qquad m = 0,1,2,\cdots$$

$$\sin\theta(\tfrac{\pi}{2}) = 0 \rightarrow \theta(\tfrac{\pi}{2}) = \bar{m}\pi \qquad \bar{m} = 0,1,2,\cdots$$

Since we seek the first mode anti-symmetric solution, we require a minimum number of nodes in $[0,\pi]$; therefore, by taking $|m - \bar{m}| = 1$, we can choose $m = 0$ and $\bar{m} = 1$ which gives

$$\theta(0) = 0 \quad ; \quad \theta(\tfrac{\pi}{2}) = \pi \tag{C-13}$$

The constant ϕ_o can be obtained from (C-12) at $\xi = \frac{\pi}{2}$ yielding

$$\phi_o = \left\{\left[\frac{n+1}{\bar{p}}\right]^{1/2}(\frac{2}{\pi}) \int_o^{\pi} (\sin\xi)^n d\xi\right\}^{-(\frac{n+1}{n})} \tag{C-14}$$

To determine the optimum $\bar{p}_{cr}$ we make use of the constant volume constraint (C-4)

$$\int_o^{\pi/2} A(\xi)d\xi = \frac{\bar{v}}{2}$$

assuming that the distribution of area is symmetric

with

$$A(\xi) = \left[\frac{I(\xi)}{\bar{\rho}}\right]^{\frac{1}{n}}$$

from (C-3), and the relation $I(\xi) = [\phi(\xi)]^{\frac{2n}{n+1}}$. Using (C-10), (C-11) and (C-14), we obtain

$$(\bar{p}_{opt})_{cr} = \bar{\rho}(n+1)\left(\frac{\bar{v}}{2}\right)^{n}\left(\frac{2}{\pi}\int_{o}^{\pi}\sin^{n}\xi d\xi\right)^{n+2}\left(\int_{o}^{\pi}(\sin\xi)^{n+2}d\xi\right)^{-n} \qquad \text{(C-15)}$$

Example

For n = 2 this becomes,

$$(\bar{p}_{opt})_{cr} = \frac{16}{3}\bar{\rho}\left(\frac{\bar{v}}{\pi}\right)^{2} \qquad \text{(C-16)}$$

For $\bar{\rho} = 1$ and $\bar{v} = \pi$, the critical value of $\bar{p}$ is 5.33 which compares quite well with the value of 5.17 obtained via the methods of Chapter II. Using (C-14) in (C-10) with the optimality condition we can determine the optimum area distribution given by

$$A(\xi) = \frac{4\bar{v}}{3\pi}\sin^{2}\theta(\xi) \qquad 0 \leq \xi \leq \pi \qquad \text{(C-17)}$$

where from (C-12), $\theta(\xi)$ is given by

$$2\theta(\xi) - \sin 2\theta(\xi) = 4\xi \qquad 0 \leq \xi \leq \pi \qquad \text{(C-18)}$$

It is worthy to note at this point that the optimum area distribution given by (C-17) and (C-18) as well as the corresponding critical axial load parameter $\bar{p}_{opt}$ given by (C-16) were determined as a result of the optimality condition and the buckling condition and are not affected by the distribution of the lateral load $q(\xi)$ nor by the initial configuration $\eta_o(\xi)$. The optimum inertia distribution from Eqs. (C-17) and (C-18) is plotted in Fig. C1 along with the results depicted by Fig. 5b. They are in excellent agreement. Moreover, the above solution was obtained for the case n = 2 and simply supported boundary conditions. For other values of n and other boundary conditions the determination of $\theta(0)$, ϕ_o and $\bar{p}_{opt}$ will require a minor numerical root finding scheme for a transcendental equation before the necessary integrations can be carried out to determine $A(\xi)$.

Consider the general rotationally restrained case:
Boundary conditions

$$\phi(0)\left[1 + \frac{\frac{\pi}{2}\bar{p}}{\beta_o}\right] + \phi'(0)\,\frac{\pi}{2} = 0 \qquad \text{(A)}$$

$$\phi\left(\frac{\pi}{2}\right) = 0 \qquad \text{(B)}$$

Recalling that

$$\phi(\xi) = \phi_o[\sin\,\theta(\xi)]^{n+1} \qquad \text{(C-10)}$$

at

$$\xi = \frac{\pi}{2}$$

$$\phi(\tfrac{\pi}{2}) = \phi_o[\sin\,\theta(\tfrac{\pi}{2})]^{n+1} = 0 \rightarrow \sin\,\theta(\tfrac{\pi}{2}) = 0 \rightarrow \theta(\tfrac{\pi}{2}) = \bar{m}\pi$$

$$\bar{m} = 0,1,2,\cdots$$

Consider boundary condition (A): From (C-10)

$$\phi(0) = \phi_o[\sin\,\theta(0)]^{n+1}$$

$$\phi'(\xi) = [n+1]\phi_o[\sin\,\theta(\xi)]^{n}\cos\,\theta(\xi)\theta'(\xi)$$

$$\phi'(0) = [n+1]\phi_o[\sin\,\theta(0)]^{n}\cos\,\theta(0)\theta'(0)$$

and from (C-11)

$$\theta'(0) = \left[\frac{\bar{p}}{n+1}\right]^{1/2}\phi_o^{-\frac{n}{n+1}}[\sin\,\theta(0)]^{-n}$$

Substituting into the above, obtain

$$\phi'(0) = [n+1]\phi_o^{\frac{1}{n+1}}\cos\,\theta(0)\left[\frac{\bar{p}}{n+1}\right]^{1/2}$$

so boundary condition (A) becomes

$$\phi_o[\sin\,\theta(0)]^{n+1}\left(1 + \frac{\frac{\pi}{2}\bar{p}}{\beta_o}\right) + \frac{\pi}{2}(n+1)\phi_o^{\frac{1}{n+1}}\cos\,\theta(0)\left[\frac{\bar{p}}{n+1}\right]^{1/2} = 0 \quad \text{(C-19)}$$

From (C-12)

$$\phi_o = \left[\left(\frac{n+1}{\bar{p}}\right)^{1/2} \frac{2}{\pi} \int_{\theta(0)}^{\bar{m}\pi} (\sin t)^n dt\right]^{-\left(\frac{n+1}{n}\right)} \tag{C-20}$$

From the constant volume constraint

$$\bar{p} = \bar{\rho}(n+1)\left[\frac{\bar{v}}{2}\right]^2\left[\frac{2}{\pi} \int_{\theta(0)}^{\bar{m}\pi} (\sin t)^n dt\right]^{n+2} \left[\int_{\theta(0)}^{\bar{m}\pi} (\sin t)^{n+2} dt\right]^{-n} \tag{C-21}$$

Given n we can use (C-20) and (C-21) to eliminate ϕ_o and $\bar{p}$ from (C-19) and obtain an expression in terms of $\theta(0)$ alone. For different β_o (restraint) we obtain different $\theta(0)$. With $\theta(0)$ known, we can find $\bar{p}_{cr}$ from (C-21) and with $(\bar{p}, \theta(0))$ we may find ϕ_o from (C-20). With $(\phi_o, n, \bar{p}_{cr}, \theta(0))$ we may determine from (C-12) values of $\theta(\xi)$ for different $0 \leq \xi \leq \pi$. From (C-10) and (C-8) we determine the optimum $I(\xi)$. The relation $I(\xi) = \bar{\rho}A(\xi)$ determines optimum area.

Through the use of this analytic approach, one can determine $\bar{P}_{cr_{opt}}$ and $I_{opt}(\xi)$ for n = 2, 3 and general boundary restraints. What remains is to determine the critical response of these designs for various initial configurations $\eta_o(\xi)$ and load distributions.

Recalling the equilibrium equation, Eq. (21),

$$[Iy"]" + \bar{p}y" = q(\xi) - \bar{p}\eta_o(\xi)$$

with boundary conditions:

$$y(0) = y(\pi) = 0$$

$$I(0)y''(0) = \beta_o y'(0)$$

$$I(\pi)y''(\pi) = -\beta_o y'(\pi)$$

and

$$\bar{p} = J \int_o^{\pi} (y'^2 - 2y'\eta_o')d\xi$$

where

$$J = 1 \div 2 \left(\int \frac{d\xi}{A(\xi)} + \hat{\alpha} \right)$$

The load function $q(\xi)$ and initial shape $\eta_o(\xi)$ can be represented as $QN(\xi)$ and $e\bar{\eta}_o(\xi)$, respectively. For a given e one seeks a simultaneous solution of the above relations to find $Q_{cr_{opt}}$. Numerous illustrative examples of this portion of the analysis are found in Appendix A for the uniform arch.

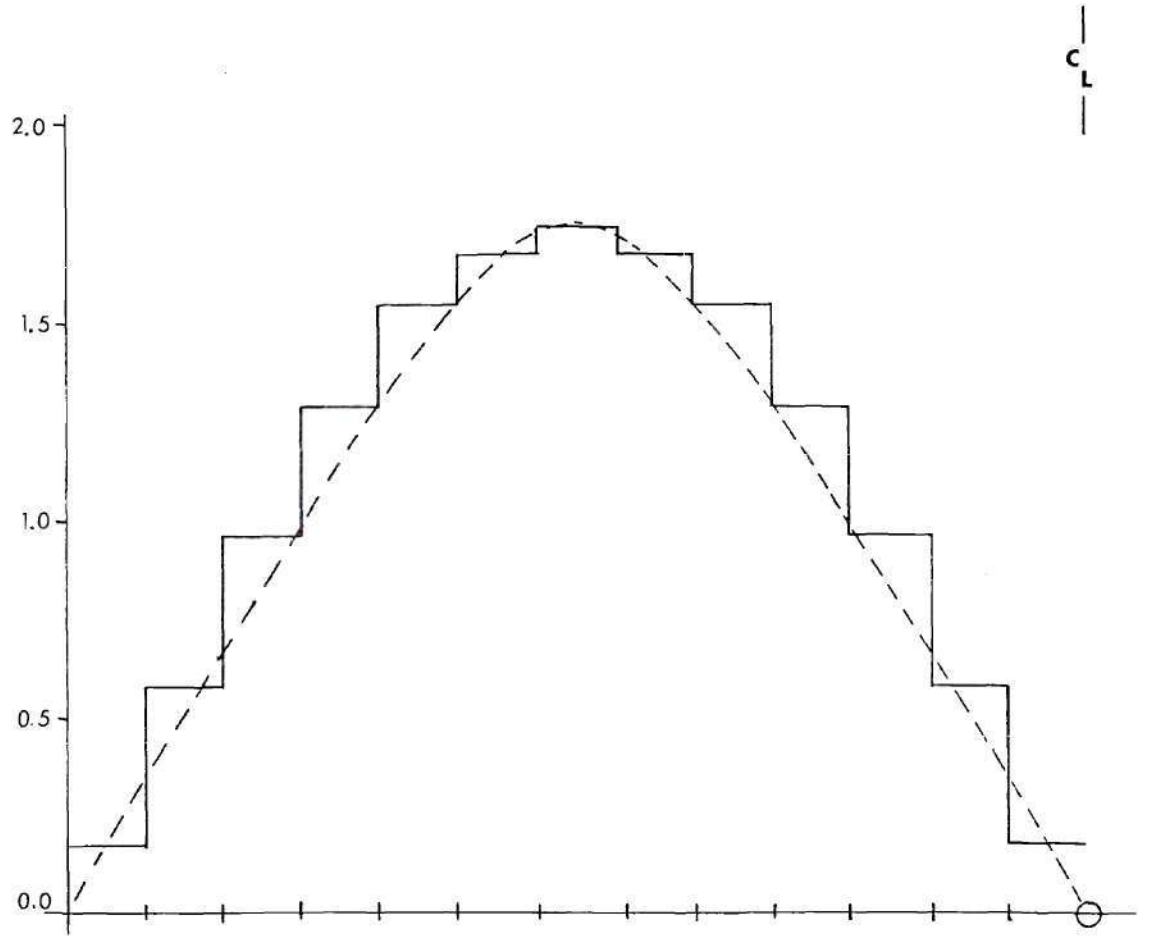

Fig. C1. Comparison of Analytic and Finite Element Optimum Shapes, Anti-Symmetric Buckling, $\beta_o = \infty$, n = 2.

APPENDIX D

DATA GENERATION AND PROGRAM LISTING

Two separate computer programs are presented: the first for the anti-symmetric optimization and the second for symmetric mode optimization. Many of the subroutines are identical or differ only slightly for the different programs. One could conceivably merge the programs together into a single code and control the different optimization processes through specifying some input parameter. However, during the course of developing the solution methodology for each case, it was found expedient to develop the program logic separately.

Basic mathematical functions and routines referenced in the program, but not listed, can be obtained through Refs. 51 and 52. Such standard routines are used to calculate the eigenvalues and vectors of matrices and calculate inverses which are essential to the assembly and solution process.

Details regarding input, output, parameter definition and programming peculiarities and difficulties are discussed herein.

Following is a descriptive summary of subroutines and variables for each program:

BASIC OPERATIONS ROUTINES

FMVX - Matrix vector multiplication

FMMX - Matrix matrix multiplication

FMTMX - Matrix transpose matrix multiplication

FMTVX - Matrix transpose vector multiplication

SINVRS - Computes inverse of a symmetric matrix using IMSL subroutine LINV2F

INVERS - Computes inverse of a matrix using IMSL subroutine LINV1F

GENERATION AND ASSEMBLY OF STRUCTURAL MATRICES AND LOAD VECTORS

ASS1 - Assembles the stiffness matrix $\underline{\underline{K}}_1$; imposes boundary conditions as specified by BETA; imposes either symmetric (MODE=1) or anti-symmetric (MODE=-1) transformation.

COMEK1 - Generates element stiffness matrix EK1 for given element I, and inertia XI(I).I=1,m.

ASS2 - Assembles the geometric matrix $\underline{\underline{K}}2$; imposes boundary conditions as specified by BETA; imposes either symmetric (MODE=1) or anti-symmetric (MODE=-1) mode transformation.

COMEK2 - Generates element geometric matrix EK2 for given element I, and inertia XI(I).I=1,m.

ASV5 - Assembles the load vector $\underline{V5}$; imposes boundary conditions as specified by BETA; imposes symmetric (MODE=1) transformation.

COMEV5 - Generates element load vector EV5 for specified load distribution (LOAD=1,2, or 3).

ASV6 - Assembles the load vector $\underline{V6}$; imposes boundary conditions as specified by BETA; imposes symmetric transformation (MODE=1).

COMEV6 - Generates element load vector EV6 for specified initial shape (ISHAPE=1, or 2).

SPECIAL OPERATIONS ROUTINES

1. Anti-Symmetric Program:

SOLVE - The primary subroutine for anti-symmetric optimization. Contains the iteration process for $\bar{p}$; checks for energy convergence; and calls the buckling analysis program BUKLOD.

EIGEN - Solves the eigenvalue problem $|\underline{K}_1 - \bar{p}\underline{K}_2| = 0$ for all positive eigenvalues and returns them in an array called EVAL. The lowest value is selected and called $\bar{p}_{cr}$. The corresponding global eigenvector is generated for $\bar{p} = \bar{p}_{cr}$ and specified boundary conditions.

ENERGY - Computes the bending energy density corresponding to the current inertia distribution, and global deformation vector and stores in an array called

ENER. A convergence test is made and, if warranted, a new inertia distribution is generated via the iterative scheme of Chapter III.

INRTIA - Generates new inertia distribution given energy density and old inertia by application of Eq. (54) and the volume constraint subject to a minimum inertia of XIMIN.

BUKLOD - For some set of system parameters and inertia, this subroutine generates the solution (at $\bar{p}=\bar{p}_{cr}$) to Eq. (59) giving the response (Ω_{cr},e).

TANGNT - Generates the value of rise parameter e at which the buckling mode changes from symmetric to antisymmetric by simultaneous solution of Eqs. (60) and (61) at $\bar{p}=\bar{p}_{cr}$. Called from BUKLOD only if desired.

DEFLOD - Called by BUKLOD and interacts with BUKLOD at a given value of e to solve Eq. (59), thus producing the load-deflection curve. "Deflection" is both apex deflection and change in area under the curve.

COEFB - Called by TANGNT and generates terms for use in computing coefficients of Eq. (61).

TRANS - Generates either symmetric (MODE=1) or antisymmetric (MODE=-1) transformation matrix.

2. Symmetric Optimization Program:

SYMOPT - The primary subroutine for the symmetric optimization program. Contains the iteration scheme for solving for Q_{cr} and $\bar{p}_{cr}$ at a specified value of e. Reassembles the global deformation vector at $\{Q_{cr}, \bar{p}_{cr}, e, I^J\}$ for use in the energy subroutine.

SECANT - Called by SYMOPT to locate $\bar{p}_{cr}$ by secant iteration once $\bar{p}_{cr}$ has been successfully bracketed.

COEFP - Generates coefficients of the {P, Q} relation, Eq. (59).

COEFB - Generates coefficients of the buckling equation, Eq. (61).

ENERGY - Generates energy density distribution for some inertia utilizing Eq. (50); tests for convergence and, if warranted, generates new inertia distribution.

INRTIA - Generates new inertia via iterative scheme of Eq. (54) with constant volume constraint.

TRANS - Generates the symmetric transformation matrix (see Appendix B) for MODE=1.

EIGEN - Locates all positive eigenvalues of the system $|\underline{\underline{K}}1 - \bar{p}\underline{\underline{K}}2| = 0$ when the matrices $\underline{\underline{K}}1$ and $\underline{\underline{K}}2$ have been symmetrically transformed.

PROGRAM VARIABLES

1. Antisymmetric Program:

EXP1 - This variable defines the exponent $n/(n\alpha+1)$ in the recurrence relation Eq. (57). α is arbitrarily taken to be unity (see Ref. 49 for details).

EXP - The value n in Eq. (57) taken as 1, 2, or 3.

ITR - Iteration parameter in subroutine SOLVE.

REDEXP - Iteration parameter for the number of times EXP1 can be reduced.

MODE - Equal to -1 or +1 according to the kind of transformation to be made on the equilibrium solution $\underset{\sim}{u}$.

SYMM - Equal to ± 1 according to the kind of apex condition to apply.

SUMJ - The parameter J.

MAX - Array dimension greater than 2m+2.

m - Number of elements.

LDTEST - If DEFLOD is called, LDTEST is set equal to one and BUKLOD will generate load deflection data only after the first pass.

T(,) - Transformation matrix.

mor - Integer specifying the matrix order; or the number of unrestrained degrees of freedom for a particular case of boundary and symmetry conditions.

ESTOP - In subroutine BUKLOD is maximum value of rise parameter for which the critical load will be computed.

QCRP - Quadratic root with positive sign in Eq. (49a).

QCRM - Quadratic root with negative sign in Eq. (49a).

DEFP - Apex deflection corresponding to QCRP.

DEFM - Apex deflection corresponding to QCRM.

DELAP - Change in area under arch corresponding to QCRP.

DELAM - Change in area under arch corresponding to QCRM.

2. Symmetric Program:

PSTOP - Maximum value of $\bar{p}$ to be considered during the solution process for $\bar{p}_{cr}$ in SYMOPT.

ICRIT - Iteration parameter for redesign.

ITMXOP - Maximum number of iterations to obtain energy convergence.

SIGN - ± 1 depending upon whether the critical value of Q comes from QCRP or QCRM.

NEG - Number of times DISC becomes negative resulting in an imaginary solution for Q.

E - Rise parameter.

IT - Iteration parameter for critical conditions at a specific inertia.

DATA GENERATION

As mentioned in Chapters III and IV and discussed in detail by Kamat in Ref.(49), the maximization of the lowest

eigenvalue $\bar{p}$ for the antisymmetric case depends upon starting the iteration scheme and the subsequent redesign process with a judicious choice of the exponent $n/(m+1)$ in Eq. (57). Setting $\alpha = 1$, the exponent EXP1 is equal to 1/2, 2/3, and 3/4 for values of n = 1, 2, or 3 in the inertia area relation. Best results were obtained by starting with EXP1 at 75% of its true value. Higher values seemed to cause a more severe change in inertia distribution from the uniform and subsequent reductions were made necessary because successive values of $\bar{p}$ were not increasing; on the other hand, lower values cause the second design to be very close to uniform and thus greatly increased the time necessary for energy convergence. Figure D1 gives a quantitative picture of this trend. Boundary conditions did not significantly affect this trend. Energy convergence criterion was set at 3% for the fully clamped case. Lower values are achievable, but at a great cost in computer time due to the increased number of iterations necessary. Once energy convergence is obtained, the critical response of I_{opt} is computed by solving the $\{\bar{p}_{cr}, Q_{cr}\}$ relation for various values of rise parameter e in BUKLOD. The bifurcation load invariably was the root from the negative sign of the quadratic. This root gave the smallest value of negative deflection at the apex and as e increased, this root increased.

By specifying the value of e in BUKLOD, DEFLOD can be used to plot the load deflection curve for any inertia, thus providing an alternative for computing a possible limit point.

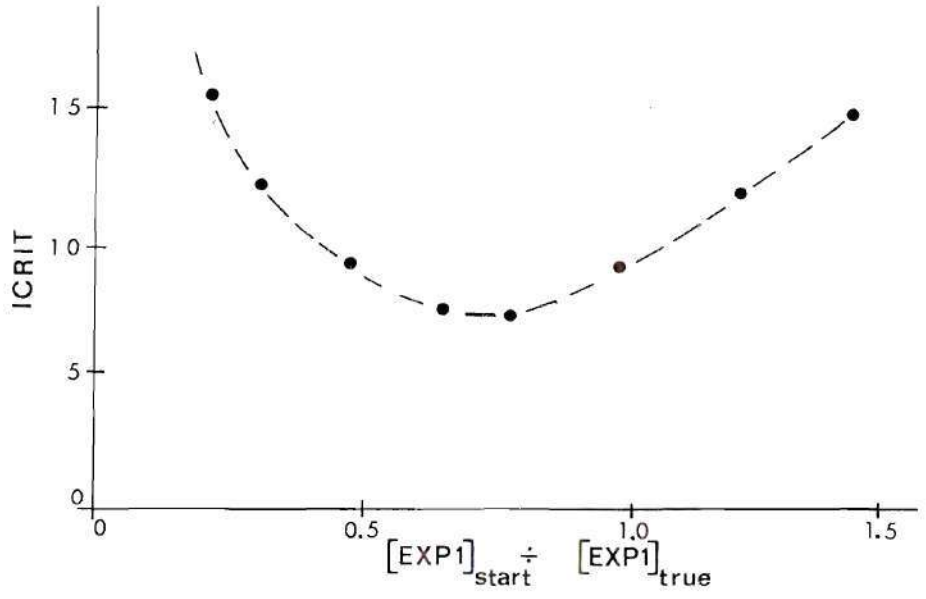

Fig. D1. Relation Between Number of Iterations to Convergence and Starting Value of EXP 1

Note from the flowchart, Fig. D2, that the first assembly of $\underline{\underline{K}}1$ and $\underline{\underline{K}}2$ is antisymmetric since the buckling mode $\underset{\sim}{v}$, in Eq. (57) is required to be antisymmetric. After energy convergence is obtained and an optimum inertia is generated, the call to BUKLOD symmetrically reassembles these matrices as well as the vectors $\underset{\sim}{V}_6$ and $\underset{\sim}{V}_5$ for use in computing the coefficients of Eq. (59).

In Fig. D3, the flowchart for the symmetric optimization process is presented. The analysis portion is much more complicated for this case and consists of solving two nonlinear

algebraic equations [Eqs. (59) and (61)] for the lowest positive value of $\bar{p}$ and the corresponding Q at a given value of rise e. Because of the nonlinearity, an iterative approach is used to increment on $\bar{p}$ until a root is bracketed. The routine SECANT is then called to converge to a more accurate (10^{-4}) solution. The rise parameter is held constant in the computation of the interaction energy U^I in accordance with the optimality criterion, Eq. (48), thus producing an optimum design for each value of rise. Coincident with the generation of the optimum design is the solution for $\bar{p}_{cr}$ and Q_{cr} together with the apex deflection. One major numerical peculiarity occurring in the solution scheme is the fact that the eigenvalues of the system [$\underline{K}1 - \bar{p}\underline{K}2$] are singularities and must be avoided during the iteration scheme. The process of avoiding these particular values of $\bar{p}$ is to create an array called SING, the elements of which are values differing from the eigenvalues by ± 0.05. The inversion routine for [$\underline{K}1 - \bar{p}\underline{K}2$] maintains its accuracy as long as $\bar{p}$ is not too close to an eigenvalue.

After many cases, it was consistently found that the critical load Q_{cr} came from the negative sign solution of the $\{\bar{p}, Q\}$ relation. (No physical or mathematical significance is attached to this.) If one wishes to include in the analysis process the possibility that QCRP may be critical, a minor change of the logic sequence in the bracket process is necessary. The synthesis logic is basically the same as for

antisymmetric optimization, except that the energy density is computed on the basis of interaction and bending energy. Each redesign requires a complete nonlinear analysis for the critical conditions. Due to the sensitivity of the design process to the starting value of EXP1, it is begun at 75% of its real value at $\alpha = 1$. For the symmetric problem, many more iterations are required to obtain convergence in energy; sometimes as many as twelve. Fewer iterations are required for clamped boundaries than for simply supported.

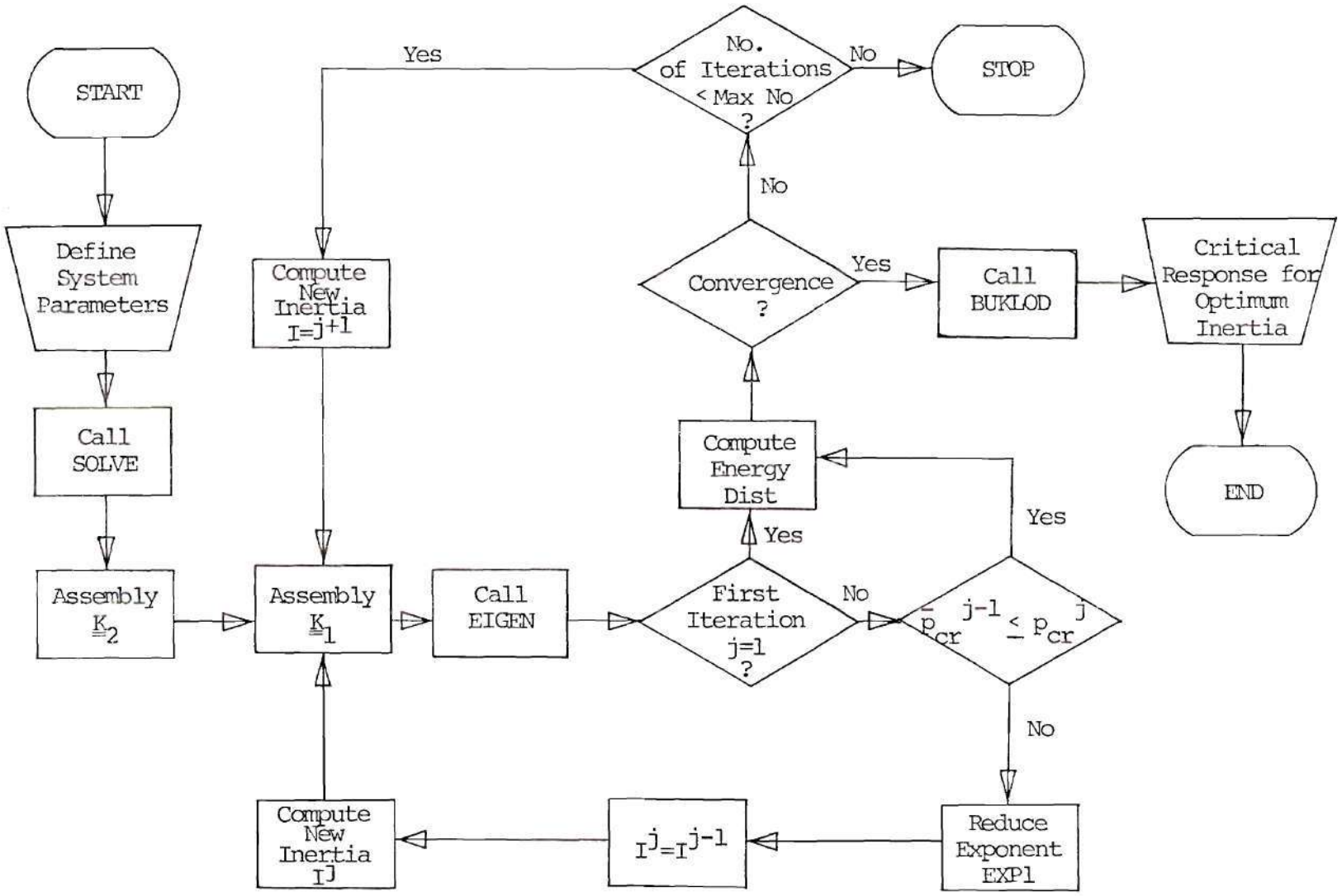

Fig. D2. Flow Chart for Anti-Symmetric Optimization

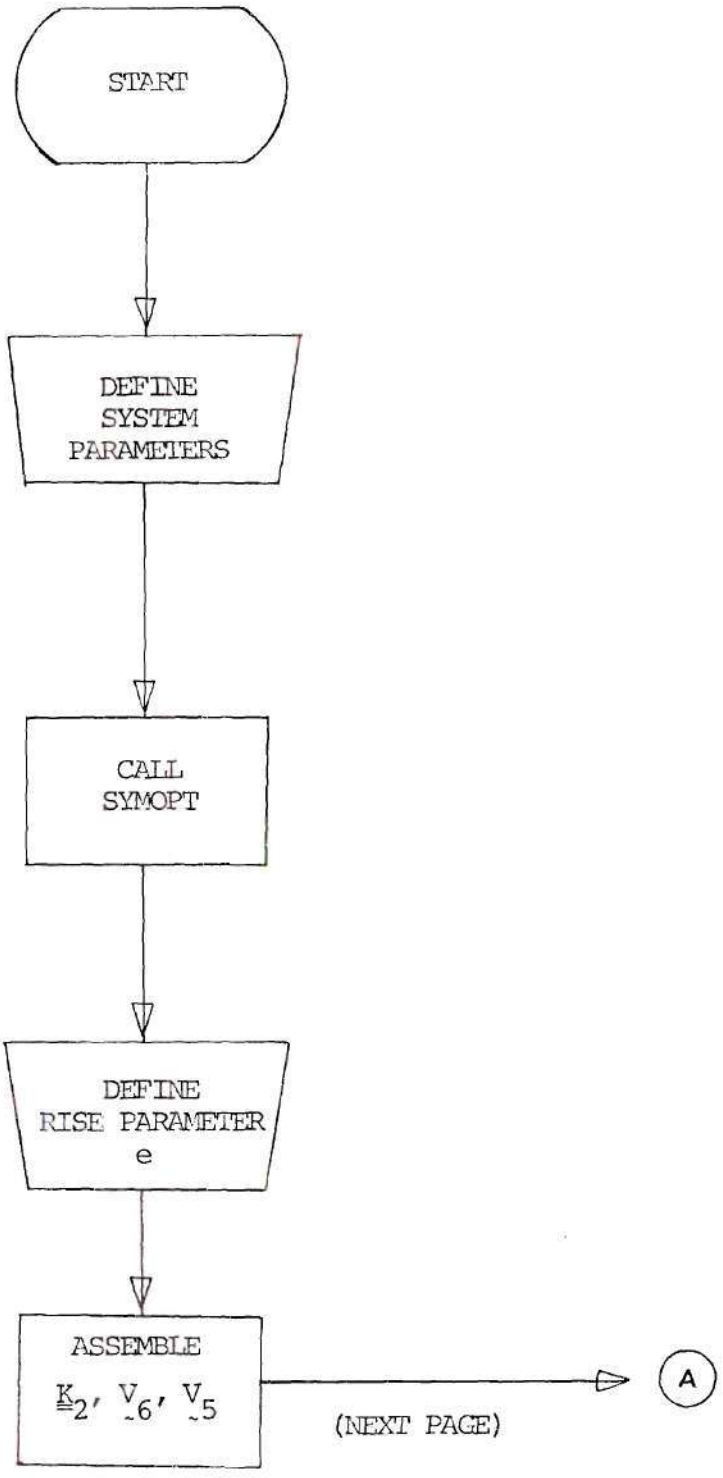

Fig. D3. Flow Chart for Symmetric Optimization

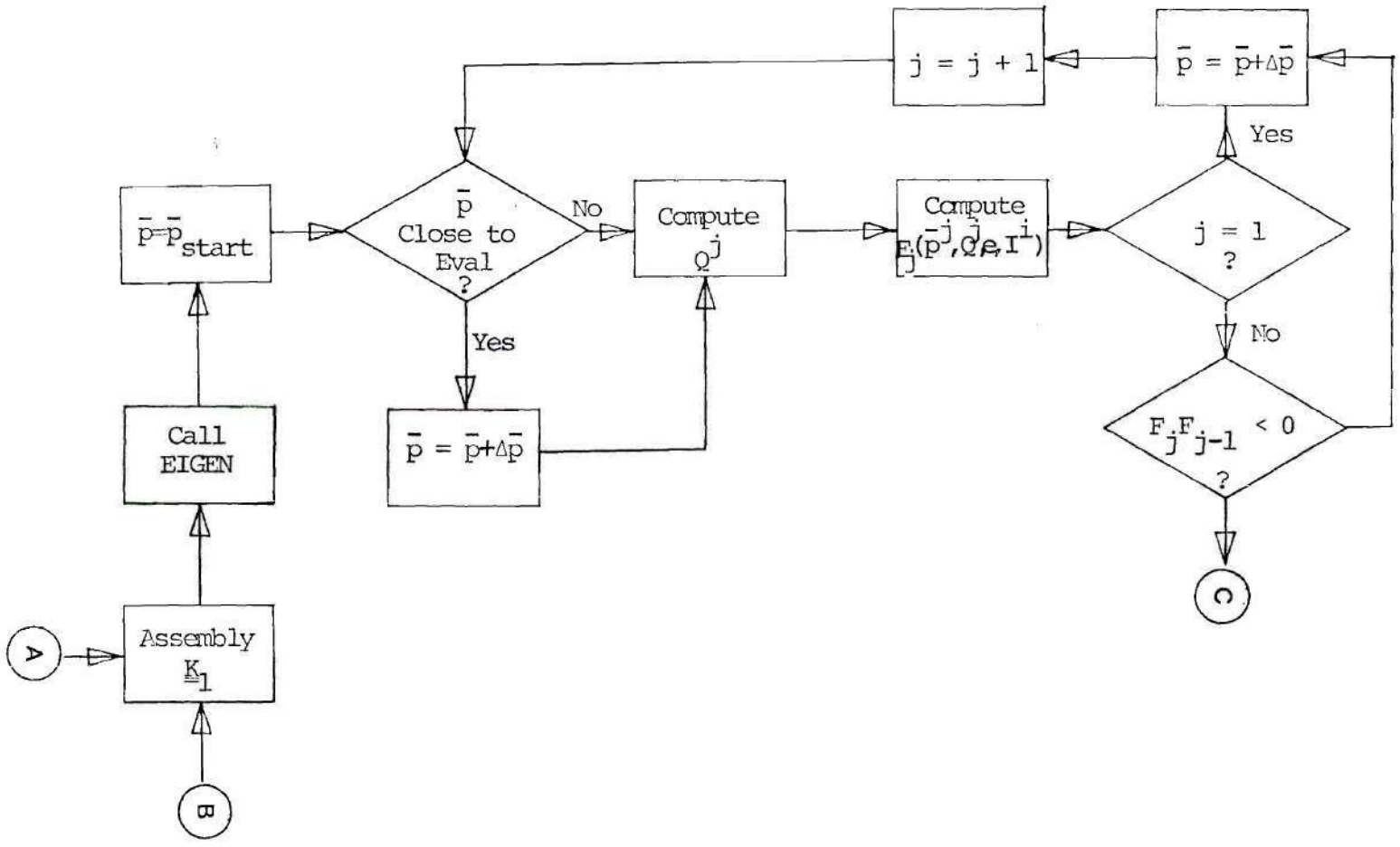

Fig. D3. (Continued)

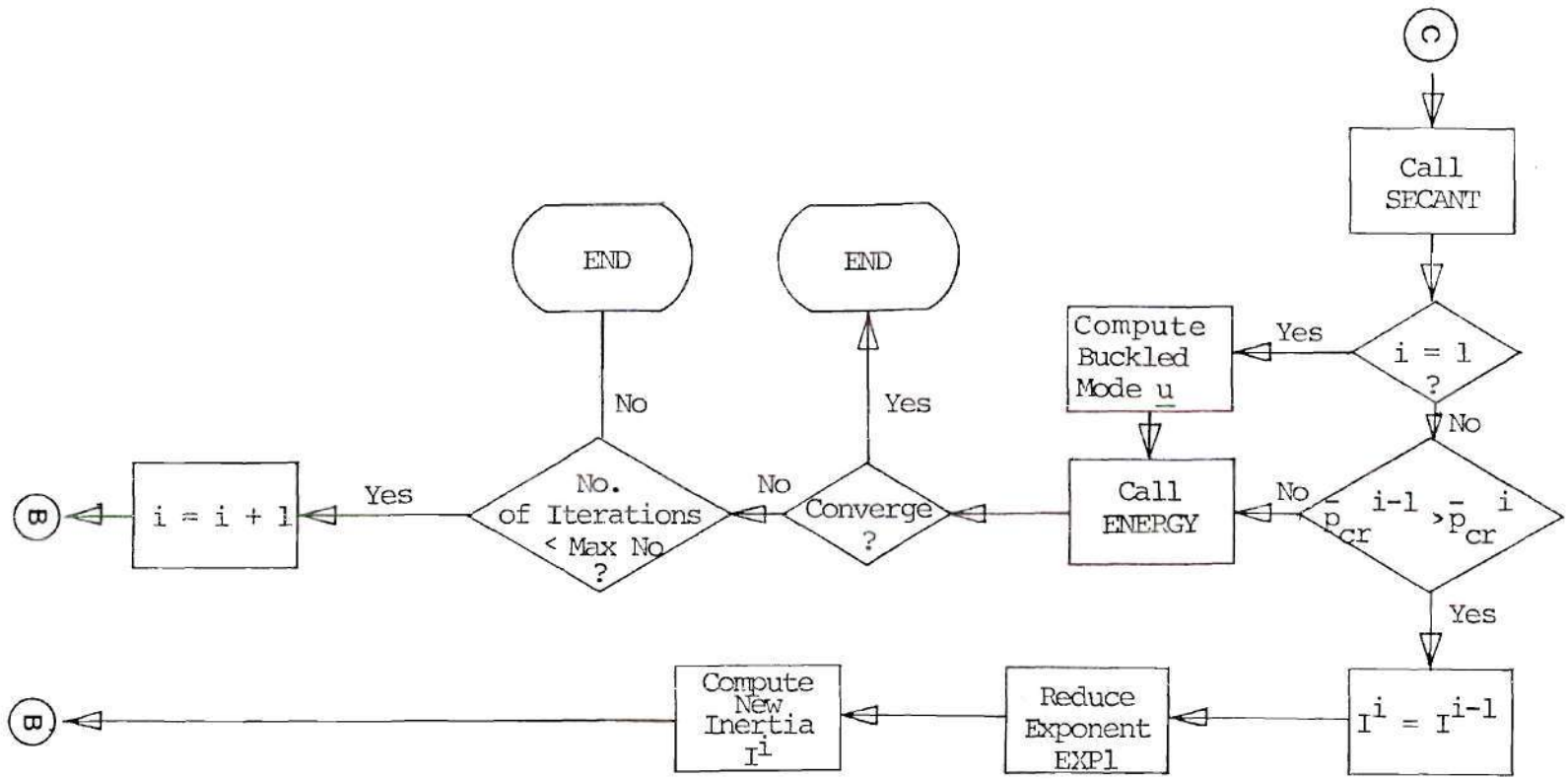

Fig. D3. (Continued)

PROGRAM LISTINGS

ANTI-SYMMETRIC OPTIMIZATION PROGRAM

```
L,A,S                                                                  G
      PROGRAM OPTRCH(OUTPUT,TAPE6=OUTPUT)
      REAL MODE
      COMMON /1/ BETA
      COMMON /2/ LOAD                                                  C     ARL LIBRARY ROUTINES
      COMMON /3/ ISHAPE                                                C
      COMMON /6/ MODE                                                        LOGICAL EXIT
      COMMON /9/ BETAF                                                       REAL K1,K2,K,LINV
      COMMON /7/ VOL,XIMIN,EXP1                                              DIMENSION DIAG(40), EVAL(MOR), DUEC(40)
      COMMON /4/ RHO,EXP                                                     COMMON /B1/ K1(40,40)/B2/K2(40,40)
      COMMON /5/ EL                                                          COMMON /B11/ PROD(40,40)
      COMMON /8/ PSTOP                                                       COMMON /B7/ T(70,40)/B8/K(40,40)
C     ***************************************************************      COMMON /10/ SYMM
                                                                             COMMON /1/ BETA
***                                                                          DIMENSION LINV(40,40), IPR(40)
C                                                                      C
C                          DEFINITION OF PARAMETERS
C
C          THE INERTIA AREA RELATION IS TAKEN AS I=RHO*(A**EXP)
C               RHO WILL BE TAKEN AS 1
C               EXP WILL ASSUME VALUES 1,2,OR3                               MAX=40
C          M,(AND EN) ARE TOTAL NUMBER OF ELEMENTS.                    C     ITRE=1
C          BETA, MODULUS OF ROTATIONAL RESTRAINT.  USED TO SPECIFY           STEP 1:  CHOLESKY DECOMP OF K2=LL(TRANS)
C          BOUNDARY CONDITIONS.                                        C     CALL LUS (MOR,K2,MAX,DIAG,EXIT)
C          BETA = 0.                SIMPLY SUPPORTED                   C     DIAG CONTAINS INVERSES OF DIAGONAL ELEMENTS OF L
C          0<BETA<100               RESTRAINED CASE                    C     STEP 2:  FORMATION OF SYMM MATRIX K= L-INV*K1*L-INT-TRANS
C                                                                      C          AND RECON OF FULL K2
C          BETA>100                 CLAMPED CASE                       C     K2 =L*LTRANS
C          ISHAPE = 1,2   HALF SINE OR PARABOLIC INITIAL CONFIG.             DEFINE L AND STORE IN PROD
C          LOAD = 1,2, OR 3  HALF SINE, PARABOLIC OR UNIFORM LOAD.           DO 1 I=1,MOR
C          VOL IS THE  VOLUME PRESCRIBED                               1     DO 1 J=1,MOR
C          XIMIN IS THE MINIMUM VALUE OF THE INERTIA                         PROD(I,J)=0.
C
C     ***************************************************************
***                                                                          DO 2 IX=1,MOR
      MAX=70                                                                 DO 2 IY=IX,MOR
      BETA=0.1                                                         2     PROD(IY,IX)=K2(IX,IY)
      ISHAPE=1                                                               DO 3 IX=1,MOR
      LOAD=3                                                           3     PROD(IX,IX)=1./DIAG(IX)
                                                                       C     NOW FIND L INV
C     DEFINE A NEW VARIABLE EN = M                                           CALL INVERS (PROD,40,MOR,IPR,LINV,D1)
      M=26                                                             C     FORM K= LINV*K1*LINV TRANS
      EN=26.                                                                 CALL FMMX (LINV,K1,PROD,MOR,MOR,40,40,40,MOR)
      VOL=3.141592658                                                  C     FORM LINV TRANS =LINV AND RECON K2
      XIMIN=0.                                                               DO 4 IZ=1,MOR
      RHO=1.                                                                 DO 4 JZ=IZ,MOR
      EXP=2.
      EXP1=EXP/(EXP+1.)
      M1=M+1
      M2=2*M+2                                                               K2(IZ,JZ)=K2(JZ,IZ)
      BETAF=0.                                                         4     LINV(IZ,JZ)=LINV(JZ,IZ)
      PI=3.141592658                                                   C     ZERO THE LOWER TRIANGLE
                                                                             DO 5 IZ=1,MOR
      EL=PI/EN                                                               DO 5 JZ=IZ,MOR
      MODE=1.                                                                IF (IZ.EQ.JZ) GO TO 5
      PSTOP=25.                                                              LINV(JZ,IZ)=0.
C     NOTE***PSTOP IS THE LARGEST VALUE OF P TO BE CONSIDERED          5     CONTINUE
      CALL SYMOPT (M,M1,M2,MODE,MAX)                                   C     NOW LINV CONTAINS L INV-TRANS
      STOP                                                             C       FORM K
      END                                                                    CALL FMMX (PROD,LINV,K,MOR,MOR,40,40,40,MOR)
**************************************                                 C
      SUBROUTINE EIGEN (M,MOR,MAX,EVAL,NPE)
**************************************
C     THE EIGEN SYSTEM K1-PK2 IS SOLVED FOR LOWEST MB EVALUES USIN
```

```
C     STEP 3:   TRIDIAG OF K
      CALL TRI1 (MOR,K,MAX)
C     THE NEC INFO FOR NEXT STEP IS IN COMMON WITH BISEC
C     STEP 4:   EVAL OF SYMM TRIDIAG FORM BY METHOD OF BISECTION
      MA=1
      MB=MOR
      TOL1=0.
      CALL BISEC (MOR,MA,MB,TOL1,DVEC,TOL2,ISUM,ANORM)
C     ***ALL E.VALUES WILL RETURN IN DVEC IN INC.ORDER.
C
      DO 6 I=1,MOR
      IF (DVEC(I)) 6,6,7

6     CONTINUE
C     NO POS EIGENVALUES***
      NPE=0
      WRITE (6,9)
      RETURN
7     CONTINUE
C
C     FOR SOME I .LE.MOR THE E.VALUES BECOME POS.
C        FOR N POS E.VALUES THERE ARE N POSSIBLE FEAS REGIONS
C
      NPE=MOR-I+1
C     DEFINE EVAL TO BE THE ARRAY OF POS E.VALUES.

      DO 8 J=1,NPE
8     EVAL(J)=DVEC(J+MOR-NPE)
C
C     NOW WE HAVE IDENTIFIED AND STORED NPE + E.VALUES.
C     FOR SYMM WE NEED ONLY EVAL
C
      RETURN
C
9     FORMAT (10X,1H*,NOPOSE.VALUES,1H*,//)
      END
*****************************
      SUBROUTINE ASS1 (M,M1,M2,MAX,MODE,X,XI,AK1)

*************************************
      REAL K1
      COMMON /B7/ T(70,40)/B15/ET(70,40)/B11/PROD(40,40)
      COMMON /B1/ K1(40,40)
      COMMON /1/ BETA
      DIMENSION EK1(4,4)
      DIMENSION AK1(MAX,2), X(M1), XI(M)
      REAL MODE
C     INITIALIZ  TO XERO
      DO 2 IR=1,M2
      DO 1 IC=IR,M2
      AK1(IR,IC)=0.

      AK1(IC,IR)=0.
1     CONTINUE
2     CONTINUE
C     START ASSEMBLY
      DO 5 I=1,M
      CALL COMEK1 (I,M,M1,X,XI,EK1)
      DO 4 JR=1,4
      DO 3 LC=1,4
      AK1(2*I-2+JR,2*I-2+LC)=EK1(JR,LC)+AK1(2*I-2+JR,2*I-2+LC)
C
3     CONTINUE
4     CONTINUE
5     CONTINUE
      IF (BETA.GT.100.) GO TO 6
      AK1(2,2)=AK1(2,2)+2.*BETA
6     CONTINUE
      MP2=M+2
C     NOW FORM K1 = T TRANSPOSE *AK1*T
      CALL FMMX (AK1,T,ET,M2,M2,70,70,70,MP2)
C     NOW FORM T TRANSPOSE * PROD
      CALL FMTMX (T,ET,AK1,M2,MP2,70,70,70,MP2)
      IF (BETA.GT.100.) GO TO 9
      DO 8 NK=1,M
      DO 7 JK=1,M


      K1(NK,JK)=AK1(NK+1,JK+1)
7     CONTINUE
8     CONTINUE
      RETURN
9     CONTINUE
C     CLAMPED CASE
      MM1=M-1
      DO 11 JK=1,MM1
      DO 10 NK=1,MM1
      K1(NK,JK)=AK1(NK+2,JK+2)
10    CONTINUE
11    CONTINUE


C     NOW AK1 HAS BEEN COMPLETELY TRANSFORMED. RTURN FOR E.VALUES
      RETURN
      END
*****************************
      SUBROUTINE COMEK1 (I,M,M1,X,XI,EK1)
*****************************
      DIMENSION CEN1(4,4), EK1(4,4), BINV(4,4), C(4,4)
      DIMENSION X(M1), XI(M)
      DIMENSION B(4,4), IPR(4)
      COMMON /5/ EL
C     DEFINE THE MATRIX CEN1 GIVEN BY INTEGRAL XI(I)*(L,,L,,T)
C     COMPUTE THE TERMS OF CEN1 FOR GIVEN ELEMENT I.


C     INTEGRATIONS HAVE BEEN DONE BY HAND.
C     THE INDEP VARIABLE IS X.
C     THE INERTIA VECTOR XI CONTAINS M ELEMENTS.
C
      DO 2 K=1,2
      DO 1 L=1,4
      CEN1(K,L)=0.
      CEN1(L,K)=0.
1     CONTINUE
2     CONTINUE
C     XI(I) IS THE INERTIA OF ITH ELEMENT ASSUMED CONSTANT.
      CEN1(3,3)=4.*(X(I+1)-X(I))*XI(I)


      CEN1(3,4)=6.*(X(I+1)**2-X(I)**2)*XI(I)
      CEN1(4,3)=CEN1(3,4)
```

```
      CEN1(4,4)=12.*(X(I+1)**3-X(I)**3)*XI(I)
C      COMPUTE ELEMENT MATRIX EK1
      B(1,1)=1.
      B(1,2)=X(I)
      B(1,3)=X(I)**2
      B(1,4)=X(I)**3
      B(2,1)=0.
      B(2,2)=1.
      B(2,3)=2.*X(I)
      B(2,4)=3.*(X(I)**2)

      B(3,1)=1.
      B(3,2)=X(I+1)
      B(3,3)=X(I+1)**2
      B(3,4)=X(I+1)**3
      B(4,1)=0.
      B(4,2)=1.
      B(4,3)=2.*X(I+1)
      B(4,4)=3.*(X(I+1)**2)
      CALL INVERS (B,4,4,IPR,BINV,D1)
C     EK1 = BINVT*CEN1*BINV
C
      CALL FMTMX (BINV,CEN1,C,4,4,4,4,4,4)

C     NOW FOR EK1 = C*BINV
      CALL FMMX (C,BINV,EK1,4,4,4,4,4,4)
      RETURN
      END
**********************************
      SUBROUTINE ASSE (M,M1,M2,MAX,MODE,X,AK2)
**********************************
      COMMON /1/ BETA
      COMMON /10/ SYMM
      COMMON /B7/ T(70,40)/B15/ET(70,40)/B11/PROD(40,40)
      COMMON /B2/ K2(40,40)
      DIMENSION AK2(MAX,2), X(M1)

      DIMENSION EK2(4,4)
      REAL K2
      REAL MODE
      M2=2*M+2
C     INITIALIZE MATRIX AK2 TO ZERO BEFORE IMPUTTING ITS VALUES
C     BY SUCCESSIVE ADDITION.
C
      DO 2 IR=1,M2
      DO 1 IC=IR,M2
      AK2(IR,IC)=0.
      AK2(IC,IR)=0.
1     CONTINUE

2     CONTINUE
C
C     START THE ASSEMBLY PROCESS.
C
      DO 5 I=1,M
      CALL COMEK2 (I,M1,X,EK2)
      DO 4 JR=1,4
      DO 3 LC=1,4
      AK2(2*I-2+JR,2*I-2+LC)=EK2(JR,LC)+AK2(2*I-2+JR,2*I-2+LC)
C
3     CONTINUE
4     CONTINUE

5     CONTINUE
      IF (MODE.EQ.0.) RETURN
      MP2=M+2
      CALL TRANS (MODE,M)
C     NOW FORM K2 = T TRANSPOSE * AK2*T
      CALL FMMX (AK2,T,ET,M2,M3,70,70,70,MP2)
C     NOW FORM T TRANSPOSE * PROD
      CALL FMTMX (T,ET,AK2,M2,MP2,70,70,70,MP2)
      IF (BETA.GT.100.) GO TO 8
      MOR=M
      DO 7 NK=1,MOR
      DO 6 JK=1,MOR


      K2(NK,JK)=AK2(NK+1,JK+1)
6     CONTINUE
7     CONTINUE
      RETURN
8     CONTINUE
C     CLAMPED CASE
      MOR=M-1
      DO 10 NK=1,MOR
      DO 9 JK=1,MOR
      K2(NK,JK)=AK2(NK+2,JK+2)
9     CONTINUE
10    CONTINUE


C     NOW AK2 HAS BEEN COMPLETELY TRANSFORMED. RTURN FOR E.VALUES
      RETURN
      END
**********************************
      SUBROUTINE COMEK2 (I,M1,X,EK2)
**********************************
      DIMENSION CEN2(4,4), EK2(4,4), BINV(4,4), C(4,4)
      DIMENSION X(M1)
      DIMENSION B(4,4), IPR(4)
      COMMON /5/ EL
C     DEFINE THE MATRIX(4,4) GIVEN BY INTEGRAL(L,L,T) AS CEN2
C     COMPUTE THE TERMS OF CENT FOR GIVEN I.  THIS WILL INVOLVE


C     SIMPLE INTEGRATIONS WHICH FOR THIS ASSEMBLY ARE DONE BY
C     HAND.  THE INDEP VARIABLE IS X.
C
      CEN2(1,1)=0.
      CEN2(1,2)=0.
      CEN2(1,3)=0.
      CEN2(1,4)=0.
      CEN2(2,1)=0.
      CEN2(3,1)=0.
      CEN2(4,1)=0.
      CEN2(2,2)=X(I+1)-X(I)
      CEN2(2,3)=(X(I+1))**2-(X(I))**2


      CEN2(2,4)=(X(I+1))**3-(X(I))**3
      CEN2(3,2)=CEN2(2,3)
      CEN2(4,2)=CEN2(2,4)
      CEN2(3,3)=4.*(CEN2(4,2))/3.
      CEN2(4,3)=3.*CEN2(2,3)*(X(I+1)**2+X(I)**2)/2.
```

```
      CEN2(3,4)=CEN2(4,3)
      CEN2(4,4)=9.*(X(I+1)**5-X(I)**5)/5.
C
C     FORM THE ELEMENT MATRIX EK2
C
      B(1,1)=1.
      B(1,2)=X(I)

      B(1,3)=X(I)**2
      B(1,4)=X(I)**3
      B(2,1)=0.
      B(2,2)=1.
      B(2,3)=2.*X(I)
      B(2,4)=3.*(X(I)**2)
      B(3,1)=1.
      B(3,2)=X(I+1)
      B(3,3)=X(I+1)**2
      B(3,4)=X(I+1)**3
      B(4,1)=0.
      B(4,2)=1.

      B(4,3)=2.*X(I+1)
      B(4,4)=3.*(X(I+1)**2)
      CALL INVERS (B,4,4,IPR,BINV,D1)
C
      CALL FMTMX (BINV,CEN2,C,4,4,4,4,4,4)
C     NOW FOR  EK2 = C*BINV
      CALL FMMX (C,BINV,EK2,4,4,4,4,4,4)
      RETURN
      END
**********************************
      SUBROUTINE TRANS (MODE,M)
**********************************

      COMMON /B7/ T(70,40)
      REAL MODE
C     THE ASSEMBLY OF T IS BASED ON EVEN NUMBER OF ELEMENTS,M
C     INITIALIZE TO ZERO
      MP2=M+2
      M2=2*M+2
      DO 2 MM=1,M2
      DO 1 KM=MM,M2
      T(KM,MM)=0.
      T(MM,KM)=0.
1     CONTINUE
2     CONTINUE

      DO 3 IR=1,M,2
      I=MP2+IR+1
      J=M+1-IR
      T(I,J)=-(MODE)
      I=IR+MP2
      J=M-IR
      T(I,J)=MODE
3     CONTINUE
      DO 4 NI=1,MP2
      T(NI,NI)=1.
4     CONTINUE
C

      RETURN
      END
**********************************
      SUBROUTINE FMVX (A,X,Y,M,N,MA)
**********************************
C     MATRIX VECTOR MULTIPLICATION.  Y = A*X
      DIMENSION A(MA,1), X(1), Y(1)
      DO 1 I=1,M
      Y(I)=0.
      DO 1 J=1,N
1     Y(I)=X(J)*A(I,J)+Y(I)
      RETURN


      END
**********************************
      SUBROUTINE FMMX (A,B,C,M,N,MA,MB,MC,K)
**********************************
C     MATRIX MATRIX MULT  C = A*B
      DIMENSION A(MA,1), B(MB,1), C(MC,1)
      DO 1 L=1,K
      DO 1 I=1,M
      C(I,L)=0.
      DO 1 J=1,N
1     C(I,L)=A(I,J)*B(J,L)+C(I,L)
      RETURN


      END
**********************************
      SUBROUTINE FMTMX (A,B,C,M,N,MA,MB,MC,K)
**********************************
C      MATRIX TRANS * MATRIX  C = A TRANS * B
      DIMENSION A(MA,1), B(MB,1), C(MC,1)
      DO 1 L=1,K
      DO 1 I=1,N
      C(I,L)=0.
      DO 1 J=1,M
1     C(I,L)=A(J,I)*B(J,L)+C(I,L)
      RETURN


      END
**********************************
      SUBROUTINE INVERS (A,IA,N,IPR,AINV,D1)
**********************************
C     TO CALC INVERSE OF A USING IMSL SUBROUTINE LINV1F
      DIMENSION A(IA,1), AINV(IA,1), IPR(1)
      REAL IPR
C     PARAMETER IDGT IF .GT. 0 LINV1F PERFORMS ACCURACY TEST
      IDGT=4
      CALL LINV1F (A,N,IA,AINV,IDGT,IPR,D1)
      RETURN
      END


**********************************
      SUBROUTINE SYMOPT (M,M1,M2,MODE,MAX)
**********************************
C     SYMOPT IS THE PRIMARY SUBROUTINE FOR THE SYMM OPT PROBLEM.**
***
      REAL K1,K2,MODE
      DIMENSION CRIT(40,2), DVEC(70)
      DIMENSION ENER(40)
```

```
      COMMON /B7/ T(70,40)/B16/VEC2(40)
      DIMENSION AK1(70,70), AK2(70,70)
      DIMENSION X(40), XI(40), EVAL(40), SING(80)
      COMMON /4/ RHO,EXP/5/EL

      COMMON /B14/ VEC1(40)/B12/VEC(40)
      COMMON /1/ BETA/10/SYMM/11/SUMJ
      COMMON /B1/ K1(40,40)/B2/K2(40,40)/B3/AU5(70)/B4/U6(40)
      COMMON /N1/ FB(100)
      COMMON /B11/ PROD(40,40)
      COMMON /8/ PSTOP/13/E
      DIMENSION XIOLD(40)
      COMMON /7/ U0L,XIMIN,EXP1/12/U
C
C
      SIGN=-1.
      ICRIT=0

      ITMXOP=15
      EXP1=1./EXP1
      E=6.
C     PSTART IS THE STARTING VALUE OF P FOR THE FIRST ITERATION
C     ON T-E BUCKLING OF THE UNIFORM ARCH.
      PSTART=6.
C
      IF (BETA.GT.100.) GO TO 1
      MOR=M
      GO TO 2
1     MOR=M-1
2     CONTINUE

      SYMM=1.
C     DEFINE THE SPATIAL VECTOR X
C
      X(1)=0.
      DO 3 LT=2,M1
3     X(LT)=X(LT-1)+EL
      DELP=.10
      CALL ASS2 (M,M1,M2,MAX,MODE,X,AK2)
      CALL ASS5 (M,M1,M2,MAX,MODE,X)
      CALL ASS6 (M,M1,M2,MAX,MODE,X)
C     THE RESULT OF THIS CALL IS THE ASSEMBLY OF K2,AU5,U6,STORED
IN COM

C
C     DEFINE THE INITIAL(UNIFORM) INERTIA DISTRIBUTION XI
      DO 4 I=1,M
4     XI(I)=1.
5     CONTINUE
      SUMJ=0.
      DO 6 IA=1,M
6     SUMJ=SUMJ+(XI(IA)/RHO)**(-1./EXP)
      SUMJ=1./(2.*EL*SUMJ)
C
      CALL ASS1 (M,M1,M2,MAX,MODE,X,XI,AK1)
      CALL EIGEN (M,MOR,MAX,EVAL,NPE)

      MAX=70
      IF (NPE) 12,12,7
7     CONTINUE
C
C     DETERMINATION OF THE SINGULARITY VECTOR SING FOR
C          NPE .GT. 0.
      DO 8 JJ=1,NPE
      IF (EVAL(JJ)-PSTOP) 8,8,9
8     CONTINUE
      NSING=NPE
      GO TO 10
9     NSING=JJ-1


10    CONTINUE
      DO 11 NX=1,NSING
      SING(2*NX-1)=0.95*EVAL(NX)
11    SING(2*NX)=1.05*EVAL(NX)
C
      WRITE (6,34)
      ISING=2*NSING
      WRITE (6,35) (SING(J),J=1,ISING)
C      THE E.VALUES OF K1-P*K2 ARE SINGULARITIES IN THE
C       SUBSEQUENT MATH SCHEME
C
C


C     START ITERATION FOR CRITICAL CONDS FOR (E,XI)
C                         STAGE 1: COARSE BRACKET
C
12    CONTINUE
C     EACH OPT ITERATION BEGINS AT ONE LESS THAN PREVIOUS PCR
C        RATHER THAN AT P=0.
      IF (ICRIT) 14,13,14
13    POLD=PSTART
      GO TO 15
14    POLD=CRIT(ICRIT,1)-.3
15    CONTINUE
      IT=0


      NEG=0
C     IT IS THE ITERATION PARAMETER FOR A PARTIC  E.
16    CONTINUE
      P=POLD+DELP
      IF (ICRIT.EQ.0) GO TO 17
      PLIM=1.5*CRIT(ICRIT,1)
      IF (P.GE.PLIM) GO TO 26
17    CONTINUE
      IF (NPE.EQ.0) GO TO 20
C
C     TEST P AGAINST SING***
C


      DO 18 NS=1,NSING
      IF (P.LT.SING(2*NS).AND.P.GT.SING(2*NS-1)) GO TO 19
C     P IS NOT IN SINGULAR ZONE.ARE P AND POLD IN SAME REGION
      IF (POLD.LT.SING(2*NS-1).AND.P.GT.SING(2*NS)) GO TO 19
18    CONTINUE
      IF (P.LE.PSTOP) GO TO 20
C     THE BRACKET WAS UNSUCCESSFUL***
      WRITE (6,36)
      WRITE (6,37) (FB(J),J=1,IT)
      RETURN
19    CONTINUE
```

```
      WRITE (6,38) P,POLD,NS

      P=SING(2*NS)
      IT=0
C
20    CONTINUE
C     COEFP WILL COMPUTE THE COEFFS IN THE P,Q RELATION
      CALL COEFP (P,E,MOR,S1,S2,S3,APEX1,APEX2)
      DISC=S2**2-4.*S1*S3
C     IF DISC IS NEG. INCREMENT P AND RECOMP COEFP
      IF (DISC) 21,23,23
21    POLD=P
      WRITE (6,39) P
      IF (NEG.GT.0) GO TO 22

      WRITE (6,40) (FB(IA),IA=1,IT)
22    NEG=NEG+1
      IF (NEG.GT.20) GO TO 33
      GO TO 16
23    CONTINUE
C     COMPUTE COEF IN BUCKLING EQUATION
      CALL COEFB (P,E,MOR,A1,A2,A3)
C
      WRITE (6,41) S1,S2,S3,A1,A2,A3,P,E
C     FORM THE FUNCTIONS OF P
C
      IT=IT+1

      Q=(-S2+SIGN*SQRT(DISC))/(2.*S1)
      FB(IT)=(Q**2)*A1+Q*A2+A3
C     TEST FOR ROOTS IF IT > 1
      IF (IT.EQ.1) GO TO 24
      TESTB=FB(IT)*FB(IT-1)
      IF (TESTB.LE.0.) GO TO 25
24    POLD=P
      GO TO 16
25    CONTINUE
C                ***STAGE 2: SECANT ITERATION ***
      CALL SECANT (P,Q,E,SIGN,MOR,IT,DELP,APEXD)
C     THE RESULT WILL BE PCR,QCR.

      PCR=P
      QCR=Q
      ICRIT=ICRIT+1
      CRIT(ICRIT,1)=PCR
      CRIT(ICRIT,2)=QCR
      IF (ICRIT.EQ.1) GO TO 28
C     COMPARE SUCCESSIVE VALUES OF PCR
      IF (CRIT(ICRIT,1)-CRIT(ICRIT-1,1)) 26,26,28
C     REDUCE THE EXPONENT EXP1 AND REPEAT THE ITERATION
C
26    CONTINUE
      REDEXP=REDEXP+1

      EXP1=.8*EXP1
      WRITE (6,42) REDEXP
      IF (REDEXP.GT.6.) GO TO 33
C
      DO 27 JJ=1,M
27    XI(JJ)=XIOLD(JJ)
      CALL INRTIA (M,U,ENER,XI,XIOLD)
C     NOW WE HAVE A NEW INERTIA THAT WILL HOPEFULLY LEAD TO
C           AN INCREASE IN QCR.
C     GO BACK AND RECOMPUTE QCR FOR THIS INERTIA
      GO TO 5
28    CONTINUE


      IF (ICRIT.GE.ITMXOP) GO TO 33
C     STEP1)  DETER BUCK MODE
C     THE BUK MODE CAN BE COMPUTED FROM VEC AND VEC1 FROM
C        COEFP AND COEFB.
      WRITE (6,43) BETA,MOR,P,Q,E
      MP2=M+2
      IF (BETA.GT.100) GO TO 30
C     ASSEMBLY OF DEFORMATION VECTOR FOR RESTRAINED CASE.
      VEC2(MP2)=0.
      VEC2(1)=0.
      DO 29 I=1,MOR
29    VEC2(I+1)=PCR*VEC1(I)*E+QCR*VEC(I)


      CALL FMUX (T,VEC2,DVEC,M2,MP2,70)
C     WITH DVEC, CALL ENERGY.
      GO TO 32
30    CONTINUE
C     ASSEMBLY OF DEFORMATION VECTOR FOR CLAMPED CASE
      VEC2(1)=0.
      VEC2(2)=0.
      VEC2(MP2)=0.
      DO 31 J=1,MOR
31    VEC2(J+2)=PCR*VEC1(J)*E+QCR*VEC(J)
      CALL FMUX (T,VEC2,DVEC,M2,MP2,70)
32    CONTINUE


      WRITE (6,44) (DVEC(I),I=1,M2)
C
C
C        ***ENERGY AND NEW INERTIA***
C
      CALL ENERGY (M,M1,M2,X,XI,DVEC,ENER,CONVG,XIOLD,AK2,PCR)
      IF (CONVG.GT.3.) GO TO 5
      RETURN
33    WRITE (6,45) ITMXOP,REDEXP,EXP1,CONVG,E
      WRITE (6,46) ((CRIT(I,J),J=1,2),I=1,ICRIT)
      WRITE (6,47) (XI(J),J=1,M)
      RETURN



C
34    FORMAT (/,10X,1H*,SINGULARITYVECTOR,1H*,/)
35    FORMAT (10X,5E12.5,/)
36    FORMAT (//,10X,1H*,BRACKETWASUNSUCCESSFUL,1H*,//)
37    FORMAT (10X,5(E12.5,3X))
38    FORMAT (//,10X,2(E12.5,5X),5X,I4,/)
39    FORMAT (//,10X,1H*,DISCBECAMENEG,1H*,7H,/,10X,,P=,8H,E12.5,/
     )
40    FORMAT (/,10X,5E12.5)
41    FORMAT (10X,8(E12.5,3X))
42    FORMAT (//,10X,1H*,THE,6H,F4.0,,REDUCTIONINEXP1ISMADE,1H*,//
     )
```

```
43    FORMAT (10X,30H*EQUIL SOLN AT CRITICAL POINT*,/,10X,5HBETA=,
F4.0,5
     1X,4HMOR=,I4,5X,4HPCR=,E12.5,5X,4HQCR=,E12.5,5X,2HE=,F4.0,//)
44    FORMAT (10X,6E12.5)
45    FORMAT (10X,1H*,OPTIMIZATIONPROC.DIDNOTCONVERGEIN,4H,I5,,ITE
RATION
     1S,1H*,/,20X,7HREDEXP=,E12.5,/,20X,5HEXP1=,E12.5,/,20X,6HCONV
G=,E12
     2.5,/,20X,2HE=,F4.0,/,)
46    FORMAT (/,20X,2(E12.5,5X))
47    FORMAT (20X,E12.5)
      END

*************************************
      SUBROUTINE ASSS (M,M1,M2,MAX,MODE,X)
*************************************
C     THE ASSEMBLY OF KS
      REAL MODE
      DIMENSION X(M1), EVS(4)
      COMMON /B7/ T(70,40),/B3/AVS(70)
      COMMON /B12/ VEC(40)
      COMMON /10/ SYMM
      COMMON /1/ BETA
      COMMON /2/ LOAD
C     AVS IS A VECTOR OF SIZE 2M + 2

C     INITIALIZE TO XERO
      MP2=M+2
      MM1=M-1
      DO 1 IC=1,M2
      AVS(IC)=0.
1     CONTINUE
C     START ASSEMBLY
      DO 3 I=1,M
      CALL COMEVS (I,M1,X,EVS)
      DO 2 LC=1,4
      AVS(2*I-2+LC)=EVS(LC)+AVS(2*I-2+LC)
2     CONTINUE

3     CONTINUE
C     THE ASSEMBLED VECTOR AVS MUST BE MODIFIED TO ACCOUNT FOR
C     BOUNDARY AND SYMMETRIC CONDITIONS
C     FORM T TRANSPOSE * AVS
      CALL FMTUX (T,AVS,VEC,M2,MP2,70)
      IF (SYMM.GT.0.) GO TO 6
C     FOR SYMMETRY Q(M+2) = 0
      DO 4 IA=1,MP2
      AVS(IA)=VEC(IA)
4     CONTINUE
      AVS(1)=0.
      AVS(MP2)=0.

      IF (BETA.GT.100.) GO TO 5
      RETURN
5     CONTINUE
6     CONTINUE
      IF (BETA.GT.100.) GO TO 8
      MOR=M
      DO 7 JK=1,MOR
      AVS(JK)=VEC(JK+1)
7     CONTINUE
      RETURN
8     CONTINUE
      MOR=MM1


      DO 9 JB=1,MOR
      AVS(JB)=VEC(JB+2)
9     CONTINUE
      RETURN
      END
*************************************
      SUBROUTINE COMEVS (I,M1,X,EVS)
*************************************
C     B IS BASED ON CUBIC INTERPOLATION FCN
      DIMENSION B(4,4), IPR(4)
      DIMENSION CENS(4), EVS(4), BINV(4,4)
      DIMENSION X(M1)


      COMMON /2/ LOAD
      PI=3.1415926
      B(1,1)=1.
      B(1,2)=X(I)
      B(1,3)=X(I)**2
      B(1,4)=X(I)**3
      B(2,1)=0.
      B(2,2)=1.
      B(2,3)=2.*X(I)
      B(2,4)=3.*(X(I)**2)
      B(3,1)=1.
      B(3,2)=X(I+1)


      B(3,3)=X(I+1)**2
      B(3,4)=X(I+1)**3
      B(4,1)=0.
      B(4,2)=1.
      B(4,3)=2.*X(I+1)
      B(4,4)=3.*(X(I+1)**2)
      CALL INVERS (B,4,4,IPR,BINV,D1)
C
C     THE PARAMETER LOAD DETERMINES THE TYPE OF LOAD DISTRIBUTION
C     LOAD = 1, SINE DIST
C     LOAD = 2,, PARABOLIC DIST
C     LOAD = 3,  UNIFORM DIST


C     CENS IS THE VECTOR DEFINED BY INTEGRAL F*L
      IF (LOAD-2) 1,2,3
1     CONTINUE
      CENS(1)=-(COS(X(I+1))-COS(X(I)))
      CENS(2)=(SIN(X(I+1))-X(I+1)*COS(X(I+1)))-(SIN(X(I))-X(I)*COS
(X(I))
     1)
      CENS(3)=(2.*X(I+1)*SIN(X(I+1))-(X(I+1)**2-2.)*COS(X(I+1)))-(
2.*X(I
     1)*SIN(X(I))-(X(I)**2-2.)*COS(X(I)))
      CENS(4)=((3.*(X(I+1)**2-2.)*SIN(X(I+1))-(X(I+1)**3-6.*(X(I+1
)))*CO
```

```
     1S(X(I+1))))-((3.*(X(I)**2-2.)*SIN(X(I))-(X(I)**3-6.*(X(I)))*
COS(X(
     2I)))
      GO TO 4
2     CONTINUE
C     PARABOLIC DIST
      C1=2./(3.*(PI**2))
      C2=1./(3.*(PI**2))
      C3=1./(5.*(PI**2))
      C4=2./(12.*(PI**2))
      CEN5(1)=C1*(3.*PI*(X(I+1)**2-X(I)**2)-2.*(X(I+1)**3-X(I)**3)
)
      CEN5(2)=C2*(4.*PI*(X(I+1)**3-X(I)**3)-3.*(X(I+1)**4-X(I)**4)
)
      CEN5(3)=C3*(5.*PI*(X(I+1)**4-X(I)**4)-4.*(X(I+1)**5-X(I)**5)
)
      CEN5(4)=C4*(6.*PI*(X(I+1)**5-X(I)**5)-5.*(X(I+1)**6-X(I)**6)
)
      GO TO 4
3     CONTINUE
C     UNIFORM LOAD DIST
      CEN5(1)=X(I+1)-X(I)
      CEN5(2)=(X(I+1)**2-X(I)**2)/2.
      CEN5(3)=(X(I+1)**3-X(I)**3)/3.

      CEN5(4)=(X(I+1)**4-X(I)**4)/4.
4     CONTINUE
C     COMPUTE THE ELEMENT VECTOR EV5
C
      CALL FMTUX (BINV,CEN5,EV5,4,4,4)
      RETURN
      END
**********************************
      SUBROUTINE ASV6 (M,M1,M2,MAX,MODE,X)
**********************************
C     THE ASSEMBLY OF V6
      REAL MODE

      DIMENSION X(M1), EV6(4)
      COMMON /B7/ T(70,40)/B4/V6(40)/B12/VEC(40)
      COMMON /1/ BETA
      COMMON /20/ AV6(70)
      COMMON /3/ ISHAPE
      COMMON /10/ SYMM
C     AV6 IS A GLOBAL VECTOR SIZE M2
C     INITIALIZE TO ZERO
      MP2=M+2
      MM1=M-1
      DO 1 IC=1,M2
      AV6(IC)=0.

1     CONTINUE
C     START ASSEMBLY
      DO 3 I=1,M
      CALL COMEV6 (I,M1,X,EV6)
      DO 2 LC=1,4
      AV6(2*I-2+LC)=EV6(LC)+AV6(2*I-2+LC)
2     CONTINUE
3     CONTINUE
      IF (MODE.EQ.0.) RETURN
C     MODIFY FOR BC AND SYMM
C     FORM T TRANSPOSE*AV6
      CALL FMTUX (T,AV6,VEC,M2,MP2,70)
      IF (SYMM.GT.0.) GO TO 6
C     FOR SYMMETRY G(M+2) = 0.
      DO 4 IA=1,MP2
      V6(IA)=VEC(IA)
4     CONTINUE
      V6(1)=0.
      V6(MP2)=0.
      IF (BETA.GT.100.) GO TO 5
      RETURN
5     CONTINUE
6     CONTINUE
      IF (BETA.GT.100.) GO TO 8


      MOR=M
      DO 7 JK=1,MOR
      V6(JK)=VEC(JK+1)
7     CONTINUE
      RETURN
8     CONTINUE
      MOR=MM1
      DO 9 JB=1,MOR
      V6(JB)=VEC(JB+2)
9     CONTINUE
      RETURN
      END


**********************************
      SUBROUTINE COMEV6 (I,M1,X,EV6)
**********************************
      DIMENSION CEN4(4), EV6(4), BINV(4,4), B(4,4)
      DIMENSION X(M1)
      DIMENSION IPR(4)
      COMMON /3/ ISHAPE
      PI=3.1415926
C     THE PARAMETER ISHAPE DETS THE INITIAL SHAPE
C     THE RISE PARAMETER E WILL BE CARRIED EXPLICITLY BY P,Q RELAT
ION
C     THE INTERRATIONS ARE DONE BY HAND.


C     CEN4 IS THE VECTOR DEFINED BY ETAOPRIME*L,
      IF (ISHAPE-1) 1,1,2
1     CONTINUE
      CEN4(1)=0.
      CEN4(2)=SIN(X(I+1))-SIN(X(I))
      CEN4(3)=2.*((COS(X(I+1))+X(I+1)*SIN(X(I+1)))-(COS(X(I))+X(I)
*SIN(X
     1(I))))
      CEN4(4)=3.*((2.*X(I+1)*COS(X(I+1))+(X(I+1)**2-2.)*SIN(X(I+1)
))-(2.
     1*X(I)*COS(X(I))+(X(I)**2-2.)*SIN(X(I))))
      GO TO 3


2     CONTINUE
C     CEN4 PARABOLIC
```

```
      CEN4(1)=0.
      CEN4(2)=4.*(PI*(X(I+1)-X(I))-(X(I+1)**2-X(I)**2))/(PI**2)
      CEN4(3)=8.*(3.*PI*(X(I+1)**2-X(I)**2)-4.*(X(I+1)**3-X(I)**3)
     1)/(8.*
     1(PI**2))
      CEN4(4)=(4.*PI*(X(I+1)**3-X(I)**3)-6.*(X(I+1)**4-X(I)**4))/(
     PI**2)
3     CONTINUE
      B(1,1)=1.
      B(1,2)=X(I)

      B(1,3)=X(I)**2
      B(1,4)=X(I)**3
      B(2,1)=0.
      B(2,2)=1.
      B(2,3)=2.*X(I)
      B(2,4)=3.*(X(I)**2)
      B(3,1)=1.
      B(3,2)=X(I+1)
      B(3,3)=X(I+1)**2
      B(3,4)=X(I+1)**3
      B(4,1)=0.
      B(4,2)=1.

      B(4,3)=2.*X(I+1)
      B(4,4)=3.*(X(I+1)**2)
      CALL INVERS (B,4,4,IPR,BINV,D1)
C     COMPUTE THE ELEMENT VECTOR EV6
      CALL FMTVX (BINV,CEN4,EV6,4,4,4)
      RETURN
      END
**********************************
      SUBROUTINE COEFP (P,E,MOR,S1,S2,S3,APEX1,APEX2)
**********************************
C     ASSEMBLE THE COEFS OF PQ RELATION AND ITERATE ON P UNTIL A F
EASIBL

C        SOLN  IS OBTAINED.
      REAL K1,K2,K,KINV
      COMMON /11/ SUMJ
      COMMON /B1/ K1(40,40)/B2/K2(40,40)/B3/AV5(70)/B4/V6(40)
      COMMON /B8/ K(40,40)/B9/KINV(40,40)/B11/PROD(40,40)
      COMMON /B12/ VEC(40)/B13/PROD1(40,40)/B14/VEC1(40)
      DO 1 IA=1,MOR
      DO 1 JA=1,MOR
1     K(IA,JA)=K1(IA,JA)-P*K2(IA,JA)
      CALL SINVRS (K,KINV,MOR,40)
      CALL FMMX (KINV,K2,PROD,MOR,MOR,40,40,40,MOR)
      CALL FMMX (PROD,KINV,PROD1,MOR,MOR,40,40,40,MOR)

      CALL FMUX (PROD1,AV5,VEC,MOR,MOR,40)
C
      S1=0.
      DO 2 IB=1,MOR
2     S1=S1+AV5(IB)*VEC(IB)
      IF (S1.EQ.0.) STOP
      CALL FMUX (KINV,AV5,VEC1,MOR,MOR,40)
      APEX1=VEC1(MOR)
      S2=0.
      DO 3 IC=1,MOR
3     S2=S2+2.*P*V6(IC)*VEC(IC)+2.*V6(IC)*VEC1(IC)
      S2=E*S2

      CALL FMUX (KINV,V6,VEC1,MOR,MOR,40)
      APEX2=VEC1(MOR)
      CALL FMUX (PROD1,V6,VEC,MOR,MOR,40)
      S3=0.
      DO 4 ID=1,MOR
4     S3=S3+(P**2)*V6(ID)*VEC(ID)+2.*P*V6(ID)*VEC1(ID)
      S3=(E**2)*S3+P/SUMJ
      RETURN
      END
**********************************
      SUBROUTINE SINVRS (A,AINV,N,IA)
**********************************


C     TO COMPUTE INVERSE OF SYM MATRIX USING IMSL LINV2F.
C     THE PARAM IDGT = 0 ITERATIVE IMPROVEMENT IS AUTO.
      DIMENSION A(IA,1), AINV(IA,1), WKAR(800)
      IDGT=0
      CALL LINV2F (A,N,IA,AINV,IDGT,WKAR,IER)
      RETURN
      END
**********************************
      SUBROUTINE FMTVX (A,X,Y,M,N,MA)
**********************************
      DIMENSION A(MA,1), X(1), Y(1)
C      FIND Y = A TRANS*X


C      WHERE A(M,N)
C      MA IS ROW DIM OF A IN CALLING PROG
C
      DO 1 I=1,N
      Y(I)=0.
      DO 1 J=1,M
1     Y(I)=A(J,I)*X(J)+Y(I)
      RETURN
      END
**********************************
      SUBROUTINE COEFB (P,E,MOR,A1,A2,A3)
**********************************


      REAL KINV
      COMMON /11/ SUMJ
      COMMON /B9/ KINV(40,40)/B12/VEC(40)
      COMMON /B14/ VEC1(40)/B3/AV5(70)/B4/V6(40)
C     NOTE THAT VEC1 IS IN COMMON WITH SUBROUTINE COEFP***
      CALL FMUX (KINV,AV5,VEC,MOR,MOR,40)
      B1=0.
      DO 1 I=1,MOR
1     B1=B1+AV5(I)*VEC(I)
      B2=0.
      DO 2 J=1,MOR
2     B2=B2+AV5(J)*VEC1(J)


      B2=B2*E
      B3=0.
      DO 3 IA=1,MOR
3     B3=B3+V6(IA)*VEC1(IA)
      B3=B3*(E**2)
```

```
C       THE BUCKLING EQN COEFF. ARE
        A1=B1+2.*SUMJ*(B2**2)
        A2=(2.*P**1.+2.*SUMJ*(B3+1./SUMJ))*B2
        A3=(P**2)*(B3+2.*SUMJ*(B3+1./SUMJ)**2))
        RETURN
        END
*************************************

        SUBROUTINE SECANT (P,Q,E,SIGN,MOR,IT,DELP,APEXD)
*************************************
C
C       THIS SUB WILL CONVERGE TO PCR AND QCR BY SECANT METHOD
C           ONCE BRACKET HAS SUCCEEDED.
C
        COMMON /N1/ FB(100)/11/SUMJ
        ITSEC=0
        P1=P
        P0=P-DELP
C       THE ROOT IS BRACKETED IN SOME FEASIBLE REGION BETWEEN
C          P0 AND P1.

        J=IT
        K=J-1
1       PNEW=(-P0*FB(J)+P1*FB(K))/(-FB(J)+FB(K))
        WRITE (6,9) P0,P1,FB(IT),IT,PNEW
        IF (PNEW.LT.P0.OR.PNEW.GT.P1) GO TO 6
        IT=IT+1
        CALL COEFP (PNEW,E,MOR,S1,S2,S3,APEX1,APEX2)
        DISC=S2**2-4.*S1*S3
        IF (DISC) 6,2,2
2       CONTINUE
        Q=(-S2-SIGN*SQRT(DISC))/(2.*S1)
        CALL COEFB (PNEW,E,MOR,A1,A2,A3)

        FB(IT)=(Q**2)*A1+Q*A2+A3
        PDIF=PNEW-P1
        TEST=FB(IT)
        FPROD=FB(IT)*FB(J)
        IF (ABS(TEST).LE.1.E-5.OR.ABS(PDIF).LE.1.E-5) GO TO 5
        ITSEC=ITSEC+1
        IF (ITSEC.GT.5) GO TO 7
        IF (FPROD) 3,5,4
3       P0=PNEW
        K=IT
        GO TO 1
4       P1=PNEW

        J=IT
        GO TO 1
5       CONTINUE
        P=PNEW
        Q=(-S2+SIGN*SQRT(DISC))/(2.*S1)
        APEXD=P*APEX2+E+Q*APEX1
        WRITE (6,11) APEXD,PDIF,PNEW,Q,E,ITSEC,IT
        GO TO 8
6       WRITE (6,10) ITSEC,IT,PNEW,P1,P0,DISC
        STOP
7       WRITE (6,12)
        ITMAX=IT+ITSEC

        WRITE (6,13) (FB(JA),JA=IT,ITMAX)
        WRITE (6,14) PNEW,P1,P0,IT,SIGN
C       **NOTE* EVEN THOUGH SECANT DID NO CONVERGE,I AM CONT
C               INUING THE OPTIMIZATION PROCESS.**********
        GO TO 5
8       CONTINUE
        RETURN
C
5       FORMAT (10X,3HP0=,E12.5,10X,3HP1=,E12.5,10X,7HFB(IT)=,E12.5,
10X,3H
       1IT=,I4,10X,5HPNEW=,E12.5,//)
10      FORMAT (10X,/,1H*,SECANTMETHODAPPARENTLYDIVERGES,1H*,/,10X,1


2HSEC4
       1NT ITER=,F4.0,/,10X,3HIT=,I4,/,10X,5HPNEW=,E12.5,/,10X,3HP1=
,E12.5
       2,/,10X,3HP0=,E12.5,/,10X,5HDISC=,E12.5,//)
11      FORMAT (10X,/,1H*,SECANTMETHODCONVERGED,1H*,/,10X,6HAPEXD=,E
12.5,/
       1,10X,5HPDIF=,E12.5,/,10X,4HPCR=,E12.5,/,10X,4HQCR=,E12.5,/,1
0X,2HE
       2=,F4.0,/,10X,6HITSEC=,I4,/,10X,3HIT=,I4,//)
12      FORMAT (/,10X,1H*,SECANTMETHODDIDNOTCONVERGEIN5ITERATIONS,1H
*,/,10
       1X,8H,TREFEVALUATIONSARE,8H,/)



13      FORMAT (10X,E12.5)
14      FORMAT (10X,/,5HPNEW=,E12.5,/,10X,3HP1=,E12.5,/,10X,3HP0=,E1
2.5,/,
       110X,3HIT=,I4,/,10X,5HSIGN=,E12.5,/)
        END
*************************************
        SUBROUTINE ENERGY (M,M1,M2,K,XI,DVEC,ENER,CONVG,XIOLD,AK2,PC
*************************************
R)
        REAL MAXE,MINE
        DIMENSION PROD1(70)
        DIMENSION XIOLD(M), AK2(70,2)



        DIMENSION ENER(M), X(M1), XI(M), DVEC(M2)
        DIMENSION ELVEC(4), EK1(4,4), PROD(4)
        COMMON /12/ U/13/E/11/SUMJ
        COMMON /20/ AV6(70)
        COMMON /4/ RHO,EXP
        COMMON /5/ EL/10/SYMM
C       IN SUB ENERGY COMPUTE AVE ENERGY DIST. OUTPUT WILL B  THE
C       CURRENT ENERGY DIST STORED AS A VECTOR, ENER(M).
C
C       AT THIS STAGE WE MUST SPECIFY THE EXPONENT AND COEF
C       IN THE INERTIA AREA RELATION, I = RHO*(A**EXP)
        UB=0.



        U=0.
C       FORM TOTAL INTERACTION ENERGY UI
C       SET MODE=0
        IF (SYMM.EQ.-1.) GO TO 3
        CALL ASS2 (M,M1,M2,70,0.,X,AK2)
        CALL FMUX (AK2,DVEC,PROD1,M2,M2,M2)
        T1=0.
        DO 1 IN=1,M2
```

```
1       T1=T1+DVEC(IN)*PROD1(IN)
        CALL ASUB (M,M1,M2,MAX,0.,X)
        T2=0.
        DO 2 IM=1,M2

2       T2=T2+DVEC(IM)*AUB(IM)*E
        UI=2.*SUMJ*((T1+T2)**2)
3       CONTINUE
C
        DO 6 I=1,M
C       DEFINE THE ELEMENT DISPL VECTOR ELVEC FROM DVEC
        DO 4 J=1,4
        ELVEC(J)=DVEC(2*I-2+J)
4       CONTINUE
        CALL COMEX1 (I,M,M1,X,XI,EK1)
C       NOW FORM MATRIX VECTOR PRODUCT
        CALL FMUX (EK1,ELVEC,PROD,4,4,4)

C       NOW MULT ELVEC AND PROD
        ENUM=0.
        DO 5 K=1,4
        ENUM=(ELVEC(K))*(PROD(K))+ENUM
5       CONTINUE
C       NOW COMPUTE THE DENOM
        REXP=1. EXP
        DENOM=(((XI(I))/RHO)**REXP)*EL
C       FINALLY THE ENERGY.  DENOM WILL BE GREATER THAN ZERO SINCE
C       XI(I) WILL BE RESTRICTED GREATER THAN ZERO.
        ENER(I)=ENUM/DENOM
        U=U+DENOM

        UB=UB+ENUM
        IF (SYMM.EQ.-1.) GO TO 6
C       NOW FORM THE INTERACTION ENERGY FOR THE ITH ELEMENT
C
        SUMJI=DENOM/(2.*(EL**2))
        ENER(I)=ENER(I)*EXP+(UI*SUMJ/SUMJI)/DENOM
6       CONTINUE
C       NOW ENER IS THE CRITICAL ENERGY DENSITY FOR EACH ELEMENT
C       UB IS TOTAL BENDING ENERGY;UI IS TOTAL INTERACTION ENERGY
        IF (SYMM-1.) 8,7,8
7       U=UB*EXP+UI
        GO TO 9

8       U=UB
9       CONTINUE
C       U  WILL BE THE TOTAL ENERGY
        WRITE (6,16) U,U
        WRITE (6,17)
        WRITE (6,18) (ENER(I),I=1,M)
C       WE NOW HAVE THE AVE ENERGY FOR EACH ELEMENT CORRES TO THE
C       PARTICULAR INERTIA IN EACH ELEMENT.
C       WE HAVE THE ENERGY DENSITY DIST FOR GIVEN INERTIA
C       NOW CHECK FOR CONVERGENCE.
C       ************CONVERGENCE TEST*************************************
******

        MM1=M-1
        MAXE=ENER(1)
        DO 11 J=1,MM1
        DIF=MAXE-ENER(J+1)
        IF (DIF) 10,10,11
10      MAXE=ENER(J+1)
11      CONTINUE

C       MAXE IS THE LARGEST ELEMENT OF ENER. SELECT THE SMALLEST.
C
        MINE=ENER(1)
        DO 13 J=1,MM1
        DIF=ENER(J+1)-MINE


        IF (DIF) 12,12,13
12      MINE=ENER(J+1)
13      CONTINUE
C       IF THE DIF BETWEEN MAXE AND MINE IS SMALL ENOUGH,THEN
C          THE ENERGY DENSITY IS ALMOST UNIFORM AND OPTIMUM
C       IS ACHIEVED WITHIN SELECTED CONVERGENCE CRITERIA.
C
        WRITE (6,19) MAXE,MINE
        CONVG=((MAXE/MINE)-1.)*100.
        IF ((CONVG.GT.3.) GO TO 14
        WRITE (6,20)
        GO TO 15


C        COMPUTE NEW INERTIA
14      CONTINUE
        CALL INRTIA (M,U,ENER,XI,XIOLD)
        WRITE (6,21)
15      WRITE (6,22) (XI(J),J=1,M)
C       TEST****
        SYMM=1.
        RETURN
C
16      FORMAT (//,5X,14HTOTAL ENERGY,U,3X,E12.5,/,5X,23HTOTAL VOLUM
E
     1       ,3X,E12.5,///)


17      FORMAT (/,20X,19HENERGY DISTRIBUTION,//)
18      FORMAT (/,25X,E12.5)
19      FORMAT (/,5X,7HMAXE IS,3X,E12.5,/,5X,7HMINE IS,3X,E12.5,///)
20      FORMAT (//,22X,30HENERGY CONVERGENCE IS OBTAINED,//)
21      FORMAT (//,10X,17HNEW INERTIA DIST.,//)
22      FORMAT (/,10X,E12.5)
        END
*******************************
        SUBROUTINE INRTIA (M,U,ENER,XI,XIOLD)
*******************************
        DIMENSION ENER(M), XI(M), DELU(40)
        DIMENSION XIOLD(M)


        DIMENSION TXI(40)
        COMMON /5/ EL
        COMMON /4/ RHO,EXP
        COMMON /7/ VOL,XIMIN,EXP1
C
C       LET XI BE TXI
        DO 1 IM=1,M
        TXI(IM)=XI(IM)
1       CONTINUE
C       COMPUTE NEW INERTIA TXI
        COUNT=0.
```

```
      DO 2 IK=1,M

      DELV(IK)=0.
2     CONTINUE
      VEFF=VOL
      NXI=0
3     CONTINUE
      DENOM=0.
      DO 4 I=1,M
      DENOM=DENOM+((((VEFF*ENER(I)/U)**EXP1)*XI(I))**(1./EXP)*EL)
4     CONTINUE
      B=(RHO*(VEFF**EXP))/(DENOM**EXP)
      DO 5 J=1,M
      IF (TXI(J).EQ.XIMIN) GO TO 6

      TXI(J)=B*((ENER(J)*VEFF/U)**EXP1)*TXI(J)
5     CONTINUE
6     CONTINUE
C     WE HAVE THE NEW INERTIA DIST. EXAMINE TO SEE WHICH IF ANY AR
E LESS
C     THAN XIMIN
      IF (COUNT.EQ.1.) GO TO 12
      DO 9 KI=1,M
      XIDIF=TXI(KI)-XIMIN
      IF (XIDIF) 7,3,8
C     COMPUTE VOLUME CHANGE
7     DELV(KI)=EL*((1./RHO)**(1./EXP))*(XIMIN**(1./EXP)-TXI(KI)**(

1. /EXP
     1.)
      TXI(KI)=XIMIN
      NXI=NXI+1
8     CONTINUE
9     CONTINUE
C     DEFINE THE NEW EFFECTIVE VOLUME
      SUM=0.
      DO 10 KI=1,M
      SUM=SUM+DELV(KI)
10    CONTINUE
      IF (SUM.EQ.0.) GO TO 12

      VEFF=VOL-SUM
      DO 11 JJ=1,M
      IF (TXI(JJ).EQ.XIMIN) GO TO 11
      TXI(JJ)=XI(JJ)
11    CONTINUE
C     RECALCULATE THE UNSPECIFIED INERTIAS.
      COUNT=1.
      GO TO 3
12    CONTINUE
      DO 13 NK=1,M
      XIOLD(NK)=XI(NK)
      XI(NK)=TXI(NK)

13    CONTINUE
C     XI(K) HAS BEEN SUITABLY RESTRAINED TO ACCOUNT FOR XIMIN
C
C     **********************************************TEST**************
******
C     CHECK TO INSURE THAT THE CONSTANT VOLUME CONSTRAINT IS SATIS
FIED.
      SUM1=0.
      DO 14 JK=1,M
      SUM1=SUM1+((XI(JK)/RHO)**(1./EXP))*EL
14    CONTINUE
C     SUM1 SHOULD EQUAL VOL EXACTLY.


      ERROR=SUM1-VOL
      WRITE (6,15) ERROR
      RETURN
C
15    FORMAT (//,10X,57H THE VOLUME ERROR IN THE NEW INERTIA DIST.
     1       IS,3X,E12.5,//)
      END
```

SYMMETRIC OPTIMIZATION PROGRAM

```
L,A,S
      PROGRAM OPTROH(OUTPUT,TAPE6=OUTPUT)
      COMMON /1/ BETA
      COMMON /2/ LOAD
      COMMON /3/ ISHAPE
      COMMON /9/ BETAF
      COMMON /7/ VOL,XIMIN,EXP1
      COMMON /4/ RHO,EXP
      COMMON /5/ EL
C     ***********************************************************
***                                                               1
C                                                                 2
C                          DEFINITION OF PARAMETERS               C
C
C          THE INERTIA AREA RELATION IS TAKEN AS I=RHO*(A**EXP)   3
C               RHO WILL BE TAKEN AS 1
C               EXP WILL ASSUME VALUES 1,2,OR3
C          M,(AND EN) ARE TOTAL NUMBER OF ELEMENTS.
C          BETA, MODULUS OF ROTATIONAL RESTRAINT.  USED TO SPECIFY
C          BOUNDARY CONDITIONS.
C          BETA = 0.                SIMPLY SUPPORTED
C          0<BETA<100               RESTRAINED CASE               C
C          BETA>100                 CLAMPED CASE
C          ISHAPE = 1,2   HALF SINE OR PARABOLIC INITIAL CONFIG.  4
C          LOAD = 1,2, OR 3  HALF SINE, PARABOLIC OR UNIFORM LOAD.
C                                                                 C
C          VOL IS THE PRESCRIBED VOLUME                           5
C          XIMIN IS THE MINIMUM VALUE OF THE INERTIA
C                                                                 C
C     ***********************************************************
***
      MAX=70
      BETA=0.
      EXP=2.
      ISHAPE=1                                                    C
      LOAD=3
C     DEFINE A NEW VARIABLE EN = M                                C
      M=EE
                                                                  6
      EN=26.
      VOL=3.141592658
      XIMIN=0.
      RHO=1.
      EXP1=EXP/(EXP+1.)
      M1=M+1                                                      C
      M2=2*M+2
      BETAF=0.
      PI=3.141592658
      EL=PI/EN
      CALL SOLVE (M,M1,M2,MAX)                                    8
      STOP
                                                                  C
      END
*****************************
      SUBROUTINE SOLVE (M,M1,M2,MAX)
*****************************                                     9
C
C     *PRIMARY SUBROUTINE FOR ANTI-SYMM OPT PROBLEM******        10
C
      REAL K1,K2,MODE                                             11
      DIMENSION X(40), XI(40), XIOLD(40), AK1(70,70), AK2(70,70)  C
      DIMENSION EVEC(70), EVAL(40), ENER(40)
      COMMON /B1/ K1(40,40)/B2/K2(40,40)
      COMMON /13/ U/10/SYMM/5/EL/7/VOL,XIMIN,EXP1


      COMMON /1/ BETA

      EXP1=.75*EXP1
      IF (BETA.GT.100.) GO TO 1
      MOR=M
      GO TO 2
      MOR=M-1
      CONTINUE
C     DEFINE THE SPATIAL VECTOR X
      X(1)=0.
      DO 3 I=2,M1
      X(I)=X(I-1)+EL


      SYMM=-1.
      MODE=-1.
      CALL ASS2 (M,M1,M2,MAX,MODE,X,AK2)
C     DEFINE THE UNIFORM INERTIA,XI
      DO 4 J=1,M
      XI(J)=1.
      ITR=0
C     BEGIN OPT PROCESS FOR XI
      CONTINUE
      CALL ASS1 (M,M1,M2,MAX,MODE,X,XI,AK1)
C     DETERMINE THE EIGEN VALUES
      CALL EIGEN (M,MOR,EVAL,NPE,PORDIF,ITR,EVEC,P)


      WRITE (6,14) P
C     TEST***FOR BUCKLING ANALYSIS SKIP OPT PROCESS*******
      GO TO 11
C     COMPARE SUCCESSIVE VALUES OF LOWEST EVALUES
      IF (PORDIF) 6,8,8
      REDEXP=REDEXP+1.
      EXP1=.75*EXP1
      IF (REDEXP.GT.3.) GO TO 12
      DO 7 JJ=1,M
      XI(JJ)=XIOLD(JJ)
      CALL INRTIA (M,U,ENER,XI,XIOLD)
C     WITH NEW XI CORRES TO EXP1,COMPUTE NEW POR.


      GO TO 5
      CONTINUE
      CALL ENERGY (M,M1,M2,X,XI,EVEC,ENER,CONVG,XIOLD)
C     NOTE THAT CONVERGENCE CRITERIA IS 3%***
      IF (CONVG.GT.3.) GO TO 9
      WRITE (6,15)
      GO TO 11
      ITR=ITR+1
      IF (ITR-20) 5,5,10
      WRITE (6,16)
      CONTINUE
C     WITH THE OPTIMUM INERTIA,XI,AND THE CORRES POR,FIND
```

```
C     QCR FOR VARIOUS VALUES OF E.
C
      LDTEST=0
      CALL BUKLOD (M,M1,M2,MOR,SUMJ,P,X,XI,AK1,AK2,LDTEST,E)
      GO TO 13
12    WRITE (6,17)
13    RETURN                                                          5
C                                                                     C
14    FORMAT (10X,//,1H*,PCR=,7H,E12.5,,1H*,//)                       C
15    FORMAT (//,10X,1H*,CONVERGENCEISACHIEVED,1H*,3H,//)
16    FORMAT (/,10X,1HX,ENERGYCONVERGENCENOTOBTAINEDIN25ITERATIONSC
     ,1H*,                                                            C
     1)
17    FORMAT (/,10X,71H***THREE REDUCTIONS IN EXP1 DID NOT
     1 PRODUCE CONVERGENCE**,3H,//)
      END
*****                                                                 C
      SUBROUTINE EIGEN (M,MOR,EVAL,NPE,PCRDIF,ITR,EVEC,PCR)
*****
C     THE EIGEN SYSTEM K1-PK2 IS SOLVED FOR LOWEST MB EVALUES USIN
G
C     ARL LIBRARY ROUTINES                                            C
C                                                                     C
      LOGICAL EXIT

      REAL K1,K2,K,LINV                                               6
      DIMENSION DIAG(40), EVAL(MOR), EVEC(70,1), DVEC(40)             C
      COMMON /B1/ K1(40,40)/B2/K2(40,40)
      COMMON /B11/ PROD(40,40)
      COMMON /B7/ T(70,40)/B8/K(40,40)
      COMMON /10/ SYMM
      COMMON /1/ BETA
      DIMENSION LINV(40,40), IPR(40)
C                                                                     7
      MAX=40                                                          C
      ITRE=1                                                          C
C     STEP 1:  CHOLESKY DECOMP OF K2=LL(TRANS)                        C
                                                                      C
      CALL LUS (MOR,K2,MAX,DIAG,EXIT)
C     DIAG CONTAINS INVERSES OF DIAGONAL ELEMENTS OF L                C
C     STEP 2:  FORMATION OF SYMM MATRIX K= L-INV*K1*L-INT-TRANS
C           AND RECON OF FULL K2                                      8
C     K2 =L*LTRANS                                                    C
C     DEFINE L AND STORE IN PROD
      DO 1 I=1,MOR
      DO 1 J=1,MOR
1     PROD(I,J)=0.                                                    C
      DO 2 IX=1,MOR                                                   C
      DO 2 IY=IX,MOR                                                  C
2     PROD(IY,IX)=K2(IX,IY)

      DO 3 IX=1,MOR                                                   C
3     PROD(IX,IX)=1./DIAG(IX)                                         C
C     NOW FIND L INV                                                  C
      CALL INVERS (PROD,40,MOR,IPR,LINV,D1)
C     FORM K= LINV*K1*LINV TRANS
      CALL FMMX (LINV,K1,PROD,MOR,MOR,40,40,40,MOR)
C     FORM LINV TRANS =LINV AND RECON K2                              10
      DO 4 IZ=1,MOR
      DO 4 JZ=IZ,MOR
      K2(IZ,JZ)=K2(JZ,IZ)
4     LINV(IZ,JZ)=LINV(JZ,IZ)
C     ZERO THE LOWER TRIANGLE

      DO 5 IZ=1,MOR
      DO 5 JZ=IZ,MOR
      IF (IZ.EQ.JZ) GO TO 5
      LINV(JZ,IZ)=0.
5     CONTINUE
C     NOW LINV CONTAINS L INV-TRANS                                   C
C        FORM K                                                       C
      CALL FMMX (PROD,LINV,K,MOR,MOR,40,40,40,MOR)

C     STEP 3:   TRIDIAG OF K
      CALL TRI1 (MOR,K,MAX)
C     THE NEC INFO FOR NEXT STEP IS IN COMMON WITH BISEC              C


C     STEP 4:   EVAL OF SYMM TRIDIAG FORM BY METHOD OF BISECTION
      MA=1
      MB=5
      TOL1=0.
      CALL BISEC (MOR,MA,MB,TOL1,DVEC,TOL2,ISUM,ANORM)
C     ***ALL E.VALUES WILL RETURN IN DVEC IN INC.ORDER.               C
C                                                                     C
      DO 6 I=1,MOR
      IF (DVEC(I)) 6,6,7
6     CONTINUE
C     NO POS EIGENVALUES***                                           C
      NPE=0



      WRITE (6,24)
      RETURN
7     CONTINUE
C                                                                     C
C     FOR SOME I .LE.MOR THE E.VALUES BECOME POS.                     C
C        FOR N POS E.VALUES THERE ARE N POSSIBLE FEAS REGIONS         C
C                                                                     C
      NPE=MOR-I+1
C     DEFINE EVAL TO BE THE ARRAY OF POS E.VALUES.                    C
      DO 8 J=1,NPE
8     EVAL(J)=DVEC(J+MOR-NPE)
C



C     NOW WE HAVE IDENTIFIED AND STORED NPE + E.VALUES.               C
C     FOR SYMM WE NEED ONLY EVAL                                      C
C                                                                     C
      IF (SYMM-1.) 9,23,9
9     CONTINUE                                                        C
C     THIS STAGE APPLIES ONLY TO ANTI-SYMM CASE                       C
C                                                                     C
C     STEP 5:   SELECTION OF LOWEST POS EIGEN VAL.AND CONVG CHECK
      DO 10 IA=MA,MB
      PCR=EVAL(IA)
      IF (PCR) 10,10,11
10    CONTINUE


      WRITE (6,25)
      STOP
```

```
11    IF (IA-1) 13,13,12
12    WRITE (6,26)
      WRITE (6,27) (EVAL(IA),IA=MA,MB)
13    CONTINUE
      IF (ITR-1) 14,15,15
14    PORN=0.
15    CONTINUE
      PORDIF=POR-PORN
      IF (PORDIF) 16,16,17
16    CONTINUE

      RETURN
17    PORN=POR
C
C     STEP 6: COMPUTE EIGEN VEC OF TRIDIAG FORM FOR THE EIGEN VAL
      CALL INIT (MOR,1,EVAL(IA),ANORM,EVEC,MAX)
C
C     STEP 7: COMPUTE E VEC OF SYMM MATRIX K
      CALL BAK1 (MOR,K,MAX,EVEC,1)
C     EVEC NOW CONTAINS THE EVECTOR OF K CORRES TO THE EVAL
C     SELECTED AS CRITICAL.
C     RECOVERY OF EVECTOR OF ORIGINAL SYSTEM BY
C      L-TRANS*VEC(ORIG) = EVEC

      CALL FMUX (LINU,EVEC,DIAG,MOR,MOR,40)
C     DIAG CONTAINS THE ORIG VECTOR CORRES TO POR
      DO 18 IB=1,MOR
18    EVEC(IB)=DIAG(IB)
C     EVEC IS THE ORIG VECTOR
C
C     STEP 8:  FORMATION OF THE DOMAIN VECTOR FOR ALL B.C.
      M2=2*M+2
      MAX=70
      MP2=M+2
C     SIMPLY SUPPORTED CASE,BETA = 0. MOR = M
      IF (BETA.GT.100.) GO TO 21

      MM1=M-1
      DVEC(1)=0.
      DO 19 ID=1,MM1
19    DVEC(ID+1)=EVEC(ID)
      DVEC(M+1)=0.
      DVEC(M+2)=EVEC(M)
      CALL FMUX (T,DVEC,EVEC,M2,MP2,MAX)
20    CONTINUE
      WRITE (6,28) (EVAL(J),J=1,MB)
      WRITE (6,29) POR,TOL2
      GO TO 23
21    CONTINUE

C       CLAMPED CASE  MOR = M -1
      MM2=M-2
      DVEC(1)=0.
      DVEC(2)=0.
      DO 22 IE=1,MM2
22    DVEC(IE+2)=EVEC(IE)
      DVEC(M+1)=0.
      DVEC(M+2)=EVEC(M-1)
      CALL FMUX (T,DVEC,EVEC,M2,MP2,MAX)
      GO TO 20
23    CONTINUE
      RETURN

C

24    FORMAT (12X,1H*,NORMOSE.VALUES,1H*,//)
25    FORMAT (//,12X,2H**,NORMOSEIGENVALUES,2H**,//)
26    FORMAT (//,12X,2H**,EIGENVALUES,2H**,//)
27    FORMAT (E12.5)
28    FORMAT (10X,E12.5)
29    FORMAT (10X,2E12.5)
      END
*****************************************
      SUBROUTINE ASS1 (M,M1,M2,MAX,MODE,X,XI,AK1)
*****************************************
      REAL K1,MODE


      COMMON /B7/ T(70,40)/B15/ET(70,40)/B11/PROD(40,40)
      COMMON /B1/ K1(40,40)
      COMMON /1/ BETA
      DIMENSION EK1(4,4), EK2(4,4)
      DIMENSION AK1(MAX,2), X(M1), XI(M)
C     INITIALIZ  TO XERO
      DO 2 IR=1,M2
      DO 1 IC=IR,M2
      AK1(IR,IC)=0.
      AK1(IC,IR)=0.
1     CONTINUE
2     CONTINUE


C     START ASSEMBLY
      DO 5 I=1,M
      CALL COMEK1 (I,M,M1,X,XI,EK1)
      DO 4 JR=1,4
      DO 3 LC=1,4
      AK1(2*I-2+JR,2*I-2+LC)=EK1(JR,LC)+AK1(2*I-2+JR,2*I-2+LC)
C
3     CONTINUE
4     CONTINUE
5     CONTINUE
      IF (BETA.GT.100.) GO TO 6
      AK1(2,2)=AK1(2,2)+2.*BETA


6     CONTINUE
      MP2=M+2
C     NOW FORM K1 = T TRANSPOSE *AK1*T
      CALL FMMX (AK1,T,ET,M2,M2,70,70,70,MP2)
C     NOW FORM T TRANSPOSE * PROD
      CALL FMTMX (T,ET,AK1,M2,MP2,70,70,70,MP2)
      IF (MODE) 7,7,10
7     CONTINUE
C     DEFINE THE ELEM TRANSFORMATION
      DO 8 II=1,MP2
      DO 8 JJ=1,MP2
8     ET(II,JJ)=0.


      DO 9 NI=1,M
9     ET(NI,NI)=1.
      ET(M+1,M+2)=1.
      ET(M+2,M+1)=1.
C     PRE AND PST AK BY ET
```

```
      CALL FMMX (ET,AK1,PROD,MP2,MP2,70,70,40,MP2)
      CALL FMMX (PROD,ET,AK1,MP2,MP2,40,70,70,MP2)
C     USE BETA TO SPECIFY BC AND REDUCE THE ORDER OF AK1 BY
C     ELIMINATING THE UNCANTED EQUATIONS
10    CONTINUE
      IF (BETA.GT.100.) GO TO 13
      DO 12 NK=1,M

      DO 11 JK=1,M
      K1(NK,JK)=AK1(NK+1,JK+1)
11    CONTINUE
12    CONTINUE
      RETURN
13    CONTINUE
C     CLAMPED CASE
      MM1=M-1
      DO 15 JK=1,MM1
      DO 14 NK=1,MM1
      K1(NK,JK)=AK1(NK+2,JK+2)
14    CONTINUE

15    CONTINUE
C     NOW AK1 HAS BEEN COMPLETELY TRANSFORMED. RTURN FOR E.VALUES
      RETURN
      END
xxxxxxxxxxxxxxxxxxxxxxxxxxxxxx
      SUBROUTINE COMEK1 (I,M,M1,X,XI,EK1)
xxxxxxxxxxxxxxxxxxxxxxxxxxxxxx
      DIMENSION CEN1(4,4), EK1(4,4), BINV(4,4), C(4,4)
      DIMENSION X(M1), XI(M)
      DIMENSION B(4,4), IPR(4)
      COMMON /5/ EL
C     DEFINE THE MATRIX CEN1 GIVEN BY INTEGRAL XI(I)*(L,,L,,T)

C     COMPUTE THE TERMS OF CEN1 FOR GIVEN ELEMENT I.
C     INTEGRATIONS HAVE BEEN DONE BY HAND.
C     THE INDEP VARIABLE IS X.
C     THE INERTIA VECTOR XI CONTAINS M ELEMENTS.
C
      DO 2 K=1,2
      DO 1 L=1,4
      CEN1(K,L)=0.
      CEN1(L,K)=0.
1     CONTINUE
2     CONTINUE
C     XI(I) IS THE INERTIA OF ITH ELEMENT ASSUMED CONSTANT.

      CEN1(3,3)=4.*(X(I+1)-X(I))*XI(I)
      CEN1(3,4)=6.*(X(I+1)**2-X(I)**2)*XI(I)
      CEN1(4,3)=CEN1(3,4)
      CEN1(4,4)=12.*(X(I+1)**3-X(I)**3)*XI(I)
C     NOW COMPUTE ELEMENT MATRIX EK1 USING LIBRARY ROUTINES FOR
      B(1,1)=1.
      B(1,2)=X(I)
      B(1,3)=X(I)**2
      B(1,4)=X(I)**3
      B(2,1)=0.
      B(2,2)=1.
      B(2,3)=2.*X(I)

      B(2,4)=3.*(X(I)**2)
      B(3,1)=1.
      B(3,2)=X(I+1)
      B(3,3)=X(I+1)**2
      B(3,4)=X(I+1)**3
      B(4,1)=0.
      B(4,2)=1.
      B(4,3)=2.**X(I+1)
      B(4,4)=3.*(X(I+1)**2)
      CALL INVERS (B,4,4,IPR,BINV,D1)
C     EK1 = BINVT*CEN1*BINV
C

      CALL FMTMX (BINV,CEN1,C,4,4,4,4,4,4)
C     NOW FOR EK1 = C*BINV
      CALL FMMX (C,BINV,EK1,4,4,4,4,4,4)
      RETURN
      END
xxxxxxxxxxxxxxxxxxxxxxxxxxxxxx
      SUBROUTINE ASS2 (M,M1,M2,MAX,MODE,X,AK2)
xxxxxxxxxxxxxxxxxxxxxxxxxxxxxx
      COMMON /1/ BETA
      COMMON /10/ SYMM
      COMMON /B7/ T(70,40)/B15/ET(70,40)/B11/PROD(40,40)
      COMMON /B2/ K2(40,40)


      DIMENSION AK2(MAX,2), X(M1)
      DIMENSION EK2(4,4)
      REAL K2
      REAL MODE
      M2=2*M+2
C     INITIALIZE MATRIX AK2 TO ZERO BEFORE INPUTTING ITS VALUES
C     BY SUCCESSIVE ADDITION.
C
      DO 2 IR=1,M2
      DO 1 IC=IR,M2
      AK2(IR,IC)=0.
      AK2(IC,IR)=0.


1     CONTINUE
2     CONTINUE
C
C     START THE ASSEMBLY PROCESS.
C
      DO 5 I=1,M
      CALL COMEK2 (I,M1,X,EK2)
      DO 4 JR=1,4
      DO 3 LC=1,4
      AK2(2*I-2+JR,2*I-2+LC)=EK2(JR,LC)+AK2(2*I-2+JR,2*I-2+LC)
C
3     CONTINUE


4     CONTINUE
5     CONTINUE
      IF (MODE.EQ.0.) RETURN
      MP2=M+2
      CALL TRANS (MODE,M)
C     NOW FORM K2 = T TRANSPOSE * AK2*T
      CALL FMMX (AK2,T,ET,M2,M2,70,70,70,MP2)
C     NOW FORM T TRANSPOSE * PROD
```

```
      CALL FMTMX (T,ET,AK2,M2,MP2,70,70,70,MP2)
      IF (MODE) 9,9,6
6     CONTINUE
      IF (SYMM.GT.0.) GO TO 13

      DO 8 IC=1,MP2
      DO 7 ID=1,MP2
      K2(IC,ID)=AK2(IC,ID)
7     CONTINUE
8     CONTINUE
      RETURN
9     CONTINUE
C     DEFINE THE ELEM TRANSFORMATION
      DO 11 II=1,MP2
      DO 10 JJ=1,MP2
      ET(II,JJ)=0.
10    CONTINUE

11    CONTINUE
      DO 12 NI=1,M
      ET(NI,NI)=1.
12    CONTINUE
      ET(M+1,M+2)=1.
      ET(M+2,M+1)=1.
C     PRE AND POST AK BY ET
      CALL FMMX (ET,AK2,PROD,MP2,MP2,70,70,40,MP2)
      CALL FMMX (PROD,ET,AK2,MP2,MP2,40,70,70,MP2)
C     USE BETA TO SPECIFY BC AND REDUCE THE ORDER OF AK2 BY
C     ELIMINATING THE UNWANTED EQUATIONS
13    CONTINUE

      IF (BETA.GT.100.) GO TO 16
      MOR=M
      DO 15 NK=1,MOR
      DO 14 JK=1,MOR
      K2(NK,JK)=AK2(NK+1,JK+1)
14    CONTINUE
15    CONTINUE
      RETURN
16    CONTINUE
C     CLAMPED CASE
      MOR=M-1
      DO 18 NK=1,MOR

      DO 17 JK=1,MOR
      K2(NK,JK)=AK2(NK+2,JK+2)
17    CONTINUE
18    CONTINUE
C     NOW AK2 HAS BEEN COMPLETELY TRANSFORMED. RTURN FOR E.VALUES
      RETURN
      END
**********
      SUBROUTINE COMEK2 (I,M1,X,EK2)
**********
      DIMENSION CEN2(4,4), EK2(4,4), BINV(4,4), C(4,4)
      DIMENSION X(M1)

      DIMENSION B(4,4), IPR(4)
      COMMON /S/ EL
C     DEFINE THE MATRIX(4,4) GIVEN BY INTEGRAL(L,L,T) AS CEN2
C     COMPUTE THE TERMS OF CENT FOR GIVEN I.  THIS WILL IVOLVE
C     SIMPLE INTEGRATIONS WHICH FOR THIS ASSEMBLY ARE DONE BY
C     HAND.  THE INDEP VARIALE IS X.
C
      CEN2(1,1)=0.
      CEN2(1,2)=2.
      CEN2(1,3)=2.
      CEN2(1,4)=0.
      CEN2(2,1)=0.


      CEN2(3,1)=0.
      CEN2(4,1)=0.
      CEN2(2,2)=X(I+1)-X(I)
      CEN2(2,3)=(X(I+1))**2-(X(I))**2
      CEN2(2,4)=(X(I+1))**3-(X(I))**3
      CEN2(3,2)=CEN2(2,3)
      CEN2(4,2)=CEN2(2,4)
      CEN2(3,3)=4.*(CEN2(4,2))/3.
      CEN2(4,3)=3.*CEN2(2,3)*(X(I+1)**2+X(I)**2)/2.
      CEN2(3,4)=CEN2(4,3)
      CEN2(4,4)=9.*(X(I+1)**5-X(I)**5)/5.
C

C     FORM THE ELEMENT MATRIX EK2
C
      B(1,1)=1.
      B(1,2)=X(I)
      B(1,3)=X(I)**2
      B(1,4)=X(I)**3
      B(2,1)=0.
      B(2,2)=1.
      B(2,3)=2.*X(I)
      B(2,4)=3.*(X(I)**2)
      B(3,1)=1.
      B(3,2)=X(I+1)


      B(3,3)=X(I+1)**2
      B(3,4)=X(I+1)**3
      B(4,1)=0.
      B(4,2)=1.
      B(4,3)=2.*X(I+1)
      B(4,4)=3.*(X(I+1)**2)
      CALL INVERS (B,4,4,IPR,BINV,D1)
C
      CALL FMTMX (BINV,CEN2,C,4,4,4,4,4,4)
C     NOW FOR  EK2 = C*BINV
      CALL FMMX (C,BINV,EK2,4,4,4,4,4,4)
      RETURN


      END
**********
      SUBROUTINE TRANS (MODE,M)
**********
      COMMON /B7/ T(70,40)
      REAL MODE
C     THE ASSEMBLY OF T IS BASED ON EVEN NUMBER OF ELEMENTS,M
C     INITIALIZE TO ZERO
      MP2=M+2
      M2=2*M+2
      DO 2 MM=1,M2
```

```
      DO 1 KK=MM,M2

      T(KK,KK)=0.
      T(KM,MM)=0.
1     CONTINUE
2     CONTINUE
      DO 3 IR=1,M,2
      I=MP2+IR-1
      J=M+1-IR
      T(I,J)=-(MODE)
      I=IR+MP2
      J=M-IR
      T(I,J)=MODE
3     CONTINUE

      DO 4 NI=1,MP2
      T(NI,NI)=1.
4     CONTINUE
C
      RETURN
      END
**********************************
      SUBROUTINE FMUX (A,X,Y,M,N,MA)
**********************************
C     MATRIX VECTOR MULTIPLICATION.  Y = A*X
      DIMENSION A(MA,1), X(1), Y(1)
      DO 1 I=1,M

      Y(I)=0.
      DO 1 J=1,N
1     Y(I)=X(J)*A(I,J)+Y(I)
      RETURN
      END
**********************************
      SUBROUTINE FMMX (A,B,C,M,N,MA,MB,MC,K)
**********************************
C     MATRIX MATRIX MULT  C = A*B
      DIMENSION A(MA,1), B(MB,1), C(MC,1)
      DO 1 L=1,K
      DO 1 I=1,M

      C(I,L)=0.
      DO 1 J=1,N
1     C(I,L)=A(I,J)*B(J,L)+C(I,L)
      RETURN
      END
**********************************
      SUBROUTINE FMTMX (A,B,C,M,N,MA,MB,MC,K)
**********************************
C      MATRIX TRANS * MATRIX  C = A TRANS * B
      DIMENSION A(MA,1), B(MB,1), C(MC,1)
      DO 1 L=1,K
      DO 1 I=1,N

      C(I,L)=0.
      DO 1 J=1,M
1     C(I,L)=A(J,I)*B(J,L)+C(I,L)
      RETURN
      END
**********************************
      SUBROUTINE INVERS (A,IA,N,IPR,AINV,D1)
**********************************
C     TO CALC INVERSE OF A USING IMSL SUBROUTINE LINV1F
      DIMENSION A(IA,1), AINV(IA,1), IPR(1)
      REAL IPR
C     PARAMETER IDGT IF .GT. 0 LINV1F PERFORMS ACCURACY TEST


      IDGT=4
      CALL LINV1F (A,N,IA,AINV,IDGT,IPR,D1)
      RETURN
      END
**********************************
      SUBROUTINE ASS5 (M,M1,M2,MAX,MODE,X)
**********************************
C     THE ASSEMBLY OF K5
      REAL MODE
      DIMENSION X(M1), EV5(4)
      COMMON /B7/ T(70,40)/B3/AV5(70)
      COMMON /B12/ VEC(40)


      COMMON /10/ SYMM
      COMMON /1/ BETA
      COMMON /2/ LOAD
C     AV5 IS A VECTOR OF SIZE 2M + 2
C     INITIALIZE TO XERO
      MP2=M+2
      MM1=M-1
      DO 1 IC=1,M2
      AV5(IC)=0.
1     CONTINUE
C     START ASSEMBLY
      DO 3 I=1,M


      CALL COMEV5 (I,M1,X,EV5)
      DO 2 LC=1,4
      AV5(2*I-2+LC)=EV5(LC)+AV5(2*I-2+LC)
2     CONTINUE
3     CONTINUE
C     THE ASSEMBLED VECTOR AV5 MUST BE MODIFIED TO ACCOUNT FOR
C     BOUNDARY AND SYMMETRIC CONDITIONS
C     FORM T TRANSPOSE * AV5
      CALL FMTVX (T,AV5,VEC,M2,MP2,70)
      IF (SYMM.GT.0.) GO TO 6
C     FOR SYMMETRY Q(M+2) = 0
      DO 4 IA=1,MP2


      AV5(IA)=VEC(IA)
4     CONTINUE
      AV5(1)=0.
      AV5(MP2)=0.
      IF (BETA.GT.100.) GO TO 5
      RETURN
5     CONTINUE
      AV5(2)=0.
      RETURN
6     CONTINUE
      IF (BETA.GT.100.) GO TO 8
      MOR=M
```

```
      DO 7 JK=1,MOR
      AV5(JK)=VEC(JK+1)
7     CONTINUE
      RETURN
8     CONTINUE
      MOR=MM1
      DO 9 JB=1,MOR
      AV5(JB)=VEC(JB+2)
9     CONTINUE
      RETURN
      END
*******************************

      SUBROUTINE COMEV5 (I,M1,X,EV5)
*******************************
C     E IS BASED ON CUBIC INTERPOLATION FCN
      DIMENSION B(4,4), IPR(4)
      DIMENSION CEN5(4), EV5(4), BINV(4,4)
      DIMENSION X(M1)
      COMMON /2/ LOAD
      PI=3.1415926
      B(1,1)=1.
      B(1,2)=X(I)
      B(1,3)=X(I)**2
      B(1,4)=X(I)**3

      B(2,1)=0.
      B(2,2)=1.
      B(2,3)=2.*X(I)
      B(2,4)=3.*(X(I)**2)
      B(3,1)=1.
      B(3,2)=X(I+1)
      B(3,3)=X(I+1)**2
      B(3,4)=X(I+1)**3
      B(4,1)=0.
      B(4,2)=1.
      B(4,3)=2.*X(I+1)
      B(4,4)=3.*(X(I+1)**2)

      CALL INVERS (B,4,4,IPR,BINV,D1)
C
C     THE PARAMETER LOAD DETERMINES THE TYPE OF LOAD DISTRIBUTION
C     LOAD = 1, SINE DIST
C     LOAD = 2,, PARABOLIC DIST
C     LOAD = 3,  UNIFORM DIST
C     CEN5 IS THE VECTOR DEFINED BY INTEGRAL F*L
      IF (LOAD-2) 1,2,3
1     CONTINUE
      CEN5(1)=-(COS(X(I+1))-COS(X(I)))
      CEN5(2)=(SIN(X(I+1))-X(I+1)*COS(X(I+1)))-(SIN(X(I))-X(I)*COSC
(X(I))

     1)
      CEN5(3)=(2.*X(I+1)*SIN(X(I+1))-(X(I+1)**2-2.)*COS(X(I+1)))-(
2.*X(I
     1)*SIN(X(I))-(X(I)**2-2.)*COS(X(I)))
      CEN5(4)=((3.*(X(I+1)**2-2.)*SIN(X(I+1))-(X(I+1)**3-6.*(X(I+1
)))*CO
     1S(X(I+1))))-((3.*(X(I)**2-2.)*SIN(X(I))-(X(I)**3-6.*(X(I)))*
COS(X(
     2I))))
      GO TO 4
2     CONTINUE
C     PARABOLIC DIST


      C1=2./(3.*(PI**2))
      C2=1./(3.*(PI**2))
      C3=1./(5.*(PI**2))
      C4=2./(12.*(PI**2))
      CEN5(1)=C1*(3.*PI*(X(I+1)**2-X(I)**2)-2.*(X(I+1)**3-X(I)**3)
     )
      CEN5(2)=C2*(4.*PI*(X(I+1)**3-X(I)**3)-3.*(X(I+1)**4-X(I)**4)
     )
      CEN5(3)=C3*(5.*PI*(X(I+1)**4-X(I)**4)-4.*(X(I+1)**5-X(I)**5)
     )
      CEN5(4)=C4*(6.*PI*(X(I+1)**5-X(I)**5)-5.*(X(I+1)**6-X(I)**6)
     )


      GO TO 4
3     CONTINUE
C     UNIFORM LOAD DIST
      CEN5(1)=X(I+1)-X(I)
      CEN5(2)=(X(I+1)**2-X(I)**2)/2.
      CEN5(3)=(X(I+1)**3-X(I)**3)/3.
      CEN5(4)=(X(I+1)**4-X(I)**4)/4.
4     CONTINUE
C     OBTAIN THE ELEMENT LOAD VECTOR EV5
C
      CALL FMTUX (BINV,CEN5,EV5,4,4,4)
      RETURN


      END
*******************************
      SUBROUTINE ASV6 (M,M1,M2,MAX,MODE,X)
*******************************
C     THE ASSEMBLY OF V6
      REAL MODE
      DIMENSION X(M1), EV6(4)
      COMMON /B7/ T(70,40)/B4/V6(40)/B12/VEC(40)
      COMMON /1/ BETA
      COMMON /20/ AV6(70)
      COMMON /3/ ISHAPE
      COMMON /10/ SYMM


C     AV6 IS A GLOBAL VECTOR SIZE M2
C     INITIALIZE TO ZERO
      MP2=M+2
      MM1=M-1
      DO 1 IC=1,M2
      AV6(IC)=0.
1     CONTINUE
C     START ASSEMBLY
      DO 3 I=1,M
      CALL COMEV6 (I,M1,X,EV6)
      DO 2 LC=1,4
      AV6(2*I-2+LC)=EV6(LC)+AV6(2*I-2+LC)
```

```
2     CONTINUE
3     CONTINUE
      IF (MODE.EQ.0.) RETURN
C     MODIFY FOR BC AND SYMM
C     FORM T TRANSPOSE*AU6
      CALL FMTUX (T,AU6,VEC,M2,MP2,70)
      IF (SYMM.GT.0.) GO TO 6
C     FOR SYMMETRY Q(M+2) = 0.
      DO 4 IA=1,MP2
      U6(IA)=VEC(IA)
4     CONTINUE
      U6(1)=0.

      VEC(MP2)=0.
      IF (BETA.GT.100.) GO TO 5
      RETURN
5     CONTINUE
6     CONTINUE
      IF (BETA.GT.100.) GO TO 8
      MOR=M
      DO 7 JK=1,MOR
      U6(JK)=VEC(JK+1)
7     CONTINUE
      RETURN
8     CONTINUE

      MOR=MM1
      DO 9 JB=1,MOR
      U6(JB)=VEC(JB+2)
9     CONTINUE
      RETURN
      END
*******************************
      SUBROUTINE COMEU6 (I,M1,X,EU6)
*******************************
      DIMENSION CEN4(4), EU6(4), BINU(4,4), B(4,4)
      DIMENSION X(M1)
      DIMENSION IPR(4)

      COMMON /3/ ISHAPE
      PI=3.1415926
C     THE PARAMETER ISHAPE DETS THE INITIAL SHAPE
C     THE RISE PARAMETER E WILL BE CARRIED EXPLICITLY BY P,Q RELAT
ION
C     THE INTEGRATIONS ARE DONE BY HAND.
C     CEN4 IS THE VECTOR DEFINED BY ETAOPRIME*L,
      IF (ISHAPE-1) 1,1,2
1     CONTINUE
      CEN4(1)=0.
      CEN4(2)=SIN(X(I+1))-SIN(X(I))
      CEN4(3)=2.*((COS(X(I+1))+X(I+1)*SIN(X(I+1)))-(COS(X(I))+X(I)

*SIN(X
     1(I))))
      CEN4(4)=3.*((2.*X(I+1)*COS(X(I+1))+(X(I+1)**2-2.)*SIN(X(I+1)
))-(2.
     1*X(I)*COS(X(I))+(X(I)**2-2.)*SIN(X(I))))
      GO TO 3
2     CONTINUE
C     CEN4 PARABOLIC
      CEN4(1)=0.
      CEN4(2)=4.*(PI*(X(I+1)-X(I))-(X(I+1)**2-X(I)**2))/(PI**2)
      CEN4(3)=8.*(3.*PI*(X(I+1)**2-X(I)**2)-4.*(X(I+1)**3-X(I)**3)
)/(6.*
     1(PI**2))
      CEN4(4)=(4.*PI*(X(I+1)**3-X(I)**3)-6.*(X(I+1)**4-X(I)**4))/(
PI**2)
3     CONTINUE
      B(1,1)=1.
      B(1,2)=X(I)
      B(1,3)=X(I)**2
      B(1,4)=X(I)**3
      B(2,1)=0.
      B(2,2)=1.
      B(2,3)=2.*X(I)
      B(2,4)=3.*(X(I)**2)



      B(3,1)=1.
      B(3,2)=X(I+1)
      B(3,3)=X(I+1)**2
      B(3,4)=X(I+1)**3
      B(4,1)=0.
      B(4,2)=1.
      B(4,3)=2.*X(I+1)
      B(4,4)=3.*(X(I+1)**2)
      CALL INVERS (B,4,4,IPR,BINU,D1)
C     OBTAIN THE ELEMENT LOAD VECTOR EU6
      CALL FMTUX (BINU,CEN4,EU6,4,4,4)
      RETURN


      END
*******************************
      SUBROUTINE BUKLOD (M,M1,M2,MOR,SUMJ,P,X,XI,AK1,AK2,LDTEST,E)
*******************************
      REAL K1,K2,K,KINV,MODE
      COMMON /B1/ K1(40,40)/B2/K2(40,40)/B3/AU6(70)/B4/U6(40)
      COMMON /B8/ K(40,40)/B9/KINV(40,40)/B11/PROD(40,40)
      COMMON /B12/ VEC(40)/B13/PROD1(40,40)/B14/VEC1(40)
      COMMON /4/ RHO,EXP/5/EL/10/SYMM
      COMMON /1/ BETA
      DIMENSION AK1(70,2), AK2(70,2)
      DIMENSION XI(40), X(40)


      DIMENSION WKAREA(800)
C
      MODE=1.
      SYMM=1.
      MAX=70
C     COMPUTE SUMJ
      IF (LDTEST.EQ.1) GO TO 2
      SUMJ=0.
      DO 1 IA=1,M
1     SUMJ=SUMJ+(XI(IA)/RHO)**(-1./EXP)
      SUMJ=1./(2.*EL*SUMJ)
      CALL ASS2 (M,M1,M2,MAX,MODE,X,AK2)


      CALL ASS1 (M,M1,M2,MAX,MODE,X,XI,AK1)
      CALL ASU6 (M,M1,M2,MAX,MODE,X)
```

```
      CALL ASSS (M,M1,M2,MAX,MODE,X)
C
C     THE RESULT OF THESE CALLS IS THE SYMM ASSM MATRICES
C     K1,K2,V6,AV5 OF ORDER MOR CORRES TO BC INDICATED BY BETA
C
2     CONTINUE
      DO 3 IA=1,MOR
      DO 3 JA=1,MOR
3     K(IA,JA)=K1(IA,JA)-P*K2(IA,JA)
      CALL SINVRS (K,KINV,MOR,42)

      CALL FMMX (KINV,K2,PROD,MOR,MOR,40,40,40,MOR)
      CALL FMMX (PROD,KINV,PROD1,MOR,MOR,42,42,40,MOR)
      CALL FMUX (PROD1,AV5,VEC,MOR,MOR,40)
C
      S1=0.
      DO 4 IB=1,MOR
4     S1=S1+AV5(IB)*VEC(IB)
      CALL FMUX (KINV,AV5,VEC1,MOR,MOR,40)
      APEX1=VEC1(MOR)
C     NOW FORM S2
      S2=0.
      DO 5 IC=1,MOR

5     S2=S2+2.*P*V6(IC)*VEC(IC)+2.*V6(IC)*VEC1(IC)
      CALL FMUX (KINV,V6,VEC1,MOR,MOR,40)
      APEX2=VEC1(MOR)
      CALL FMUX (PROD1,V6,VEC,MOR,MOR,40)
      S3=0.
      DO 6 ID=1,MOR
6     S3=S3+(P**2)*V2(ID)*VEC(ID)+2.*P*V6(ID)*VEC1(ID)
C
C
C     COMPUTE QCR FOR VARIOUS RISE PARAMETERS E.
      WRITE (6,27) S1,S2,S3,SUMJ
      IF (LDTEST.EQ.1) GO TO 15

      DMIN=(4.*S1*P/SUMJ)/(S2**2-4.*S1*S3)
      IF (DMIN) 7,8,8
7     CONTINUE
      WRITE (6,28)
      STOP
8     EMIN=SQRT(DMIN)
      ESTART=0.
C     COMPUTE QCR FOR VARIOUS VALUES OF E BEGINNING WITH
C     ESTART IF ESTART .GE.EMIN OR EMIN IF ESTART.LT.EMIN
C
      WRITE (6,29) EMIN,P
      WRITE (6,30)

      IF (ESTART-EMIN) 10,9,9
9     E=ESTART
      GO TO 11
10    E=EMIN
C     TEST*****
11    ESTOP=E+3.
      J=0
      ENT=0.
      DO 12 I=1,100
      IF (ENT-E) 12,13,13
12    ENT=ENT+1.
13    CONTINUE

      IF (E.EQ.EMIN) GO TO 14
      GO TO 15
14    SDISC=0.
      GO TO 16
15    CONTINUE
      DISC=(S**2)*(S2**2-4.*S1*S3)-4.*S1*P/SUMJ
      IF (DISC.LT.0.) STOP
      SDISC=SQRT(DISC)
16    QCRP=(-S2*E+SDISC)/(2.*S1)
      DEFP=P*E*APEX2+QCRP*APEX1
      QCRM=(-S2*E-SDISC)/(2.*S1)
      DEFM=P*E*APEX2+QCRM*APEX1


      IF (LDTEST-1) 18,17,18
17    WRITE (6,30)
      WRITE (6,32) E,QCRP,DEFP,QCRM,DEFM,P,DISC
18    CONTINUE
      DO 19 I=1,MOR
      VEC(I)=P*E*V2(I)+QCRP*AV5(I)
19    VEC1(I)=P*E*V6(I)+QCRM*AV5(I)
      IDGT=0
      CALL LEQT2F (K,1,MOR,40,VEC,IDGT,WKAREA,IER)
      DEFP1=VEC(MOR)
      CALL LEQT2F (K,1,MOR,40,VEC1,IDGT,WKAREA,IER)
      DEFM1=VEC1(MOR)


      DELAM=0.
      DELAP=0.
      MORP1=MOR+1
      DO 20 JJ=1,MOR,2
      DELAP=DELAP+VEC(MORP1-JJ)
20    DELAM=DELAM+VEC1(MORP1-JJ)
      WRITE (6,31) DELAM,DELAP
      IF (LDTEST-1) 22,21,22
21    RETURN
22    CONTINUE
      WRITE (6,32) E,QCRP,DEFP,QCRM,DEFM,DEFM1,DEFP1
      WRITE (6,33) (VEC(IA),IA=1,MOR)


      WRITE (6,33) (VEC1(IB),IB=1,MOR)
      IF (E.GT.ESTOP) GO TO 24
      IF (J.GT.0) GO TO 23
      E=ENT
      J=J+1
      GO TO 15
C
23    E=E+1.
      J=J+1
      GO TO 15
24    CONTINUE
      WRITE (6,34)


      WRITE (6,35) (XI(I),I=1,M)
      GO TO 25
      ESTART=EMIN
      CALL TANGNT (ESTART,P,MOR,M,S1,S2,S3,SUMJ,ETAN)
      GO TO 26
```

```
25    E=3.
      CALL DEFLOD (M,M1,M2,MOR,SUMJ,P,X,XI,AK1,AK2,E)
26    CONTINUE
      RETURN
C
27    FORMAT (//,4(E12.5,5X),//)
28    FORMAT (10X,1H*,DMINISNEG,2H**,//)

29    FORMAT (//,20X,1H*,CONDITIONSATOPTIMUMINERTIA,1H*,//,10X,5HE
MIN=,E
     112.5,5X,4HPCR=,E12.5,//)
30    FORMAT (//,15X,1HE,15X,4HQCRP,13X,4HDEFP,13X,4HQCRM,13X,4HDE
FM,/)
31    FORMAT (10X,1H*,CHANGEINAREA,1H*,//,10X,6HDELAM=,E12.5,6HDEL1
AP=,E1
     12.5)
32    FORMAT (/,10X,7(E12.5,5X))
33    FORMAT (10X,8E12.5,/)
34    FORMAT (//,5X,38H**OPTIMUM INERTIA DIST***,//)
35    FORMAT (10X,5(E12.5,3X))

      END
*************************************
      SUBROUTINE DEFLOD (M,M1,M2,MOR,SUMJ,PCR,X,XI,AK1,AK2,E)
*************************************
      DIMENSION X(40), XI(40), AK1(70,2), AK2(70,2)
      PSTOP=1.5*PCR
      LDTEST=1
      WRITE (6,3) LDTEST,MOR,SUMJ,PCR,E
      P=0.
      DELP=0.15
1     P=P+DELP
      CALL BUKLOD (M,M1,M2,MOR,SUMJ,P,X,XI,AK1,AK2,LDTEST,E)

C     EACH CALL TO BUKLOD WITH LDTEST =1 WILL COMPUTE QM AND
C       QP AND THE DEFLECTIONS
      PSTOP=1.5*PCR
      IF (P.GT.PSTOP) GO TO 2
      GO TO 1
2     CONTINUE
      RETURN
C
3     FORMAT (10X,//,24H**LOAD DEFLECTION DATA**,//,10X,21HLDTEST,
MOR,SU
     1MJ,PCR,E,5X,2I4,5X,3E12.5,//)
      END

*******************************
      SUBROUTINE TANGNT (EMIN,P,MOR,M,S1,S2,S3,SUMJ,ETAN)
*******************************
C
C     AFTER SUCCESSFUL ANTI-SYMM OPT, THIS SUB WILL ATTEMPT TO
C     LOCATE BY ITERATION THE VALUE OF E FOR WHICH SNAPPING WOULD
C     OCCUR WHEN P=PCR.  THIS PRESUPPOSES A TANGENT POINT FOR SOME
C     E>EMIN. CALC WILL BE MADE FOR QCRP AND QCRM.
C
      REAL K1,K2
      COMMON /N1/ TP(100),TM(100),B1/K1(40,40),B2/K2(40,40)
      COMMON /B3/ AU5(70),B4/U6(40)

C     FORM COEFFICIENTS IN BUCK EQN
C     ****TEST*************************************************
      CALL COEFB (P,A1,C1,C2,C3,C4,MOR)
      DELE=0.1
      ESTOP=EMIN+10.
C     *END TEST*************************************************
      D1=S2**2-4.*S1*S3
      D2=4.*P*S1/SUMJ
      T1=P*(2*C4+C2*U6(MOR)+P*C1*C3
      T2=P*C1/SUMJ-AU5(MOR)/(2.*SUMJ)
      T3=(P*C4+U6(MOR))*C3
      T4=(P*C4+U6(MOR))/SUMJ


      E=EMIN+DELE
      I=1
      DISC=(E**2)*D1-D2
      IF (DISC) 14,2,2
2     QP=(-S2*E+SQRT(DISC))/(2.*S1)
      QM=(-S2*E-SQRT(DISC))/(2.*S1)
      TP(I)=(QP**2)*A1*E+QP*(T1*(E**2)+T2)+P*E*(T3*(E**2)+T4-U6(MO
R)/(2.
     1*SUMJ))
      TM(I)=(QM**2)*E*A1+QM*(T1*(E**2)+T2)+P*E*(T3*(E**2)+T4-U6(MO
R)/(2.
     1*SUMJ))


      WRITE (6,16) E,QP,QM,TP(I),TM(I),I
      IF (I-1) 3,3,4
3     I=I+1
      E=E+DELE
      IF (E-ESTOP) 1,1,13
C     TEST FOR ROOT FOR I>1
4     TESTP=TP(I)*TP(I-1)
      TESTM=TM(I)*TM(I-1)
      IF (TESTP.LE.0.0.AND.TESTM.LE.0.) GO TO 7
      IF (TESTP.LE.0.0.OR.TESTM.LE.0.) GO TO 5
      GO TO 3
5     IF (TESTP) 6,6,12


6     ETAN=E-(DELE/2.)
      E=ETAN
      DISC=(E**2)*D1-D2
      QP=(-S2*E+SQRT(DISC))/(2.*S1)
      E=ETAN+(DELE/2.)
      IF (QP.GE.0.) GO TO 3
      WRITE (6,17) ETAN,P,QP
      GO TO 3
7     CONTINUE
C     BOTH TM AND TP YIELD POSSIBLE SOLNS
      ETAN=E-(DELE/2.)
      E=ETAN


      DISC=(E**2)*D1-D2
      QP=(-S2*E+SQRT(DISC))/(2.*S1)
      QM=(-S2*E-SQRT(DISC))/(2.*S1)
      IF (QP.LE.0..AND.QM.LE.0.) GO TO 8
      IF (QP.LE.0.) GO TO 9
      GO TO 10
8     IF (QP.LE.QM) GO TO 10
9     QCR=QM
```

```
      GO TO 11
10    QCR=QM
11    CONTINUE
      WRITE (6,18) E,QP,QM,P,TM(I),TP(I),QCR

      E=ETAN+(DELE/2.)
      GO TO 3
12    CONTINUE
      ETAN=E-(DELE/2.)
      E=ETAN
      DISC=(E**2)*D1-D2
      Q1=(-B3*E-SQRT(DISC))/(2.*S1)
      E=ETAN+(DELE/2.)
      IF (QM.GE.0.) GO TO 3
      WRITE (6,19) ETAN,P,QM
      GO TO 3
C     AT THIS STAGE THE TANGENT HAS BEEN DET WITH THE APPROX

C     VALUE OF THE LOAD. WE COULD REDUCE THE VALUE OF E FROM
C     ETAN AND SOLVE THE SYMM BUCKLING PROB FOR IOPT BY ITER
C     ON P .LE.PCR.
C
13    WRITE (6,20) EMIN,ESTOP,P,QP,QM
      GO TO 15
14    CONTINUE
      WRITE (6,21) I,S1,S2,S3,P,SUMJ,E
      E=E+DELE
      IF (E.GE.ESTOP) GO TO 15
      I=1
      GO TO 1

15    CONTINUE
      RETURN
C
16    FORMAT (10X,27HE,QP,QM,TP,TM,I FROM TANGNT,5E12.5,3X,I4,/)
17    FORMAT (10X,1H*,CRITICALCONDITIONSATTANGENTPOINT,14H*
     1,//,10X,5HETAN=,E12.5,5X,4HPCR=,E12.5,5X,3HQP=,E12.5,/)
18    FORMAT (10X,29H*BOTH TM AND TP CHANGED SIGN*,//,15X,25HE,QP,
QM,PCR
     1,TM,TP,QCR ARE,7E12.5,/)
19    FORMAT (10X,1H*,CRITICALCONDITIONSATTANGENTPOINT,1H*,//,10X,
5HETAN
     1=,E12.5,5X,4HPCR=,E12.5,5X,3HQM=,E12.5,/)

20    FORMAT (10X,54H*NO TANGENT POINT FOUND BET EMIN AND ESTOP
     1  *,8H,//,10X,,EMIN,ESTOP,P,QP,QMARE,13H,/,10X,5E12.5)
21    FORMAT (10X,35H*DISC IS NEG DURING ETAN SEARCH.***,3H***,//,
24HI,S
     11,S2,S3,P,SUMJ,E  ARE,I4,3X,6E12.5)
      END
**********************************
      SUBROUTINE COEFB (P,A1,C1,C2,C3,C4,MOR)
**********************************
      REAL K2,KINV
      COMMON /B2/ K2(40,40)/B9/KINV(40,40)/B12/VEC(40)
      COMMON /B14/ VEC1(40)/B3/AV5(70)/B4/V6(40)

C
      C1=0.
      CALL FMUX (KINV,AV5,VEC,MOR,MOR,40)
      DO 1 I=1,MOR
1     C1=C1+K2(MOR,I)*VEC(I)
      CALL FMUX (KINV,V6,VEC1,MOR,MOR,40)
      C2=0.
      DO 2 J=1,MOR
2     C2=C2+AV5(J)*VEC1(J)
      C3=0.
      DO 3 IA=1,MOR
3     C3=C3+V6(IA)*VEC1(IA)


      C4=0.
      DO 4 IB=1,MOR
4     C4=C4+K2(MOR,IB)*VEC1(IB)
      A1=C1*C2
      RETURN
      END
**********************************
      SUBROUTINE SINVRS (A,AINV,N,IA)
**********************************
C     TO COMPUTE INVERSE OF SYM MATRIX USING IMSL LINV2F.
C     THE PARAMETER IDGT = 0 ITERATIVE IMPROVMENT IS AUTO.
      DIMENSION A(IA,1), AINV(IA,1), WKAR(800)


      IDGT=0
      CALL LINV2F (A,N,IA,AINV,IDGT,WKAR,IER)
      RETURN
      END
**********************************
      SUBROUTINE FMTVX (A,X,Y,M,N,MA)
**********************************
      DIMENSION A(MA,1), X(1), Y(1)
C      FIND Y = A TRANS*X
C      WHERE A(M,N)
C      MA IS ROW DIM OF A IN CALLING PROG
C


      DO 1 I=1,N
      Y(I)=0.
      DO 1 J=1,M
1     Y(I)=A(J,I)*X(J)+Y(I)
      RETURN
      END
**********************************
      SUBROUTINE ENERGY (M,M1,M2,X,XI,DVEC,ENER,CONVG,XIOLD)
**********************************
      REAL MAXE,MINE
      DIMENSION XIOLD(M)
      DIMENSION ENER(M), X(M1), XI(M), DVEC(M2)


      DIMENSION ELVEC(4), EK1(4,4), PROD(4)
      COMMON /12/ U/13/E/11/SUMJ
      COMMON /4/ RHO,EXP
      COMMON /5/ EL/10/SYMM
C     IN SUB ENERGY COMPUTE AVE ENERGY DIST. OUTPUT WILL B  THE
C     CURRENT ENERGY DIST STORED AS A VECTOR,ENER(M).
C
C     AT THIS STAGE WE MUST FORMALLY SPECIFY THE EXPONENT AND COEF
C
C     IN THE INERTIA AREA RELATION, I = RHO*(A**EXP)
      UB=0.
```

```
      U=0.
C
      DO 3 I=1,M
C     DEFINE THE ELEMENT DISPL VECTOR ELVEC FROM DVEC
      DO 1 J=1,4
      ELVEC(J)=DVEC(2*I-2+J)
1     CONTINUE
      CALL COMEK1 (I,M,N1,X,XI,EK1)
C     NOW FORM MATRIX VECTOR PRODUCT
      CALL FMUX (EK1,ELVEC,PROD,4,4,4)
C     NOW MULT ELVEC AND PROD
      ENUM=0.
      DO 2 K=1,4

      ENUM=(ELVEC(K))*(PROD(K))+ENUM
2     CONTINUE
C     NOW COMPUTE THE DENOM
      REXP=1./EXP
      DENOM=(((XI(I))/RHO)**REXP)*EL
C     FINALLY THE ENERGY.  DENOM WILL BE GREATER THAN ZERO SINCE
C     XI(I) WILL BE RESTRICTED GREATER THAN ZERO.
      ENER(I)=ENUM/DENOM
      U=U+DENOM
      UB=UB+ENUM
3     CONTINUE
C     NOW ENER IS THE CRITICAL ENERGY DENSITY FOR EACH ELEMENT

C     UB IS TOTAL BENDING ENERGY;UI IS TOTAL INTERACTION ENERGY
      U=UB
C     U  WILL BE THE TOTAL ENERGY
      WRITE (6,11) U,V
C     WE NOW HAVE THE AVE ENERGY FOR EACH ELEMENT CORRES TO THE
C     PARTICULAR INERTIA IN EACH ELEMENT.
C     WE HAVE THE ENERGY DENSITY DIST FOR GIVEN INERTIA
C     NOW CHECK FOR CONVERGENCE.
C     **********CONVERGENCE TEST**********************************
******
      MM1=M-1
      MAXE=ENER(1)

      DO 5 J=1,MM1
      DIF=MAXE-ENER(J+1)
      IF (DIF) 4,4,5
4     MAXE=ENER(J+1)
5     CONTINUE
C     MAXE IS THE LARGEST ELEMENT OF ENER.  NOW SELECT THE SMALLES
C.
C
      MINE=ENER(1)
      DO 7 J=1,MM1
      DIF=ENER(J+1)-MINE
      IF (DIF) 6,6,7

6     MINE=ENER(J+1)
7     CONTINUE
C     IF THE DIF BET MAXE AND MINE IS SMALL ENOUGH,THE
C     ENERGY DENSITY DIST. IS ALMOST UNIFORM AND OPTIMUM IS ACHIEV
ED.
C        CONVG CRITERIA IS 3%
C
      WRITE (6,12) MAXE,MINE
      CONVG=((MAXE/MINE)-1.)*100.
      WRITE (6,13)
      DO 8 J=1,M
      WRITE (6,14) DVEC(2*J-1),ENER(J),XI(J)


8     CONTINUE
      WRITE (6,15) DVEC(2*M+1)
      IF (CONVG.GT.3.) GO TO 9
      WRITE (6,16)
      GO TO 10
C      COMPUTE NEW INERTIA
9     CONTINUE
      CALL INRTIA (M,U,ENER,XI,XIOLD)
10    CONTINUE
      RETURN
C
11    FORMAT (//,5X,14HTOTAL ENERGY,U,3X,E12.5,/,5X,23HTOTAL VOLUM
E
     1      ,3X,E12.5,///)
12    FORMAT (/,5X,7HMAXE IS,3X,E12.5,/,5X,7HMINE IS,3X,E12.5,///)
13    FORMAT (//,10X,12HDISPLACEMENT,8X,6HENERGY,8X,7HINERTIA,//)
14    FORMAT (10X,3(E12.5,5X))
15    FORMAT (10X,E12.5)
16    FORMAT (//,20X,30HENERGY CONVERGENCE IS OBTAINED,//)
      END
**************************************
      SUBROUTINE INRTIA (M,U,ENER,XI,XIOLD)
**********************************************
      DIMENSION ENER(M), XI(M), DELU(40)


      DIMENSION XIOLD(M)
      DIMENSION TXI(40)
      COMMON /5/ EL
      COMMON /4/ RHO,EXP
      COMMON /7/ VOL,XIMIN,EXP1
C
C     LET XI BE TXI
      DO 1 IM=1,M
      TXI(IM)=XI(IM)
1     CONTINUE
C     COMPUTE NEW INERTIA TXI
      COUNT=0.


      DO 2 IK=1,M
      DELU(IK)=0.
2     CONTINUE
      VEFF=VOL
      NXI=0
3     CONTINUE
      DENOM=0.
      DO 4 I=1,M
      DENOM=DENOM+((((VEFF*ENER(I)/U)**EXP1)*XI(I))**(1./EXP)*EL)
4     CONTINUE
      B=(RHO*(VEFF**EXP))/(DENOM**EXP)
      DO 5 J=1,M
```

```
      IF (TXI(J).EQ.XIMIN) GO TO 6
      TXI(J)=E*((ENER(J)*VEFF/U)**EXP1)*TXI(J)
5     CONTINUE
6     CONTINUE
C     WE HAVE THE NEW INERTIA DIST. EXAMINE TO SEE WHICH IF ANY AR
E LESS
C     THAN XIMIN
      IF (COUNT.EQ.1.) GO TO 12
      DO 9 KI=1,M
      XIDIF=TXI(KI)-XIMIN
      IF (XIDIF) 7,9,8
C     COMPUTE VOLUME CHANGE

7     DELV(KI)=EL*((1./RHO)**(1./EXP))*(XIMIN**(1./EXP)-TXI(KI)**(
1./EXP
     1))
      TXI(KI)=XIMIN
      NKI=NKI+1
8     CONTINUE
9     CONTINUE
C     DEFINE THE NEW EFFECTIVE VOLUME
      SUM=0.
      DO 10 KI=1,M
      SUM=SUM+DELV(KI)
10    CONTINUE

      IF (SUM.EQ.0.) GO TO 12
      VEFF=VOL-SUM
      DO 11 JJ=1,M
      IF (TXI(JJ).EQ.XIMIN) GO TO 11
      TXI(JJ)=XI(JJ)
11    CONTINUE
C     RECALCULATE THE UNSPECIFIED INERTIAS.
      COUNT=1.
      GO TO 3
12    CONTINUE
      DO 13 NK=1,M
      XIOLD(NK)=XI(NK)

      XI(NK)=TXI(NK)
13    CONTINUE
C     XI(K) HAS BEEN SUITABLY RESTRAINED TO ACCOUNT FOR XIMIN
C
C     **********************************************TEST****************
******
C     CHECK TO INSURE THAT THE CONSTANT VOLUME CONSTRAINT IS SATIS
FIED.
      SUM1=0.
      DO 14 JK=1,M
      SUM1=SUM1+((XI(JK)/RHO)**(1./EXP))*EL
14    CONTINUE

C     SUM1 SHOULD EQUAL VOL EXACTLY.
      ERROR=SUM1-VOL
      WRITE (6,15) ERROR
      RETURN
C
15    FORMAT (///,10X,57H THE VOLUME ERROR IN THE NEW INERTIA DIST.
     1       IS,3X,E12.5,//)
      END
**********************************
..
```

REFERENCES

1. Keller, J. B., "The Shape of the Strongest Column," Archive for Rational Mechanics and Analysis, Vol. 5, 1960.

2. Keller, J. B., Niordson, F. I., "The Tallest Column," Journal of Applied Mechanics, Vol. 16, No. 5, 1966.

3. Tadjbakhsh, I., Keller, J. B., "Strongest Columns and Isoperimetric Inequalities for Eigenvalues," Journal of Applied Mechanics, Vol. 29, March 1962, pp. 159-164.

4. Taylor, J. E., "Strongest Column: An Energy Approach," Journal of Applied Mechanics, Vol. 34, No. 2, June 1967, pp. 486-487.

5. Taylor, J. E. and Liu, C. V., "Optimal Design of Columns," AIAA Journal, Vol. 6, No. 8, August 1968, pp. 1497-1502.

6. Simitses, G. J., Kamat, M. P., and Smith, C. V., "Strongest Column by Finite Element Displacement Method," AIAA Journal, Vol. 11, No. 9, September 1973, pp. 1231-1232.

7. Simitses, George, J., and Ungbhakorn, Variddhi,"Weight Optimization of Stiffened Cylinders under Axial Compression," Computers and Structures, Vol. 5, pp. 305-314, Pergamon Press 1975.

8. Taig, I. C., and Kerr, R. I., "Optimization of Aircraft Structures with Multiple Stiffness Requirements" AGARD Second Symposium on Structural Optimization, April 1973, Milan, Italy.

9. Simitses, G. J., and Ungbhakorn, V., "Minimum Weight Design of Stiffened Cylinders under Axial Compression," AIAA Paper No. 74-101, January, 1974.

10. Simitses, G. J., and Caldwell, H. M., "Snap-Through Buckling of the Low Arch by the Trefftz Criterion," accepted for publication, Journal of Applied Mechanics.

11. Clausen, T., "Uber die Form Architekronischer Saulen." Bulletin Physico-Mathematique de l'Academie, Vol. 9, pp. 368, 1851.

12. Sheu, C. V. and Prager, W., "Recent Developments in Optimal Structural Design," Applied Mechanics Reviews, Vol. 21, No. 10, October 1968, pp. 985-992.

13. Prager, W. and Taylor, J. E., "Problems of Optimal Structural Design," Journal of Applied Mechanics, Vol. 35, 1968, pp. 102-106.

14. Huang, N. C., and Sheu, C. Y., "Optimal Design of an Elastic Column of Thin-walled Cross Section," Journal of Applied Mechanics, Vol. 35, pp. 285, 1968.

15. Venkayya, V. B., Khot, N. S., and Berke, L., "Application of Optimality Criteria Approaches to Automated Design of Large Practical Structures," AGARD Conference Proceedings No. 123, Second Symposium on Structural Optimization.

16. Gellatly, R. A., and Berke, L., "Optimal Structural Design," AFFDL-TR-70-165, Apr 1971.

17. Gellatly, R. A., "Development of Procedures for Large Scale Automated Minimum Weight Structural Design," AFFDL-TR-68-180, 1968.

18. Venkayya, V. B., Khot, N. S., and Reddy, V. S., "Energy Distribution in An Optimum Structural Design," AFFDL-TR-68-156.

19. Niordson, F. I., "On the Optimal Design of a Vibrating Beam," Quarterly of Applied Mathematics, Vol. 23, No. 1, 1965, pp. 47-53.

20. Turner, M. J., "Design of Minimum Mass Structures with Specified Natural Frequencies," AIAA Journal, Vol. 5, No. 3, 1967, pp. 406-412.

21. Taylor, J. E. "Minimum Mass Bar for Axial Vibration at Specified Natural Frequency," AIAA Journal, Vol. 5, No. 10, pp. 1911-1913, Oct 1967.

22. Taylor, J. E., "Optimum Design of a Vibrating Bar with Specified Minimum Cross-section, AIAA Journal, Vol. 6, No. 7, 1968, pp. 1379-1381.

23. Venkayya, V. B., Khot, N. S., Tischler, V. A., and Taylor, R. F., "Design of Optimum Structures for Dynamic Loads," presented at the 3rd Conference on Matrix Methods in Structural Mechanics, WPAFB, Ohio, October 1971.

24. Venkayya, V. B., and Khot, N. S., "Design of Optimum Structures to Impulse Type Loading," presented at the AIAA/ASME/SAE 15th Structures, Structural Dynamics and Materials Conference, Las Vegas, Nev., 17-19 Apr 1974.

25. Rudisill, C. S., Bhatia, K. G., "Optimization of Complex Structures to Satisfy Flutter Requirements," AIAA Journal Vol. 9, No. 8, Aug. 1971, pp. 1487-1491.

26. Wilkinson, K., Lerner, E., and Taylor, R. F., "Practical Design of Minimum Weight Aircraft Structures for Strength and Flutter Requirements," AIAA Paper No. 74-986, presented at the 6th AIAA Aircraft Design, Flight Test and Operations Meeting held in Los Angeles, California, 12-14 August 1974.

27. Timoshenko, S. P. and Gere, J. M., Theory of Elastic Stability, McGraw-Hill Book Co., Second Edition, 1961.

28. Marguerre, Karl, "On the Application of the Energy Method to Stability Problems," NACA TM 1138.

29. Kaplan, A., and Fung, Y. C., "Buckling of Low Arches or Curved Beams of Small Curvature," NACA TN 2840, Washington, 1952.

30. Schreyer, H. L. and Masur, E. F.,"Buckling of Shallow Arches," Journal of the Engineering Mechanics Division, ASCE, Vol. 92, August, 1966.

31. Walker, A. C., "A Non-linear Finite Element Analysis of Shallow Circular Arches," Journal of Solids and Structure, Vol. 5, pp. 97-107, 1969.

32. Thomas, Jerrell M., "A Finite Element Approach to the Structural Instability of Beams, Columns, Frames, and Arches," NASA TN D-5782, May, 1970.

33. Simitses, G. J., "Dynamic Snap-Through Buckling of Low Arches and Shallow Spherical Caps," Ph.D. Dissertation Dept. of Aeronautics and Astronautics, Stanford University, June 1965.

34. Hsu, C. S., Kuo, C. T., and Lee, S. S., "On the Final States of Shallow Arches on Elastic Foundations Subjected to Dynamicsl Loads," Journal of Applied Mechanics, Vol. 35, Series E, No. 4, Dec. 1968, pp. 713-723.

35. Hoff, N. J., and Bruce, V. G., "Dynamic Analysis of the Buckling of Laterally Loaded Flat Arches," Journal of Math. and Phys., Vol. XXXII, No. 4, Jan. 1954, pp. 276-288.

36. Wu, C.H., "The Strongest Circular Arch-A Perturbation Solution," Journal of Applied Mechanics, Vol. 35, No. 3, Trans, ASME, Vol. 90 Series E, Sept. 1968, pp. 476-480

37. Budiansky, B., Frauenthal, J. C. and Hutchinson, J. W., "On Optimal Arches," Journal of Applied Mechanics, Vol. 36, 1969, pp. 880-882.

38. Rapp, I. H., "Snap-through Buckling of Shallow Arches with Non-Uniform Stiffness Under Dynamic and Quasi-Static Loadings," Ph.D. Dissertation, Georgia Institute of Technology, Atlanta, Georgia 1974.

39. Christensen, E. N., "Optimal Design of Shallow Arches Against Buckling," Ph.D. Dissertation, Rensselaer Polytechnic Institute, June 1975.

40. Salinas, D., "On Variational Formulations for Optimal Structural Design," Ph.D. Dissertation, U.C.L.A., 1968.

41. Prager, W., and Marcal, P. V., "Optimality Criteria in Structural Design," AFFDL-TR-70-166, May 1971.

42. Berke, L., "Convergence Behavior of Iterative Resizing Procedures Based on Optimality Criteria," AFFDL-TM-72-1-FBR.

43. Prager, W., "Necessary and Sufficient Conditions for Global Structural Optimality," AGARD Conference Proceedings No. 123, 2nd Symposium on Structural Optimization, April 1973.

44. Berke, L. and Venkayya, V. B. "Review of Optimality Criteria Approaches to Structural Optimization," presented at Symposium on Structural Optimization, ASME Winter Annual Meeting, November 17-22, 1974, New York.

45. Kiusalaas, J., "Minimum Weight Design of Structures Via Optimality Criteria, NASA TN D-7115, Dec. 1972.

46. Sanders, J. L. Jr., "Non-Linear Theories for Thin Shell," Quarterly of Applied Mathematics, Vol. 21, 1963, p. 34.

47. Simitses, G. J., "Snapping of Low Pinned Arches on an Elastic Foundation," Journal of Applied Mechanics, Sept. 1973, pp. 741-744.

48. Simitses, George J., An Introduction to the Elastic Stability of Structures, Prentice-Hall, Inc., Englewood Cliffs, New Jersey, 1976.

49. Kamat, M. P., "Optimization of Structural Elements for Stability and Vibration," Ph. D. Dissertation, Georgia Institute of Technology, 1972.

50. Zienkiewicz, O. C., The Finite Element Method in Engineering Science, 2nd Edition, McGraw-Hill, London, 1971.

51. Nikolai, P. J., and Tsao, Nai-Kuan, "The ARL Linear Algebra Library Handbook," (Interim Report), ARL-TR-74-0106, Aerospace Research Laboratory, Wright-Patterson AFB, Ohio, July 1974.

52. International Mathematical and Statistical Libraries (IMSL), Inc., 5th Edition, Houston, Texas, 1976.

VITA

Hartley McMullin Caldwell, III was born in Bennettsville, South Carolina, on November 10, 1945. He received his Bachelor's Degree in Civil Engineering, with honors, from The Citadel in June, 1968. He subsequently entered the United States Air Force as a Second Lieutenant. Upon completion of his Master's Degree in Civil Engineering at Duke University, in 1969, he served for three years as an operations and maintenance officer in Air Force Civil Engineering while assigned to Headquarters 13th Air Force, Clark Air Force Base, the Philippines. Under the auspices of the Air Force Institute of Technology, he entered the Graduate Division of Georgia Institute of Technology in the School of Engineering Science and Mechanics in pursuit of his Doctor's Degree. After completion of his tour in 1975, he was assigned as a structural optimization engineer in the Structural Mechanics Division of the Air Force Flight Dynamics Laboratory, Wright-Patterson Air Force Base, Ohio. Upon completion of his doctorate, he will continue his career as an officer in the United States Air Force.